

**CONFORMATION OF THE RNA-BINDING
N-TERMINUS OF THE COAT PROTEIN
OF COWPEA CHLOROTIC MOTTLE VIRUS**

**A NUCLEAR MAGNETIC RESONANCE
AND OPTICAL SPECTROSCOPY STUDY**

Ontvangen

25 MEI 1992

UB-CARDEX



CENTRALE LANDBOUWCATALOGUS

0000 0489 6250

Promotor: dr. T. J. Schaafsma
hoogleraar in de moleculaire fysica

Co-promotor: dr. M. A. Hemminga
universitair hoofddocent bij de vakgroep Moleculaire Fysica

Marinette van der Graaf

**CONFORMATION OF THE RNA-BINDING
N-TERMINUS OF THE COAT PROTEIN
OF COWPEA CHLOROTIC MOTTLE VIRUS**

**A NUCLEAR MAGNETIC RESONANCE
AND OPTICAL SPECTROSCOPY STUDY**

Proefschrift

ter verkrijging van de graad van doctor
in de landbouw- en milieuwetenschappen
op gezag van de rector magnificus,
dr. H. C. van der Plas,
in het openbaar te verdedigen
op dinsdag 2 juni 1992
des namiddags te half twee in de Aula
van de Landbouwuniversiteit te Wageningen

BIBLIOTHEEK
LANDBOUWUNIVERSITEIT
WAGENINGEN

STELLINGEN

1. Poly(rA) en oligo(rA) zijn geen goede modelsystemen voor CCMV-RNA.

Adolph, K. W. (1975) *J. Gen. Virol.* 28, 137-145.
Dit proefschrift, hoofdstuk 6.

2. Door Vriend wordt ten onrechte op grond van exchange tussen resonanties bij 6.5 en 7.0 ppm in een 500-MHz proton-NMR-spectrum van lege capsiden van CCMV-manteleiwit geconcludeerd dat de N-terminus van dit eiwit secundaire structuur bezit en in tenminste twee verschillende metastabiele conformaties voor kan komen.

Vriend, G. (1983) Proefschrift Landbouwniversiteit Wageningen, hoofdstuk 9.
Dit proefschrift, hoofdstuk 5.

3. De aanwezigheid van een H1'/H2'-kruispijk in een COSY-spectrum van een RNA-molecuul duidt erop dat het bij deze kruispijk horende suikerresidue van tenminste een fractie van de aanwezige moleculen een C2'-endo-conformatie heeft; de afwezigheid van een dergelijke kruispijk duidt echter niet per definitie op de afwezigheid van deze conformatie.

Puglisi, J. D., Wyatt, J. R. & Tinoco, I. (1990) *J. Mol. Biol.* 214, 437-453.

4. Aan het door Palchaudhuri et al. voorgestelde helix-turn-helix motief voor het D-serine deaminase activator eiwit dient getwijfeld te worden, gezien het feit dat dit voorstel gebaseerd is op een DNA-sequentie die men kan toeschrijven aan de voor clonering gebruikte vector in plaats van het voor dit eiwit coderende *dsdC*-gen.

Palchaudhuri, S., Patel, V. & McFall, E. (1988) *J. Bacteriol.* 170, 330-334.

5. Omdat ureum bij verhitting ontleedt, dient men ureumhoudende oplossingen niet te autoclaveren.

6. De verlaging van darmepitheelbeschadiging en epitheliale proliferatie door binding van cytotoxische galzouten en vetzuren aan calciumfosfaat in de darm vormt een interessante verklaring voor het feit dat calcium in de voeding het risico op colonkanker kan verminderen.

Lapr , J. A., proefschrift Landbouwniversiteit Wageningen, te verdedigen op 2 juni 1992.

7. De publicatie door het Canadian Journal of Physics van een artikel waarin werkende moeders verantwoordelijk worden gesteld voor de toename van onethisch gedrag in de Westerse samenleving, levert geen bijdrage tot de bewustwording van de maatschappelijke verantwoordelijkheid van fysici.

Freeman, G. R. (1990) *Can. J. Phys.* 68, 794-798.

Crease, R. P. (1992) *Science* 255, 1065-1066.

8. Het door de Nederlandse Organisatie voor Wetenschappelijk Onderzoek (NWO) gehanteerde inschalingsbeleid voor ex-promovendi op post-doc posities, waarbij onderscheid wordt gemaakt tussen ex-AIO's/OIO's en overige ex-promovendi, is merkwaardig.
9. Het vermeerderingsproces dat optreedt bij cellen, laat zien dat delen een vorm van vermenigvuldigen is.

Stellingen behorende bij het proefschrift:

'Conformation of the RNA-Binding N-Terminus of the Coat Protein of Cowpea Chlorotic Mottle Virus: A Nuclear Magnetic Resonance and Optical Spectroscopy Study'

M. van der Graaf
Wageningen, 2 juni 1992.

Aan mijn ouders

'Eppur si muove'

(En toch beweegt zij zich)

Galilei

VOORWOORD

Op de omslag van dit proefschrift staat slechts één structuur van het onderzochte peptide, terwijl het zeer veel verschillende conformaties aan kan nemen. Ook wordt er maar één naam vermeld, hoewel er bij het tot stand komen van dit proefschrift veel mensen betrokken zijn geweest. Een aantal van de belangrijkste mensen wil ik hier met name noemen, maar ook alle andere wil ik hartelijk bedanken.

Tjeerd Schaafsma en Marcus Hemminga, zonder jullie optreden als respectievelijk promotor en co-promotor was er van dit proefschrift natuurlijk nooit iets terecht gekomen. Het onderzoek heeft zich voornamelijk afgespeeld binnen de virusgroep onder leiding van Marcus, die altijd zeer bedreven was in het 'regelen' van geld voor benodigde apparatuur of congresbezoek. Tijdens de laatste fase van mijn promotietijd werd de rol van Tjeerd wat groter. Ik heb zijn opbouwende kritiek op mijn manuscripten altijd zeer gewaardeerd.

Cor Wolfs heeft een deel van de optische metingen uitgevoerd en was onmisbaar bij biochemisch werk zoals virusisolaties en analyses. Cor, mede door jouw voorbeeld sta ik nu niet geheel onwennig hele dagen op het lab (dat had ik toen nooit gedacht, jij wel?). Ik hoop dat het je lukt dit jaar de Vierdaagse van Nijmegen uit te lopen.

Carlo van Mierlo en Jacques Vervoort zijn altijd bereid geweest om mij te helpen bij NMR-problemen. Carlo, jij hebt mij ingewijd in de geheimen van de 2D-NMR en bent altijd een morele steun voor mij geweest. Jacques, jij wist altijd de laatste nieuwtjes te vertellen uit de NMR-wereld.

Jos Joordens en Sybren Wijmenga zijn eigenlijk het Nijmeegse equivalent van het Wageningse duo dat ik hierboven heb genoemd. Jos, jij zorgde er altijd voor dat de AM-600 in topconditie was en Sybren, bij jou kon ik altijd terecht met theoretische vragen over pulsprogramma's en dergelijke. Ik ben dan ook blij dat ik in mijn huidige baan met jullie samen kan blijven werken. Ook alle andere mensen van Biofysische Chemie hebben er toe bijgedragen dat ik (toen en nu nog steeds) altijd met veel plezier in Nijmegen ga meten.

Martin Bos, Dirk Huckriede, Sandra Dijkstra, Katinka van der Linden en Gerard Kroon hebben als doctoraalstudenten een zeer belangrijke bijdrage geleverd aan dit onderzoek. Jullie waren niet alleen een grote steun bij het werk maar ook daarbuiten. Kennelijk is het jullie toen goed bevallen, want jullie zijn nu allemaal bezig met een eigen promotie-onderzoek. Ik wens jullie daarbij dan ook veel succes en ik hoop binnen afzienbare tijd jullie promoties

te kunnen bijwonen. Voor Sandra, Katinka en Gerard wil ik daar nog het volgende aan toevoegen: grijp niet te snel naar de Tipp-Ex; zonder lukt het uiteindelijk ook wel.

Zonder Ruud Scheek zouden er geen Distance Geometry berekeningen zijn uitgevoerd en had hoofdstuk 4 een veel kaler aanzien gehad. Ruud, hierbij geef ik je dan ook een welverdiend schouderklopje. Jij en de andere medewerkers van Fysische Chemie zorgden ervoor dat Katinka en ik onze bezoeken aan Groningen altijd zeer plezierig vonden.

Verder bedank ik Dick Verduin voor zijn aanwezigheid bij de virusgroeppbesprekingen, waarbij naar voren kwam dat ik niet alleen te maken had met spectroscopie maar ook met een virus; Paul ten Kortenaar en prof. Tesser voor hun behulpzaamheid toen bleek dat het peptide P25 niet helemaal zuiver was; Gerrit Polder en Cornelis Schillemans voor hun hulp bij mijn computerproblemen; de medewerkers van de tekenkamer en fotografie voor het voltooiën van mijn figuren; Pieter Magusin voor zijn prettige gezelschap op kamer 127 (Pieter, veel sterkte bij het schrijven van jouw boekje); en mijn huidige begeleider Kees Pleij voor het mij in de gelegenheid stellen mijn proefschrift af te ronden; I would like to thank Dagmar Hartmann and Sabine Keim for performing molecular dynamics calculations.

Alle medewerkers van Moleculaire Fysica bedank ik voor het feit dat ik ondanks wat mindere perioden de eerste verdieping van het Transitorium als een soort thuis ben gaan beschouwen. Zelfs nu nog zeg ik in Leiden wel eens 'bij ons in Wageningen' duidend op een situatie op Moleculaire Fysica (dit wordt me trouwens niet altijd in dank afgenomen). Hiertoe heeft niet alleen het werk op de vakgroep zelf bijgedragen, maar zeker ook de verjaardagen, etentjes, volleybalpartijen, zeer succesvolle roeiwedstrijden, etc. Mijn dank hiervoor is groot.

Als laatste wil ik John bedanken. John, hoewel jij niet hebt bijgedragen aan het hier beschreven onderzoek, ben ik ervan overtuigd dat de voltooiing van mijn proefschrift nog véél langer zou hebben geduurd wanneer jij niet tegelijkertijd met het schrijven van jouw proefschrift bezig was geweest.

Marinette
—

CONTENTS

List of Abbreviations

Chapter 1 1

General introduction

Chapter 2 19

Conformational studies on a peptide fragment representing the RNA-binding N-terminus of a viral coat protein using circular dichroism and NMR spectroscopy.

(Van der Graaf, M. & Hemminga, M. A. (1991) *Eur. J. Biochem.* 201, 489-494)

Chapter 3 35

Solution conformation of a peptide fragment representing a proposed RNA-binding site of a viral coat protein studied by two-dimensional NMR.

(This chapter has been published in abbreviated form: Van der Graaf, M., Van Mierlo, C. P. M. & Hemminga, M. A. (1991) *Biochemistry* 30, 5722-5727)

Chapter 4 57

Conformation of a pentacosapeptide representing the RNA-binding N-terminus of CCMV coat protein in the presence of oligophosphates. A two-dimensional proton NMR and distance geometry study.

(Van der Graaf, M., Scheek, R. M., Van der Linden, C. C. & Hemminga, M. A., submitted)

Chapter 5 77

Conformation and mobility of the RNA-binding N-terminal part of the intact coat protein of cowpea chlorotic mottle virus. A two-dimensional proton nuclear magnetic resonance study.

(Van der Graaf, M., Kroon, G. J. A. & Hemminga, M. A. (1991) *J. Mol. Biol.* 220, 701-709)

Chapter 6	95
Conformational changes in oligonucleotides upon binding to a peptide representing the N-terminal region of CCMV coat protein. An optical spectroscopy study.	
Summary	105
Samenvatting	109
Curriculum Vitae	113

LIST OF ABBREVIATIONS

1D, 2D	one-, two-dimensional
BMV	brome mosaic virus
CCMV	cowpea chlorotic mottle virus
CD	circular dichroism
COSY	2D scalar correlated spectroscopy
DG	distance geometry
DNA	deoxyribonucleic acid
DQ	double quantum
FID	free induction decay
HoHaHa	2D homonuclear Hartmann Hahn transfer experiment
NMR	nuclear magnetic resonance
NOE	nuclear Overhauser enhancement
NOESY	2D nuclear Overhauser enhancement spectroscopy
N/P	nucleotide/peptide molar ratio in nucleotide residues per P25
OD	optical density
P	monophosphate
P ₄	tetrapolyphosphate
P ₁₈	polyphosphate with an average chain length of 18 phosphates
P25	synthetic peptide containing the first 25 N-terminal amino acids of the coat protein of CCMV
P25*	P25 containing D-Valine instead of L-Valine at position 3
ppm	parts per million
rmsd	root mean square difference
RNA	ribonucleic acid
SD	standard deviation
T	triangulation number
T ₁	spin-lattice (longitudinal) relaxation time
UV	ultra violet

Ac		acetyl group	Ile	I	isoleucine
Ala	A	alanine	Leu	L	leucine
Arg	R	arginine	Lys	K	lysine
Asn	N	asparagine	Pro	P	proline
Gln	Q	glutamine	Ser	S	serine
Glu	E	glutamic acid	Thr	T	threonine
Gly	G	glycine	Val	V	valine

CHAPTER 1

GENERAL INTRODUCTION

SIMPLE SPHERICAL VIRUSES

Icosahedral structures

Viruses are nucleoprotein particles designed to transport specific genes between cells of a host and between hosts. Depending on the virus type, the genetic information is coded on RNA or DNA, which is single- or double-stranded. To protect the nucleic acid from digestion, it is packaged in a capsid composed of either protein or a lipid membrane and protein. A characteristic feature of viruses is that they cannot generate metabolic energy or synthesize proteins, but need a host for reproduction. After penetration into a host cell, the virus particle dissociates and the viral genome directs the cellular machinery to replication of viral nucleic acid and protein. Subsequently, the newly synthesized nucleic acids and coat proteins (and sometimes also lipids) assemble into new virus particles, that can be transported to other parts of the plant or other plants for new infection.

Since the gene of a simple virus is too small to code for many different proteins, Crick and Watson (1956, 1957) suggested that its protein coat consists of a large number of identical subunits. When identical protein subunits having identical environments are involved, only a few capsid structures are possible. The two most likely arrangements are a cylindrical shell having helical symmetry and a spherical shell having icosahedral symmetry. In fact, all small viruses are either rods or spheres.

Although an icosahedron requires 60 equivalent protein subunits, a large number of virus capsids is built from multiples of 60 identical proteins. Therefore, Caspar and Klug (1962) suggested the concept of quasi-symmetry. They proposed a certain flexibility in the coat protein subunits allowing slightly different interactions with their neighbours. The number of quasi-equivalent protein subunits in an icosahedral coat is $60T$, where T is the triangulation number giving the number of different quasi-equivalent units. The value of T is limited by a selection rule based upon the geometry of a trigonal lattice constructed on the surface of an icosahedron. The first high resolution X-ray structures of two $T = 3$ spherical plant RNA viruses (tomato bushy stunt virus (Harrison et al., 1978) and southern bean mosaic virus (Abad-Zapatero et al., 1980)) confirmed the $T = 3$ surface lattice, but showed more different subunit

contact regions than the quasi-equivalence theory predicted. This led to a small revision of the theory (Caspar, 1980; Harrison, 1980). Harrison showed that the building block in the icosahedron is a dimer, which can have two distinct conformations (the so called A/B and C/C states) in the virus particle. Assembly of the virus requires a selection between the two states, related by a hinge-like motion. More details about the assembly of small icosahedral viruses are given in reviews by Harrison (1984) and Rossmann and Erickson (1985). Viral disassembly has recently been reviewed by Liljas (1991).

Although Caspar and Klug developed their theory for identical protein subunits, it is now clear that the subunits of the icosahedron need not to be identical, but can also exist of different proteins with similar tertiary structure. This was first found for human rhinovirus 14 (Rossmann et al., 1985) with a protein coat consisting of three different proteins. The structure of this virus has been described as pseudo-symmetry $P = 3$ with a P instead of T number. Examples of larger and more complex spherical viruses are the polyomaviruses, the simplest viruses with double-stranded DNA genomes (Tooze, 1980). Recently, the X-ray structure of simian virus 40 has been determined at 3.8-Å resolution (Liddington et al., 1991). In this virus, the coat protein subunits do not interact in a quasi-equivalent way. However, comparison of its structure with a quasi-equivalent $T=7$ capsid shows that coat protein pentamers are present at exactly the same positions of pentamers and hexamers in a $T=7$ lattice. So, despite the lack of quasi-equivalence, the surface lattice of this polyomavirus is consistent with the concept of Caspar and Klug.

Tertiary structure of viral coat proteins

Since the first X-ray structures of tomato bushy stunt virus (Harrison et al., 1978) and tobacco mosaic virus disk protein (Bloomer et al., 1978) were published, the structures of several other viruses have been determined at atomic resolution: e.g. the spherical plant RNA viruses southern bean mosaic virus (Abad-Zapatero et al., 1980), satellite tobacco necrosis virus (Liljas et al., 1982), turnip crinkle virus (Hogle et al., 1986a,b), cowpea mosaic virus (Stauffer et al., 1987), and beanpod mottle virus (Chen et al., 1989). All the protein subunits of these viruses consist of two back-to-back four-stranded β -sheets that follow a ' β -role' topology (see Figure 1.1). This conformation is not unique for spherical plant RNA viruses, but appears also in spherical animal viruses. Generally, animal viruses show more insertions between the β -strands than plant viruses. Insertions can occur at the broad end of the

trapezoid (between the β -strands βC and βD , βE and βF , or βG and βH in Figure 1.1). An overview of the various known protein subunit structures in spherical plant and animal viruses is given by Rossmann and Johnson (1989). The only spherical bacterial virus of which the structure has been solved so far, the RNA phage MS2, has a coat protein of completely different conformation (Valegård et al., 1990).

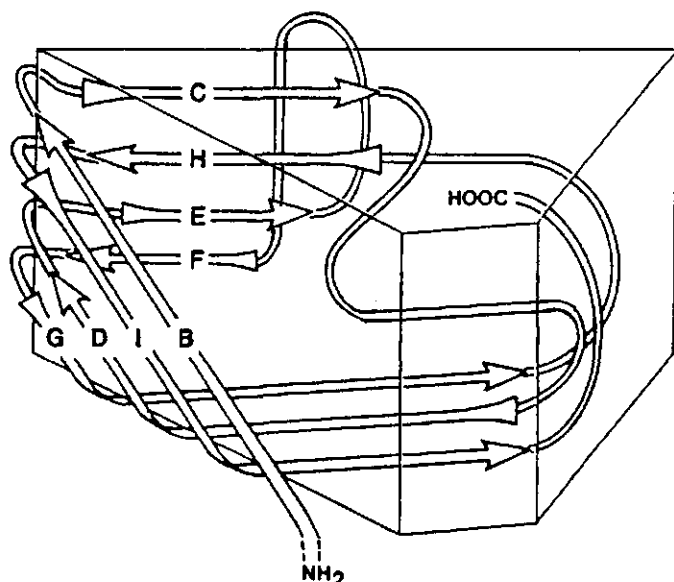


Fig. 1.1 Schematic representation of the arrangement of the eight β -sheets B to I which are common in small spherical plant and animal viruses (after Hogle et al., 1985).

Coat protein - RNA interactions in icosahedral plant viruses

In the coat proteins of many plant and insect viruses, the first 20 to 100 N-terminal residues contain a large number of basic amino acids that interact with the viral RNA (Rossmann and Johnson, 1989). Viruses without basic N-termini (tymoviruses, comoviruses and picornaviruses) contain a high concentration of polyamines such as spermidine (Cohen and McCormick, 1979). These positively charged N-termini and polyamines may be considered histone-like, because they help the RNA to fold by neutralizing the negative charges of the phosphates (Rossmann and Erickson, 1985).

The viral RNA is generally not packed in an icosahedral way, and can therefore not be seen in the electron density map obtained by X-ray crystallography. For this reason little direct information about the interactions between the coat protein and the RNA has been obtained so far. However, Rossmann presented a detailed model for the protein-RNA interactions in southern bean mosaic virus based upon the distribution of basic residues on the internal surface of the protein coat (Rossmann et al., 1983). He showed that these basic residues could be docked against double-helical A-RNA. In a few viruses, some part of the nucleic acid can be observed by X-ray crystallography (Liljas, 1991). In bean pod mottle virus, a comovirus with a coat protein lacking a basic N-terminus, nearly 20% of the RNA is visible in the electron density map (Chen et al., 1989). This part of the RNA is arranged around the threefold axis of the icosahedron and has the conformation of a single strand of an A-type RNA helix. The interactions with the protein are dominated by nonbonded electrostatic and Van der Waals interactions with few specific contacts.

Since the basic N-termini mentioned above are associated with the generally non-icosahedrally arranged RNA, they also appear as being disordered in X-ray structures. However, a portion of the basic N-terminal arm in satellite tobacco necrosis virus is ordered and forms an amphipathic α -helix (Abad-Zapatero et al., 1980). The α -helices of three coat protein subunits are clustered around the threefold axes of the icosahedron with their hydrophobic sides pointing to each other. Each helix exposes a highly basic side to the RNA. Secondary structure predictions performed by Argos (1981) show that the basic N-termini of several viruses can form amphipathic α -helices. It has been suggested that these α -helical structures can bind in one groove of double-stranded regions of the RNA.

Although the basic N-termini generally cannot be observed by X-ray crystallography, they can be observed by NMR spectroscopy under conditions giving them enough mobility. For the rod-shaped tobacco mosaic virus it has been shown that the internal mobility in the isolated coat protein can be studied by NMR (De Wit, 1978). NMR studies on the spherical alfalfa mosaic virus (Andree et al., 1981; Kan et al., 1982), cowpea chlorotic mottle virus (Vriend et al., 1981), tomato bushy stunt virus (Munowitz et al., 1980), and southern bean mosaic virus (McCain et al., 1982a,b) show that the N-termini of the coat proteins become mobile or more mobile upon swelling or disassembly of the virus. This suggests that without RNA most of the N-termini do not fold into a regular structure. Secondary structure predictions for the

N-terminus of cowpea chlorotic mottle virus (Vriend et al., 1986) indicate that the N-terminal arm shows no structural preference when the positive charges of its side chains are present. However, in the absence of these positive charges there is a tendency towards α -helix formation.

It has been shown for the rod-shaped viruses tobacco mosaic virus (Zimmern, 1977) and papaya mosaic virus (AbouHaidar and Bancroft, 1978), that the RNA has specific coat-protein binding sequences that act as initiation sites for the assembly. Also the coat protein of the spherical alfalfa mosaic virus binds to specific sites on the RNA (Houwing and Jaspars, 1982). However, after removal of the N-terminal arm by tryptic digestion, the coat protein of alfalfa mosaic virus loses its specificity for the RNA (Zuidema et al., 1983). Removal of the N-terminal arms from the coat proteins of cowpea chlorotic mottle virus and brome mosaic virus makes the coat protein unable to bind RNA (Vriend et al., 1981; Sacher and Ahlquist, 1989).

COWPEA CHLOROTIC MOTTLE VIRUS

Cowpea chlorotic mottle virus (CCMV) is an icosahedral T=3 plant virus belonging to the group of bromoviruses. CCMV consists of three types of nucleoprotein particles containing four species of single-stranded RNA molecules (RNA-1, -2, -3, and -4). RNA-1 and RNA-2 are encapsidated separately, and RNA-3 and RNA-4 are packaged together in spherical particles of about 26 nm in diameter (Lane, 1974). The protective protein coat consists of 180 identical proteins, each 189 residues long (Dasgupta and Kaesberg, 1982). CCMV particles undergo structural changes as a function of pH, ionic strength and temperature (Kaper, 1975). The *in vitro* dissociation and association processes of CCMV as a model for *in vivo* disassembly and assembly have been studied by Verduin (1978).

Figure 1.2 gives an overview of the various aggregation states of the viral RNA and coat protein. The virus particle is stable around pH 5, but it swells at increasing pH and low ionic strength ($\mu \approx 0.2$). Reversibility of this swelling is obtained in the presence of divalent cations (i.e. Mg^{2+}) (Chauvin et al., 1978; Verduin, 1978). Raising the pH at increased ionic strength ($\mu > 0.3$) results in dissociation of the virus particle into protein dimers and RNA (Bancroft and Hiebert, 1967). Both RNA and protein can be isolated and reassembled *in vitro*. In the absence of RNA, the protein subunits can be reassociated into empty protein capsids by lowering the pH to 5.0 (Bancroft et

al., 1968). These empty protein capsids have T=3 icosahedral structures similar to the native virus (Finch and Bancroft, 1968).

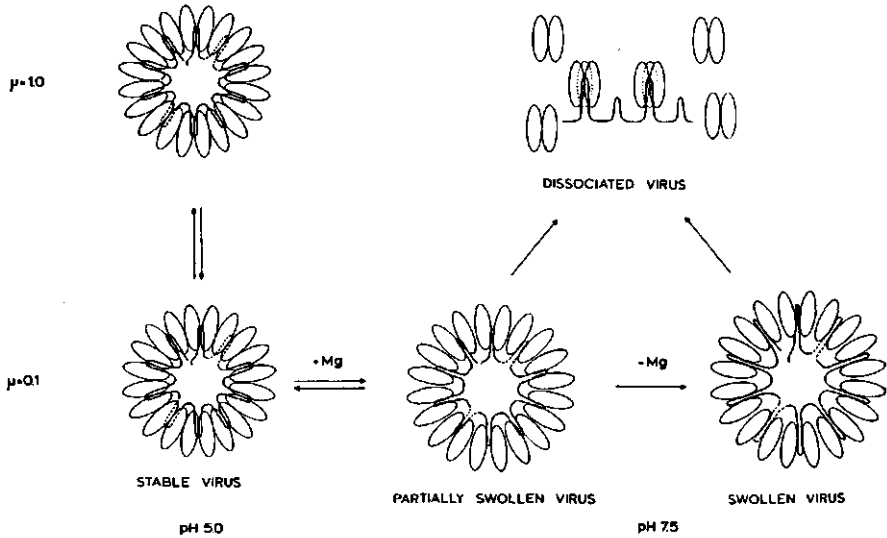


Fig. 1.2 Schematic representation of the swelling and dissociation of CCMV. Ionic strength (μ) and pH are varied in vertical and horizontal direction, respectively. At low ionic strength and pH 7.5, the influence of magnesium ions on swelling is shown. Protein subunits are represented by ellipses and the RNA by strings (from Verduin, 1978).

Krüse (1979) and Vriend (1983) used optical and magnetic resonance spectroscopy to study conformational changes appearing upon the dissociation and assembly of CCMV particles. NMR studies on empty capsids revealed an increased mobility of the highly basic N-terminal parts of the protein subunits. This mobility is absent upon binding of RNA - as in intact virions - as well as after removal of the first 25 N-terminal amino acids by tryptic digestion (Vriend et al., 1981). After removal of the highly basic N-terminal arm the coat protein shows no interaction with the RNA. Interactions between the positively charged residues present in the N-terminus (six Arg and three Lys, see Figure 1.3) and the negatively charged phosphate groups of the RNA are suggested to be responsible for protein-

RNA binding (Argos, 1981; Vriend et al., 1981). Cross-link and deletion studies on brome mosaic virus (BMV), a bromovirus closely related to CCMV, supported this suggestion. For both CCMV and BMV, the positively charged amino acids are situated between residues 7 and 25 within the significantly conserved N-terminal region of the coat protein. Sgro et al. (1986) introduced RNA-protein cross-links into brome mosaic virus by a photoreactive cross-linker with a relatively short 0.7-nm span. Residues 11-19 have been found to be cross-linked to the RNA. Sacher and Ahlquist (1989) investigated the effect of deletions in the N-terminal region of BMV coat protein on RNA packaging and systemic infection. Their results show that the RNA binding region is situated somewhere in the region 8-25, which contains all but one of the positively charged amino acids.

CCMV

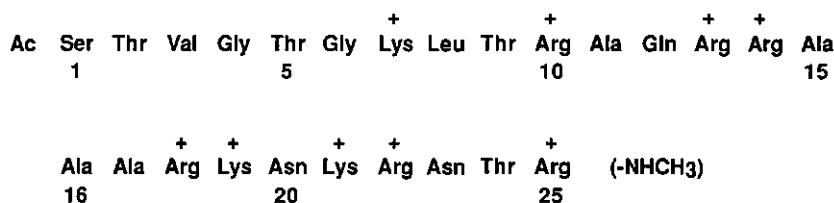


Fig. 1.3 Amino acid sequence of the N-terminal arm of CCMV coat protein (Dasgupta and Kaesberg, 1982). Positively charged residues are denoted as (+). The methyl group is present at the C terminus of the chemically synthesized peptide P25 (see text).

On the basis of NMR experiments and secondary structure predictions, Vriend et al. (1982, 1986) proposed a 'snatch-pull' model for the assembly of CCMV coat protein (Figure 1.4). In this model the N-terminal arm has a flexible random-coil conformation before interacting with the RNA. The large flexibility enhances the chance that a positively charged side chain meets a negatively charged phosphate of the RNA backbone. Upon binding the positive and negative charges neutralize each other, and the N-terminal arm adopts an α -helical conformation, thereby pulling the coat protein and RNA towards each other.

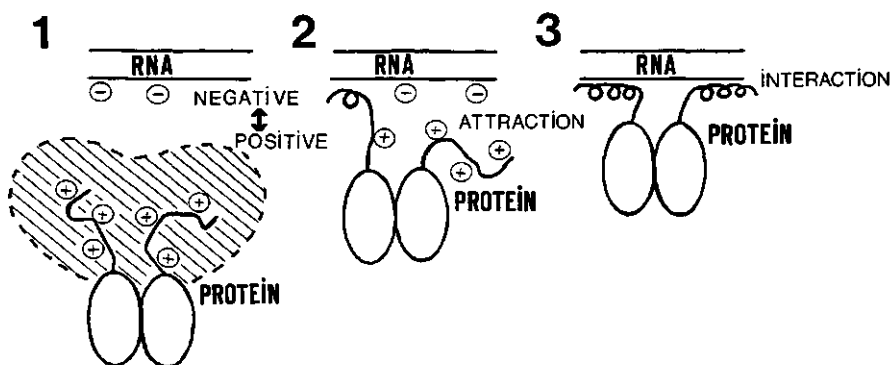


Fig. 1.4 Schematic representation of the 'snatch-pull' interaction model for binding of CCMV coat protein to RNA. In solution, CCMV coat protein exists mostly as dimers. (after Vriend, 1983)

The objective of the study described in this thesis was to obtain information about the protein-RNA interactions in the CCMV particle and to test the 'snatch-pull' model. Until recently, no experimental evidence has been presented for the α -helical conformation suggested by secondary structure predictions for the N-terminal region of CCMV coat protein (Vriend et al., 1986). Laser Raman studies on CCMV showed differences in protein conformation in the presence and the absence of RNA, but no conclusions could be drawn about the nature of the secondary structure of the N-terminus (Verduin et al., 1984). High-resolution NMR experiments have provided some information about the behaviour of the N-terminal arm of CCMV coat protein (Vriend, 1983). However, the large sizes of coat protein aggregates, intact virus particles or protein-nucleotide complexes lead to very broad NMR lines. This makes it very difficult to study the secondary structure of the N-terminus in these systems by high resolution NMR.

Chemical synthesis of the pentacosapeptide P25 (Ten Kortenaar et al., 1986) containing the first 25 amino acid residues of CCMV coat protein (Figure 1.3) made it possible to perform detailed NMR and optical spectroscopic studies on the structure of this N-terminal segment in the

absence and presence of nucleotides. The spectroscopic techniques used for structure determination are described in the following two sections. Unlike the intact coat protein, the peptide is stable over a wide range of temperature and ionic strength, so that its conformation can be studied under various conditions. It has been shown that the proton NMR spectrum of P25 closely resembles the proton NMR difference spectrum of intact coat protein and coat protein lacking the N-terminal region, except for their linewidths (Hemminga et al., 1985). This indicates that P25 is a good model for the N-terminal part of CCMV coat protein.

STRUCTURE DETERMINATION BY NMR SPECTROSCOPY

NMR spectroscopy

Nuclear magnetic resonance is based upon the interaction between the magnetic moments of atomic nuclei and magnetic fields. Only nuclei for which $I \neq 0$ (I = spin) have a magnetic moment and can be observed by NMR. The magnetization of nuclei with $I = 1/2$ (e.g. ^1H , ^{13}C , ^{15}N , and ^{31}P) can be oriented either parallel or antiparallel to an external magnetic field. For protons, the parallel state corresponding to the lower energy state has a larger population than the antiparallel state in thermal equilibrium. This equilibrium can be perturbed by a second magnetic field oscillating at an appropriate radiofrequency. The response of the system during relaxation towards equilibrium gives rise to a free induction decay, which can be Fourier transformed to the NMR signal. A simple description of NMR can be found in the text book by Sanders and Hunter (1987), and a detailed quantum mechanical treatment is given by Ernst et al. (1987).

For many years X-ray crystallography has been the only technique by which three-dimensional structures of biomolecules could be determined. However, during the last two decades NMR has become a powerful tool to study the structure of small proteins and nucleic acids. This is mainly due to the development of two-dimensional NMR techniques (Ernst et al., 1987; Jeener, 1971) and great advances in NMR instrumentation. Also of great importance was the publication of a resonance assignment strategy for two-dimensional proton NMR spectra of proteins (Wüthrich, 1986). In addition, computational facilities have been improved and algorithms have been developed for the calculation of three-dimensional structures from NMR data (Kaptein et al., 1988).

Three major advantages of NMR with respect to X-ray crystallography are: (1) the need for crystals can be avoided, (2) the possibility to measure in solution makes it possible to vary conditions such as pH and ionic strength, and (3) dynamic information can be obtained. A minor disadvantage of NMR is the restriction on the size of the macromolecule; until now only protein structures of sizes up to about 20 kDa have been determined by NMR spectroscopy. However, it may be expected that in the future also the structure of larger proteins can be studied by NMR. Developments in molecular biology and organic chemistry have made it possible to label proteins with isotopes such as ^{13}C and ^{15}N (McIntosh and Dahlquist, 1990). This isotope labelling allows the use of heteronuclear three- and four-dimensional NMR (Clore and Gronenborn, 1991; Fesik and Zuiderweg, 1990) or heteronuclear filters in two-dimensional proton NMR (Otting and Wüthrich, 1990), by which techniques severe overlap problems in the spectra can be avoided.

Dipolar cross-relaxation between protons in close vicinity of each other ($< 5 \text{ \AA}$) gives basic information for structure determination by proton NMR. This interaction can result in magnetisation transfer, which is called the nuclear Overhauser effect (NOE) (Noggle and Schirmer, 1971). The NOE shows an r^{-6} distance dependence making it possible to extract proton-proton distances from NOE intensities. These intensities can be determined by measuring the sizes of off-diagonal peaks in two-dimensional NOE (= NOESY) spectra. Assuming that all rotational correlation times within the protein are equal, inter-proton distances can be calculated on the basis of a known reference distance by using the equation:

$$r_{ij} = (\text{NOE}_{\text{ref}} / \text{NOE}_{\text{obs}})^{1/6} \times r_{\text{ref}}$$

with r_{ij} = distance between proton i and j
 r_{ref} = reference distance
 NOE_{obs} = observed NOE intensity
 NOE_{ref} = NOE intensity corresponding to the reference distance

A problem in NOE based distance determination is spin diffusion, the effect of indirect magnetisation transfer via other protons (Kalk and Berendsen, 1976). This effect, which appears especially in larger molecules, gives rise to inaccurate proton-proton distances. The iterative relaxation-matrix method

(IRMA) takes spin diffusion into account and can be used to correct the distances (Boelens et al., 1988).

Another useful NMR parameter in structure determination is the J-coupling constant between vicinal protons, giving information about dihedral angles (Karplus, 1959). The coupling constant representing the J-coupling between the amide proton and the α -proton of an amino acid residue ($^3J_{\text{HN}\alpha}$) gives information about secondary structure in proteins: $^3J_{\text{HN}\alpha} \leq 5$ corresponds with α -helical conformation and $^3J_{\text{HN}\alpha} \geq 8$ with β -structure (Wüthrich, 1986). A third NMR parameter, the chemical shift, is generally considered to be not very reliable for structure determination because of a high sensitivity to ring-current fields of aromatic amino acids and shielding effects. However, it has been shown by statistical analysis of chemical-shift distributions in 32 polypeptides and proteins that the α -protons of aliphatic amino acid residues in α -helical conformations shift upfield by 0.4 ppm, on the average (Szilágyi and Jardetzky, 1989). Therefore, it can be concluded that also the chemical shift can supply information about secondary structure. Information about molecular motions can be obtained by measuring the relaxation times T_1 (spin-lattice relaxation time) and T_2 (spin-spin relaxation time) (Ernst et al., 1987).

Distance geometry calculations

The metric matrix distance-geometry (DG) algorithm (Crippen and Havel, 1978; Crippen, 1981; Havel et al., 1983) can be used to generate structures from distances obtained from NOE intensities (Kaptein et al., 1988). At the beginning of this procedure, upper and lower bounds (u and l) are set for all atom-atom distances in the molecule. Some of these bounds follow from the NOE-derived distances and J-coupling constants and others follow from standard bond lengths and bond angles. A procedure using triangle inequalities extends the constraints to all possible distances. A structure can be generated by repeated random choices of all inter-atomic distances between upper and lower bounds. After this step, the generated structure must be optimized by minimizing an error function consisting of distance constraints and chirality constraints. By repetition of the whole procedure several DG structures can be obtained. The deviation in conformation of these structures gives information about how uniquely the structure is determined by the constraints. The possible conformations that satisfy the NMR distance constraints can be sampled more exhaustively by applying distance bounds driven dynamics to the generated DG structures. This is a simplified molecular

dynamics calculation with only geometric constraints as the driving potential. Finally, the structures can be refined by a restrained energy minimisation using steepest descent or conjugate gradient methods to bring the energy down, followed by restrained molecular dynamics (Kaptein et al., 1988).

STRUCTURE DETERMINATION BY OPTICAL SPECTROSCOPY

Circular dichroism spectroscopy

Circular dichroism (CD) is the phenomenon that the absorbance of left circularly polarized light is different from the absorbance of right circularly polarized light. Optically active molecules such as proteins and nucleic acids show this difference in absorbance. A detailed description of the quantum mechanical basis of circular dichroism is given by Schellman (1975).

In the far UV region (190-240 nm) a protein gives rise to a CD signal (expressed in ellipticity θ) of which the shape and intensity depend on its backbone conformation. The observed signal can be considered as a linear combination of CD signals originating from the various secondary structure elements present in the protein:

$$\theta_{\text{total}}(\lambda) = f_{\alpha} \cdot \theta_{\alpha}(\lambda) + f_{\beta} \cdot \theta_{\beta}(\lambda) + f_r \cdot \theta_r(\lambda)$$

with $\theta(\lambda)$ = mean residue ellipticity at wavelength λ
 λ = wavelength
 f_x = fraction of the protein having conformation x
 α = α -helix
 β = β -structure
 r = remainder structure

The secondary structure of a protein with unknown conformation can be determined by fitting its CD spectrum to sets of reference spectra, obtained from CD spectra of proteins with known amounts of the various structure elements (Cantor and Schimmel, 1980). Several sets of reference spectra have been published (Greenfield and Fasman, 1969; Saxena and Wetlaufer, 1971; Chen et al., 1972, 1974; Chang et al., 1978; Hennessey and W.C. Johnson, 1981). In modern CD analysis the various structure elements are

often more differentiated: e.g. β -turns and β -sheet instead of β -structure (Chang et al., 1978; Provencher and Glöckner, 1981). However, since the peptide P25 contains only 25 residues and only a limited amount of secondary structure elements, its CD spectra were analyzed according to the equation given above with only three different secondary structure elements.

CD spectra can be distorted due to light-scattering or contributions of aromatic amino acids (not present in P25) in the far UV region. Also uncertainties in concentration result in inaccurate fractions of the various structure elements. Structure determination from CD spectra is more accurate for proteins with a high content of α -helix or β -sheet structure than for proteins with only little secondary structure (Van Stokkum et al., 1990). For all these reasons, the values of the various structure elements in P25 determined by CD spectroscopy must be considered to give only relative information.

Since for nucleic acids the spectral differences between the different bases cannot be ignored, it is very difficult to analyze their CD spectra. Not only the base composition but also the base sequence must be taken into account. For a molecule such as tRNA with both single-strand and double-strand regions a total of up to 30 different spectral contributions must be combined to compute the CD spectrum (Cantor and Schimmel, 1980). However, some conformational information about the structure of an oligonucleotide can be obtained by comparing its CD spectrum with the CD spectrum of a polynucleotide with a corresponding sequence and known conformation (e.g. the CD spectrum of $r(A)_{12}$ can be compared to that of $\text{poly}(rA)$).

UV absorption spectroscopy

The UV absorption band of double stranded nucleic acid is 30-40% less intense than the absorption band observed for a mixture of the component monomers. The origin of this hypochromism is the interaction between one particular electronic excited state of a given chromophore and different electronic states of neighbouring chromophores (Cantor and Schimmel, 1980). This hypochromic effect makes it possible to monitor the melting of RNA and DNA, because the unstacking of the base pairs at increasing temperature results in an increase of the absorption intensity at the absorption maximum (~ 260 nm). The melting temperature, the temperature at which half of the helical structure is lost, can be determined by measuring this absorbance intensity as a function of the temperature.

OUTLINE OF THIS THESIS

The objective of the study presented in this thesis was to obtain information about protein-RNA interactions in the CCMV particle and to test the 'snatch-pull' model (see Figure 1.4). As described above, this model suggests a conformational change of the N-terminal region of the coat protein upon RNA binding. The pentacosapeptide P25 was used as a model for the N-terminus of CCMV coat protein, and oligophosphates and oligonucleotides were used as models for RNA.

Chapter 2 describes the effects of ionic strength, addition of (oligo)phosphates, and temperature on the conformation of P25 studied by one-dimensional proton NMR and CD spectroscopy. NMR relaxation measurements have been used to study the effect of oligophosphate binding on the mobility of several amino acid side chains in the peptide. Chapter 3 and 4 show how two-dimensional proton NMR experiments provide detailed information about the conformation of P25 in the presence of monophosphate (Chapter 3) or oligophosphates (Chapter 4). NMR distance constraints obtained for P25 in the presence of tetraphosphate have been used to generate peptide structures by distance geometry calculations. In Chapter 5 a description is given of two-dimensional proton NMR experiments on the intact CCMV coat protein, which can be present as a dimer or as an empty capsid consisting of 180 protein monomers. The NMR spectra of both dimer and capsid show only resonances originating from the flexible N-termini and have been interpreted by using information obtained for P25. Chapter 6 deals with the effect of P25 on the conformation and stability of three different oligonucleotides. Conformational changes of the oligonucleotides have been studied by CD and UV spectroscopy. Finally, the summary gives a review of all the results obtained.

REFERENCES

- Abad-Zapatero, C., Abel-Meguid, S. S., Johnson, J. E., Leslie, A. G. W., Rayment, I., Rossmann, M. G., Suck, D. & Tsukinara, T. (1980) *Nature* 286, 33-39.
- AbouHaidar, M. & Bancroft, J. B. (1978) *Virology* 90, 54-59.
- Andree, P. J., Kan, J. H. & Mellema, J. E. (1981) *FEBS Lett.* 130, 265-268.
- Argos, P. (1981) *Virology* 110, 55-62.
- Bancroft, J. B. & Hiebert, E. (1967) *Virology* 32, 354-356.

- Bancroft, J. B., Wagner, G. W. & Bracker, C. E. (1968) *Virology* 36, 146-149.
- Bloomer, A. C., Champness, J. N., Bricogne, G., Staden, R. & Klug, A. (1978) *Nature* 276, 362-368.
- Boelens, R., Koning, T. M. G. & Kaptein, R. (1988) *J. Mol. Struct.* 173, 299-311.
- Cantor, C. R. & Schimmel, P. R. (1980) in *Biophysical Chemistry. Part II: Techniques for the Study of Biological Structure and Function*, pp. 339-431, W.H. Freeman and Company, San Francisco.
- Caspar, D. L. D. (1980) *Biophys. J.* 32, 103-138.
- Caspar, D. L. D. & Klug, A. (1962) *Cold Spring Harbor Symp. Quant. Biol.* 27, 1-24.
- Chang, C. T., Wu, C.-S. C. & Yang, J. T. (1978) *Anal. Biochem.* 91, 13-31.
- Chauvin, C., Pfeiffer, P., Witz, J. & Jacrot, B. (1978) *Virology* 88, 138-148.
- Chen, Y. H., Yang, J. T. & Chau, K. H. (1974) *Biochemistry* 13, 3350-3359.
- Chen, Y. H., Yang, J. T. & Martinez, H. M. (1972) *Biochemistry* 11, 4120-4131.
- Chen, Z., Stauffacher, C., Li, Y., Schmidt, T., Bomu, W., Kamer, G., Shanks, M., Lomonosoff, G. & Johnson, J. E. (1989) *Science* 245, 154-159.
- Clore, G. M. & Gronenborn, A. M. (1991) *Science* 252, 1390-1398.
- Cohen, S. S. & McCormick, F. P. (1979) *Adv. Virus Res* 24, 331-387.
- Crick, F. H. C. & Watson, J. D. (1956) *Nature* 177, 473-475.
- Crick, F. H. C. & Watson, J. D. (1957) in *Ciba Foundation Symposium on the Nature of Viruses* (Wolstenholme, G. E. W. & Millar, E. C. P., Eds.) pp. 5-13, Little, Brown, Boston.
- Crippen, G. M. (1981) *Distance Geometry and Conformational Calculations*, Research Studies Press, New York.
- Crippen, G. M. & Havel, T. F. (1978) *Acta Cryst.* 34A, 282-284.
- Dasgupta, R. & Kaesberg, P. (1982) *Nucl. Acids Res.* 10, 703-713.
- De Wit, J. L. (1978) Ph.D. Thesis, Agricultural University Wageningen, The Netherlands.
- Ernst, R. R., Bodenhausen, G. & Wokaun, A. (1987) *Principles of Nuclear Magnetic Resonance in One and Two Dimensions*, Clarendon Press, Oxford.
- Fesik, S. W. & Zuiderweg, E. R. P. (1990) *Q. Rev. Biophys.* 23, 97-132.
- Finch, J. T. & Bancroft, J. B. (1968) *Nature* 220, 815-816.
- Greenfield, N. & Fasman, G. D. (1969) *Biochemistry* 8, 4108-4116.
- Harrison, S. C. (1980) *Biophys. J.* 32, 139-153.
- Harrison, S. C. (1984) *Trends Biochem. Sci.* 9, 345-351.
- Harrison, S. C., Olson, A. J., Schutt, C. E., Winkler, F. K. & Bricogne, G. (1978) *Nature* 276, 368-373.
- Havel, T. F., Kuntz, I. D. & Crippen, G. M. (1983) *Bull. Math. Biol.* 45, 665-720.
- Hemminga, M. A., Datema, K. P., ten Kortenaar, P. W. B., Krüse, J., Vriend, G., Verduin, B. J. M. & Koole, P. (1985) in *Magnetic Resonance in Biology and Medicine* (Govil, G. Khetrpal, C. L. & Saran, A., Eds.), pp. 53-76, Tata McGraw-Hill, New Delhi.

- Hennessey, J. P. & W.C. Johnson, J. (1981) *Biochemistry* 20, 1085-1094.
- Hogle, J. M., Chow, M. & Filman, D. J. (1985) *Science* 229, 1358-1365.
- Hogle, J. M., Maeda, A. & Harrison, S. C. (1986a) *J. Mol. Biol.* 159, 93-108.
- Hogle, J. M., Maeda, A. & Harrison, S. C. (1986b) *J. Mol. Biol.* 191, 625-38.
- Houwing, C. J. & Jaspars, E. M. J. (1982) *Biochemistry* 21, 3408-3414.
- Jeener, J., Ampère Summer School, Basko Polje, Yugoslavia, (1971),
- Kalk, A. & Berendsen, H. J. C. (1976) *J. Magn. Reson.* 24, 343-350.
- Kan, J. H., Andree, P. J., Kouijzer, L. C. & Mellema, J. E. (1982) *Eur. J. Biochem.* 126, 29-33.
- Kaper, J. M. (1975) *The Chemical Basis of Virus Structure, Dissociation and Reassembly*, North-Holland, Amsterdam.
- Kaptein, R., Boelens, R., Scheek, R. M. & Gunsteren, W. F. V. (1988) *Biochemistry* 27, 5389-5395.
- Karplus, M. (1959) *J. Chem. Phys.* 30, 11-15.
- Krüse, J. (1979) Ph.D. Thesis, Agricultural University Wageningen, The Netherlands.
- Lane, L. C. (1974) *Adv. Virus Res.* 19, 151-220.
- Liddington, R. C., Yan, Y., Moulai, J., Sahli, R., Benjamin, T. L. & Harrison, S. C. (1991) *Nature* 354, 278-284.
- Liljas, L. (1991) *Int. J. Biol. Macromol.* 13, 273-280.
- Liljas, L., Unge, T., Jones, T. A., Fridborg, K., Lövgren, S., Skoglund, U. & Strandberg, B. (1982) *J. Mol. Biol.* 159, 93-108.
- McCain, D. C., Virudachalam, R., Markley, J. L., Abdel-Meguid, S. S. & Rossmann, M. G. (1982a) *Virology* 117, 501-503.
- McCain, D. C., Virudachalam, R., Santini, R. E., Abdel-Meguid, S. S. & Markley, J. L. (1982b) *Biochemistry* 21, 5390-5397.
- McIntosh, L. P. & Dahlquist, F. W. (1990) *Q. Rev. Biophys.* 23, 1-38.
- Munowitz, M. G., Dobson, C. M., Griffin, R. G. & Harrison, S. C. (1980) *J. Mol. Biol.* 141, 327-333.
- Noggle, J. H. & Schirmer, R. E. (1971) *The Nuclear Overhauser Effect*, Academic Press, New York.
- Otting, G. & Wüthrich, K. (1990) *Q. Rev. Biophys.* 23, 39-96.
- Provencher, S. W. & Glöckner, J. (1981) *Biochemistry* 20, 33-37.
- Rossmann, M. G., Arnold, E., Erickson, J. W., Frankenberger, E. A., Griffith, J. P., Hecht, H. J., Johnson, J. C., Kamer, G., Luo, M., Mosser, A. G., Rueckert, R. R., Sherry, B. & Vriend, G. (1985) *Nature* 317, 145-153.
- Rossmann, M. G., Chandrasekaran, R., Abad-Zapatero, C., Erickson, J. W. & Arnott, S. (1983) *J. Mol. Biol.* 166, 73-80.
- Rossmann, M. G. & Erickson, J. W. (1985) in *Virus Structure and Assembly* (Casjens, S., Ed.), pp. 29-73, Van Nostrand Reinhold International.

- Rossmann, M. G. & Johnson, J. E. (1989) *Annu. Rev. Biochem.* 58, 533-573.
- Sacher, R. & Ahlquist, P. (1989) *J. Virol.* 63, 4545-4552.
- Sanders, J. K. M. & Hunter, B. K. (1987) *Modern NMR Spectroscopy. A Guide for Chemists*, Oxford University Press, Oxford.
- Saxena, V. P. & Wetlaufer, D. B. (1971) *Proc. Nat. Acad. Sci. USA* 68, 969-972.
- Schellman, J. A. (1975) *Chem. Revs.* 75, 323-331.
- Sgro, J., Jacrot, B. & Chroboczek, J. (1986) *Eur. J. Biochem.* 154, 69-76.
- Stauffacher, C. V., Usha, R., Harrington, M., Schmidt, T., Hosur, M. V. & Johnson, J. E. (1987) in *Crystallography in Molecular Biology* (Moras, D., Drenth, J., Strandberg, B., Suck, D. & Wilson, K., Eds.), pp. 293-308, Plenum, New York.
- Szilágyi, L. & Jardetzky, O. (1989) *J. Magn. Reson.* 83, 441-449.
- Ten Kortenaar, P. B. W., Krüse, J., Hemminga, M. A. & Tesser, G. I. (1986) *Int. J. Pept. Protein Res.* 27, 401-413.
- Tooze, J. (1980) *DNA Tumor Viruses*, Cold Spring Harbor Laboratory, New York.
- Valegård, K., Liljas, L., Fridborg, K. & Unge, T. (1990) *Nature* 345, 36-41.
- Van Stokkum, I. H. M., Spoelder, H. J. W., Bloemendal, M., Van Grondelle, R. & Groen, F. C. A. (1990) *Anal. Biochem.* 191, 110-118.
- Verduin, B. J. M. (1978) Ph.D. Thesis, Agricultural University Wageningen, The Netherlands.
- Verduin, B. J. M., Prescott, B. & Thomas, G. J., Jr. (1984) *Biochemistry* 23, 4301-4308.
- Vriend, G. (1983) Ph.D. Thesis, Agricultural University Wageningen, The Netherlands.
- Vriend, G., Hemminga, M. A., Verduin, B. J. M., de Wit, J. L. & Schaafsma, T. J. (1981) *FEBS Lett.* 134, 167-171.
- Vriend, G., Verduin, B. J. M. & Hemminga, M. A. (1986) *J. Mol. Biol.* 191, 453-460.
- Vriend, G., Verduin, B. J. M., Hemminga, M. A. & Schaafsma, T. J. (1982) *FEBS Lett.* 145, 49-52.
- Wüthrich, K. (1986) *NMR of Proteins and Nucleic Acids*, Wiley, New York.
- Zimmer, D. (1977) *Cell* 11, 463-482.
- Zuidema, D., Bierhuizen, M. F. A. & Jaspars, E. M. J. (1983) *Virology* 129, 255-260.

CHAPTER 2

CONFORMATIONAL STUDIES ON A PEPTIDE FRAGMENT REPRESENTING THE RNA-BINDING N-TERMINUS OF A VIRAL COAT PROTEIN USING CIRCULAR DICHROISM AND NMR SPECTROSCOPY

Marinette van der Graaf, and Marcus A. Hemminga

ABSTRACT

Conformational studies were performed on a synthetic pentacosapeptide representing the RNA-binding N-terminal region of the coat protein of cowpea chlorotic mottle virus. The effects of ionic strength, addition of (oligo)phosphates, and temperature on the conformation of this highly positively charged peptide containing six arginines and three lysines were studied. CD experiments show that the peptide has 15-18% α -helical and about 80% random coil conformation in the absence of inorganic salt at 25°C, and 20-21% α -helical conformation under the same conditions at 10°C. Addition of inorganic salts results in an increase of α -helix content, up to 42% in the presence of oligophosphate with an average chain length of 18 phosphates, which was used as an RNA-analog. NMR experiments show that the α -helix formation starts in the region between Thr9 and Gln12, and is extended in the direction of the C-terminus. Relaxation measurements show that binding to oligophosphates of increasing length results in reduced internal mobilities of the positively charged side chains of the arginyl and lysyl residues and of the side chain of Thr9 in the α -helical region. The α -helix formation in the N-terminal part of this viral coat protein upon binding of phosphate groups to the positively charged side chains is suggested to play an essential role in RNA-binding.

INTRODUCTION

Cowpea chlorotic mottle virus (CCMV) is a spherical bromovirus, consisting of RNA and 180 identical coat protein units, each 189 residues long (Dasgupta and Kaesberg, 1982). The virus particle can be dissociated and re-

associated *in vitro* (Bancroft and Hiebert, 1967), but after removal of the first 25 N-terminal amino acids by tryptic digestion the protein shows no interaction with the RNA anymore (Vriend et al., 1981). This indicates that this N-terminal arm containing nine positively charged amino acids (six Arg and three Lys; see Fig. 1.3) plays an essential role in RNA binding. On the basis of NMR experiments, Vriend et al. (1982, 1986) have proposed a 'snatch-pull' model for the assembly of CCMV coat protein and RNA. In this model the N-terminal arm has a flexible random-coil conformation before interacting with the RNA. The large flexibility enhances the chance of the positively charged side chains meeting the negatively charged phosphates of the RNA backbone. Upon binding the positive and negative charges neutralize each other, and the N-terminal arm attains an α -helical conformation, thereby pulling the protein core towards the RNA. This 'snatch-pull' model is in agreement with secondary structure predictions suggesting a random-coil conformation for an N-terminus with charged side chains, but an α -helical conformation between residues 10 and 20 for an N-terminus with neutralized charges (Vriend et al., 1986).

Although high-resolution NMR spectra of CCMV coat protein show several sharp resonances originating from the flexible N-terminal arm, only broad unresolved lines are present after immobilization of this region by RNA-binding (Vriend et al., 1981; 1986). The large size of the protein-RNA complex makes it impossible to monitor the conformational change of the N-terminal region of the protein upon RNA-binding by high resolution NMR spectroscopy. Chemical synthesis of the N-terminal pentacosapeptide P25 (Ten Kortenaar et al., 1986) has created the possibility to perform detailed NMR and optical spectroscopic studies on the structure of this N-terminal segment in the absence and presence of nucleotides. Unlike the intact protein, this peptide is stable over a wide range of temperature and ionic strength, which makes it possible to obtain experimental information about the conformation of the N-terminal region under various conditions. A recent two-dimensional NMR study on P25 in 200 mM sodium phosphate at pH 4 has shown that under these conditions P25 alternates among extended and helical structures with the helical region situated between residues 9 and 17 (Chapter 3). The objective of the present study is to determine how ionic strength, addition of (oligo)phosphates, and temperature affects the conformation of the synthetic P25 by using NMR and CD spectroscopy.

MATERIALS AND METHODS

Samples

The N-terminal pentacosapeptide of the coat protein of CCMV was available as the chemically synthesized N^α1-acetyl, C^α25-methylamide P25 (Ten Kortenaar et al., 1986). Sodium chloride, sodium fluoride, and sodium phosphate (NaH₂PO₄·2H₂O) were obtained from Merck. Hexaammonium tetrapolyphosphate (tetraphosphate) and sodium phosphate glass nr. 15 with an average chain length of 18 P (octadecaphosphate) were obtained from Sigma. NMR samples contained 1 mM P25 in various salt solutions made up in 10%(v/v) ²H₂O and 90%(v/v) H₂O, pH 5.0. CD samples contained 0.4 mM P25 in various salt solutions in H₂O, pH 5.0. The volumes of NMR and CD samples were 600 μl and 20 μl, respectively. Protein and phosphate concentrations were checked according to Peterson (1977) and Bartlett (1959), respectively. For CD measurements sodium fluoride was used instead of sodium chloride to obtain a better signal to noise ratio in the far UV.

Circular dichroism experiments

CD spectra were recorded at 10 and 25°C on a Jobin-Yvon Auto-Dichrograph Mark V spectrometer. The CD signal was measured between the wavelengths 190 and 250 nm with 0.1-nm steps. A sample cell of 0.1-mm path length was used. Each spectrum is the result of the average of four scans taken from the same sample minus the average of four scans taken from a reference sample containing an identical salt solution without P25. The secondary structure of the peptide was determined by fitting the CD spectra to two different sets of reference spectra (Saxena and Wetlaufer, 1971; Chen et al., 1972) by a least-squares fitting procedure using spectral points in the 190—250-nm range with 5-nm steps. The spectra were not scaled so that the absolute value of the intensity was also fitted. The basis for the analysis has been described elsewhere (Cantor and Schimmel, 1980).

NMR experiments

NMR spectra were recorded at 10 and 25°C on a Bruker AM600 spectrometer operating at 600 MHz for protons. The carrier frequency was chosen in the middle of the spectrum coinciding with the water resonance. The water signal was suppressed by gated irradiation with a saturation power at 10 dB attenuation of 0.2 Watt during the relaxation delay of 2.5 s. A very broad spectral width (about 20 ppm) was chosen to obtain a flattened

baseline at the position of the resonance peaks. The NMR spectra presented in this article were recorded with 128 scans using 8k data points. Before every experiment, two dummy scans were performed. The NMR data were processed on a VAXstation 2000 using software kindly given by Dr R. Boelens. A line broadening of 1 Hz was applied before zero-filling. The final digital resolution after Fourier transformation was 1.57 Hz/point. All chemical shifts refer to sodium 3-trimethylsilyl-(2,2,3,3- $^2\text{H}_4$) propionate, and were determined by taking the resonance of the N-terminal acetyl group as an internal standard at 2.08 ppm.

For the longitudinal relaxation time (T_1) experiments an inversion/recovery pulse scheme 180° - τ - 90° with systematically increasing τ (in the range 3.3 μs - 1 s) was used. For every value of τ , two dummy scans and 32 scans of 4k data points were recorded. The data were processed on a SUN 4/60 using the NMR software of New Methods Research, Inc. (version 3.97). T_1 values were determined by a least-squares fitting procedure after baseline correction, exponential multiplication with a line broadening of 1 Hz, zero-filling, Fourier transformation, phase correction, and baseline flattening with a fourth order polynomial (Pearson, 1977).

RESULTS

Conformation of P25

Table 2.1 shows percentages of three different conformations present in P25, which were obtained from CD spectra of P25 recorded under various conditions. The two different sets of reference spectra (Saxena and Wetlaufer, 1971; Chen et al., 1972) used in the analysis resulted in very similar values confirming each other. However, since the helical regions in P25 are very small, the values presented must be considered to give only relative information (Chen et al., 1974). CD spectra of 0.4 mM P25 in the absence of inorganic salt show 15-18% α -helix content at 25°C, and 20-21% α -helix content at 10°C (see Table 2.1). At both temperatures very little β -structure is observed. Figure 2.1 shows proton NMR spectra of 1 mM P25 under the same conditions. The resonances of the water-exchangeable protons (6-9 ppm) show more intensity at 10°C than at 25°C as a result of a reduced exchange rate with the bulk water at lower temperature (Englander et al., 1972). In the aliphatic region (0-5 ppm) of the spectrum recorded at 10°C one of the βCH -resonances of Gln12 and the γCH_3 -resonance of Thr9 are indicated by

arrows at 2.16 and 1.27 ppm, respectively. Both resonances clearly shift to lower field going from 25 to 10°C. These resonances were assigned according to a complete resonance assignment obtained by a two-dimensional NMR study on P25 in 200 mM sodium phosphate pH 4 at 10°C (see Chapter 3).

Table 2.1 Conformation of P25 in the presence of various inorganic salts as determined by CD measurements

Presence of inorganic salt	Conformation of P25					
	α -helix		β -structure		remainder	
	%					
no salt ^a	18.3	15.3	0.0	9.9	83.2	74.6
no salt	21.0	20.1	0.0	2.3	80.6	77.9
50 mM P	23.6	21.5	0.0	7.7	77.5	70.2
50 mM P (as P ₄)	35.4	35.9	0.0	0.0	65.1	64.5
50 mM P (as P ₁₈)	40.6	41.6	0.0	0.0	59.4	58.5
200 mM NaF	26.2	25.5	0.0	3.2	74.9	71.3
200 mM P	29.9	29.4	0.0	4.0	70.3	65.5

The CD spectra of P25 in the presence of various inorganic salts were recorded at 10°C or 25°C. For the rows 3-5 the total phosphorus concentration was 50 mM, present as monophosphate (P), tetraphosphate (P₄), or octadecaphosphate (P₁₈). In every column two values are given; the first value was determined by using the set of reference spectra of Saxena and Wetlauber (1971), and the second by using those of Chen et al. (1972).

Effect of addition of inorganic salt

Table 2.1 shows that an increase of ionic strength by addition of 200 mM sodium fluoride or 200 mM sodium phosphate induces more α -helical conformation in P25. At pH 5, the average charge of each phosphate is approximately -1 (Chang, 1981), which is comparable to the charge of a fluoride (or chloride) anion. However, Table 2.1 shows somewhat more α -helical conformation for P25 in 200 mM sodium phosphate (29-30%) than for P25 in 200 mM sodium fluoride (~26%).

Figure 2.2 shows the effects of addition of 200 mM sodium chloride (2.2B) and 200 mM sodium phosphate (2.2C) on the low-field region of the proton NMR spectrum of P25. After addition of 200 mM inorganic salt, the

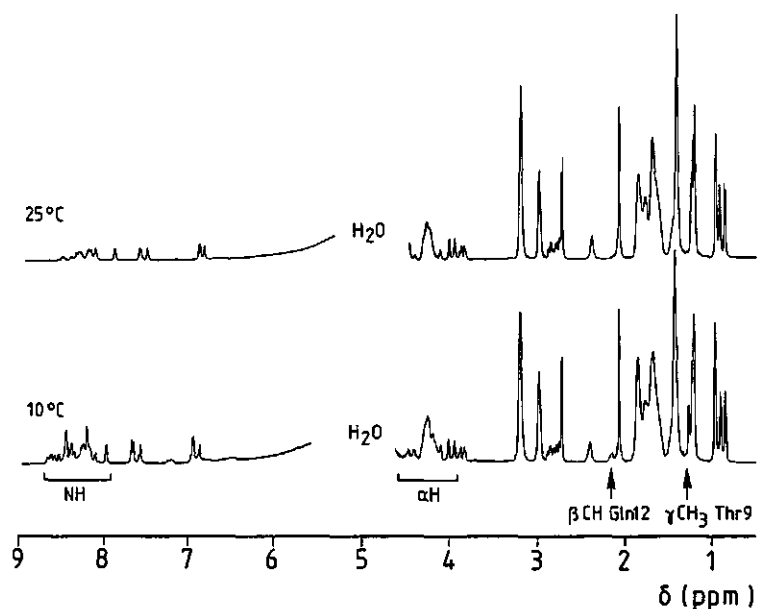


Fig. 2.1 600 MHz proton NMR spectra of P25 in water adjusted to pH 5, recorded at 25 and 10°C. The arrows indicate one of the β CH-resonances of Gln12 at 2.16 ppm and the γ CH₃-resonance of Thr9 at 1.27 ppm in the spectrum recorded at 10°C. 'NH' and ' α H' indicate the positions of the backbone NH-resonances and α H-resonances, respectively.

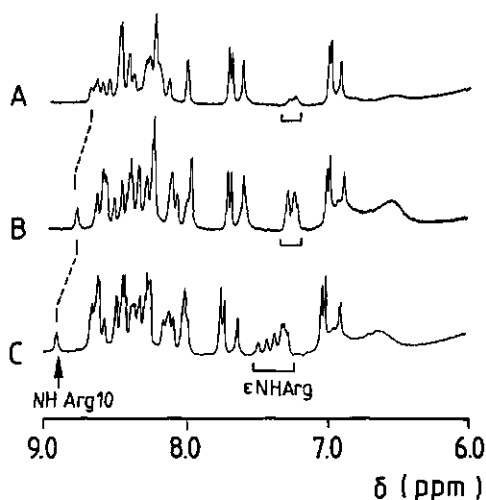


Fig. 2.2 Low field regions (6 - 9 ppm) of 600 MHz proton NMR spectra of 1 mM P25 in (A) water adjusted to pH 5 (B) 200 mM sodium chloride, pH 5 and (C) 200 mM sodium phosphate, pH 5. The positions of the ϵ NH-resonance of the arginyl residues and of the backbone NH-resonance of Arg10 are indicated. All spectra were recorded at 10°C.

intensities of a number of resonances increase, particularly of the resonances assigned to the arginyl ϵ NH (7.1-7.5 ppm) and guanidium protons (broad resonances around 6.7 and 7.0 ppm). This increase in intensity can be explained by a reduction of the exchange rate of these protons with the bulk water. The positions of the ϵ N-protons of the arginines do not change after the addition of 200 mM sodium chloride, but these resonances shift to lower field after the addition of 200 mM sodium phosphate. The largest down-field shift is observed for Arg10, followed by Arg14, Arg18, Arg22, Arg25 and Arg13. These resonances could be assigned according to a two-dimensional NMR study on P25 in 200 mM sodium phosphate (Chapter 3).

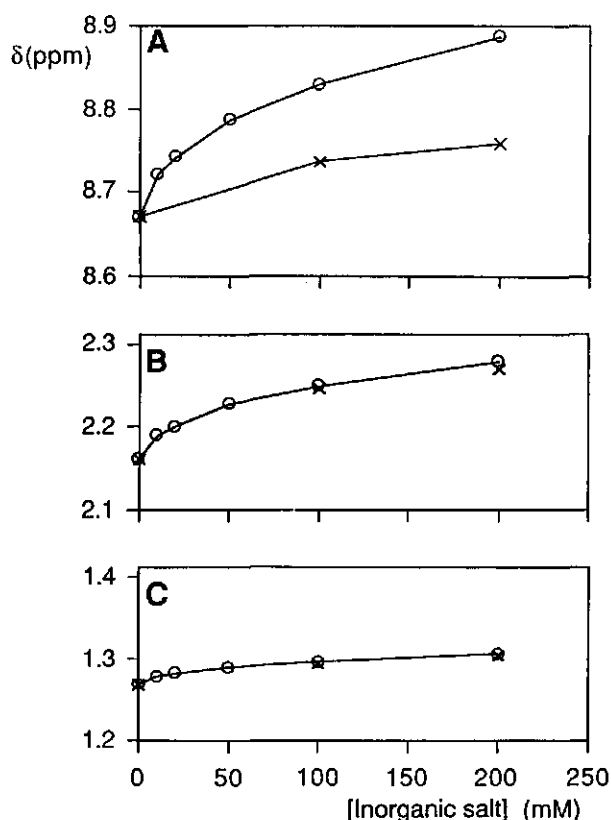


Fig. 2.3 Chemical shift values (± 0.01 ppm) of the resonances of (A) γCH_3 of Thr9, (B) βCH of Gln12, and (C) backbone NH of Arg10 as a function of the concentration of sodium chloride (X) and sodium phosphate (O). All chemical shifts were obtained from 600 MHz proton NMR spectra of P25 recorded at 10°C.

Also several backbone NH-resonances (8-9 ppm) shift after addition of inorganic salt. Particularly the backbone amide proton of Arg10 shows a clear shift to low field, which is indicated in the Figures 2.2 and 2.3A. Again, sodium chloride shows a smaller effect than sodium phosphate. In the aliphatic region of the spectra (not shown) some α H-resonances shift after addition of inorganic salt, but these resonances could not be followed due to overlapping peaks. In addition, one of the β CH-resonances of Gln12 and the γ CH₃-resonance of Thr9 show shifts to lower field (Figures 2.3B and C).

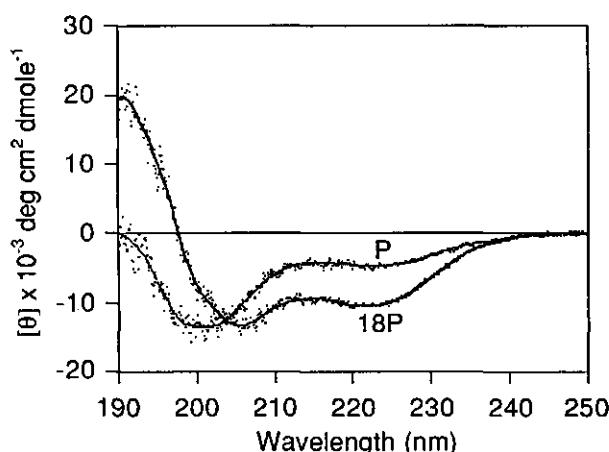


Fig. 2.4 CD spectra of 0.4 mM P25 in 50 mM phosphate, present as sodium monophosphate (P) or sodium octadecaphosphate (P₁₈). Both spectra were recorded at 10°C. The percentages α -helix, β -structure and remainder are given in Table 2.1.

Effect of oligophosphate length

CD and NMR experiments were performed on samples containing P25 in 50 mM sodium monophosphate, 50/4 mM ammonium tetrphosphate, or 50/18 mM sodium octadecaphosphate in order to study the effect of oligophosphate length on the conformation of P25. In all samples the phosphorus concentration was 50 mM, but the length of the phosphate present varied. Figure 2.4 shows that the CD spectra of P25 in monophosphate and in octadecaphosphate are clearly different. As presented in Table 2.1, P25 attains more α -helical conformation with increasing phosphate length: from 22-23% α -helix conformation for monophosphate to 41-42% α -helix conformation for octadecaphosphate. Figure 2.5 presents

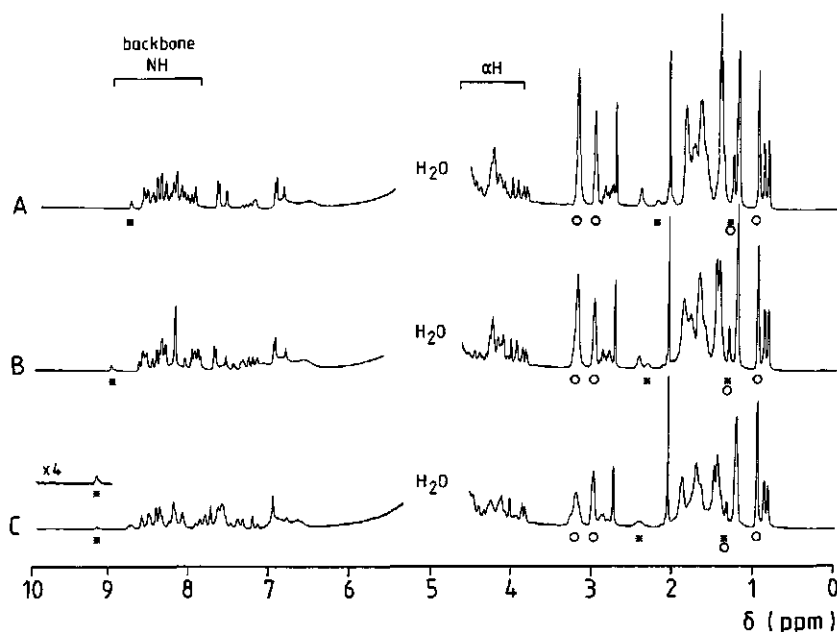


Fig. 2.5 600 MHz proton NMR spectra of 1 mM P25 in 50 mM phosphate, present as (A) sodium monophosphate, (B) ammonium tetraphosphate, and (C) sodium octadecaphosphate. All spectra were recorded at 10°C, pH 5.0. The spectral regions containing the resonances of backbone amide protons and α -protons are indicated. The chemical shifts of the resonances labelled with asterisks (NH Arg10, β CH Gln12, and γ CH₃ Thr9) are presented in Table 2.2. For the resonances labelled with open circles (δ CH₂ of Arg at ~ 3.2 ppm, ϵ CH₂ of Lys at ~ 3.0 ppm, γ CH₃ of Thr9 at ~ 1.3 ppm, and $(\gamma$ CH₃)₂ of Val3 at ~ 0.96 ppm) T₁ values are presented in Table 2.3.

proton NMR spectra of P25 in the presence of the various phosphates mentioned. This figure shows that several resonances become broadened or shift upon addition of oligophosphates, especially in the case of octadecaphosphate (Figure 2.5C). A two-dimensional proton NMR study on P25 in 10 mM octadecaphosphate, pH 5.0, has shown that the resonances corresponding to residues 6-25 of P25 show some broadening (unpublished results). This region of the peptide contains all positively charged residues which interact with the negatively charged phosphates. Although Figure 2.5 shows that several resonances shift, only a few can be followed without problems due to overlap in the one-dimensional spectra. Table 2.2 presents

the chemical shifts of the backbone NH-resonance of Arg10, one of the β CH-resonances of Gln12 and the γ CH₃-resonance of Thr9 (labelled with asterisks in Figure 2.5) under various conditions. All these resonances shift to lower field with increasing length of the phosphate present.

Table 2.2 Chemical shifts of proton resonances of P25 in the presence of phosphates of various lengths at 10 and 25°C

Phosphate present	Temperature °C	Chemical shift of		
		NH Arg10 ppm	β CH Gln12	γ CH ₃ Thr9
P	10	8.79	2.23	1.29
P ₄	10	9.02	2.34	1.33
P ₁₈	10	9.20	2.44 ^a	1.35
P	25	8.55	2.13 ^a	1.26
P ₄	25	8.79	2.25	1.30
P ₁₈	25	9.03	2.33	1.34

The chemical shifts (± 0.01 ppm) were measured relative to sodium 3-trimethylsilyl-(2,2,3,3-²H₄) propionate. The phosphorus concentration was 50 mM in all cases, present as monophosphate (P), tetraphosphate (P₄), or octadecaphosphate (P₁₈). ^a Accuracy ± 0.05 ppm due to overlap with other resonances.

Table 2.3 presents the longitudinal relaxation times T_1 measured at 10 and 25°C for the side-chain proton resonances of arginyl δ CH₂ at 3.2 ppm, lysyl ϵ CH₂ at 3.0 ppm, γ CH₃ of Thr9 at ~ 1.3 ppm and (γ CH₃)₂ of Val3 at 0.96 ppm (labelled with open circles in Figure 2.5). A single exponential decay was observed for each resonance. The values obtained for the arginyl δ CH₂-resonance at 3.2 ppm and the lysyl ϵ CH₂-resonance at 3.0 ppm should be considered to be average T_1 values, because these resonances correspond to six arginyl and three lysyl residues, respectively. In Figure 2.5C the arginyl δ CH₂-peak at 3.2 ppm shows a low-field shoulder indicating that some of the arginyl resonances shift to lower field as result of the presence of octadecaphosphate. Since the average T_1 value was measured at 3.2 ppm, the resonances most strongly affected by the presence of octadecaphosphate are less strongly weighted in the T_1 value obtained. Therefore, the T_1 value for

the arginyl δCH_2 -resonance in the presence of octadecaphosphate is less accurate.

The longitudinal relaxation times T_1 give information about the internal mobility of the corresponding side chains in the presence of phosphates of various lengths. The four side-chain resonances mentioned were chosen for the following reasons. The $(\gamma\text{CH}_3)_2$ resonance of Val3 is considered to be a reference, because the methyl groups of this valyl residue are not expected to bind to phosphate groups and are not involved in α -helix formation according to a two-dimensional NMR study on P25 in 200 mM sodium phosphate at pH 4 (Chapter 3). However, the δ -protons of the arginyl residues, the ϵ -protons of the lysyl residues, and the methyl group of Thr 9 may be affected by the length of the phosphate present. The arginyl δ -protons and the lysyl ϵ -protons are in close proximity of positively charged groups, which are expected to interact with the negatively charged phosphates, and the γCH_3 resonance of Thr9 shifts down field with increasing length of the phosphate present (see Table 2.2). Table 2.3 shows that the T_1 values of the last three resonances mentioned decrease with increasing phosphate length.

Table 2.3 Longitudinal relaxation times of proton resonances of P25 in the absence and presence of phosphates of various lengths at 10 and 25°C

Inorganic salt	Temp. °C	Longitudinal relaxation time of the ^1H resonance of			
		$(\gamma\text{CH}_3)_2$ Val3	δCH_2 Arg	ϵCH_2 Lys	γCH_3 Thr9
		s			
no salt	10	0.44 ± 0.02	0.40 ± 0.01	0.51 ± 0.02	0.42 ± 0.02
P	10	0.43 ± 0.02	0.40 ± 0.01	0.46 ± 0.02	0.41 ± 0.01
P ₄	10	0.44 ± 0.02	0.38 ± 0.01	0.36 ± 0.01	0.38 ± 0.01
P ₁₈	10	0.43 ± 0.02	0.28 ± 0.01	0.33 ± 0.01	0.27 ± 0.01
no salt	25	0.50 ± 0.02	0.43 ± 0.02	0.63 ± 0.02	n.d.
P	25	0.49 ± 0.02	0.43 ± 0.02	0.57 ± 0.02	n.d.
P ₄	25	0.49 ± 0.02	0.41 ± 0.01	0.41 ± 0.01	0.49 ± 0.02
P ₁₈	25	0.49 ± 0.02	0.38 ± 0.01	0.43 ± 0.02	0.40 ± 0.01

Longitudinal relaxation times (T_1) of several proton resonances of P25 are given as $T_1 \pm \text{SD}$. The total phosphorus concentration was 50 mM, present as monophosphate (P), tetraphosphate (P₄), or octadecaphosphate (P₁₈). n.d. = not determined due to overlap problems.

DISCUSSION

In the study presented here the effects of ionic strength, addition of (oligo)phosphates, and temperature on the conformation of P25 were studied by CD and NMR spectroscopy. Although *in vivo* the interaction between CCMV coat protein and RNA is expected to be highly specific, *in vitro* reassembly experiments showed no specificity for RNA encapsidation. CCMV coat protein can encapsidate not only CCMV-RNA, but also other RNA molecules, or even polyanions like polyvinyl sulphate or sodium dextran sulphate (Verduin, 1978). The advantage of the oligophosphates used here as compared to oligonucleotides is that they do not disturb the CD spectrum of the peptide and do not give rise to additional resonances in the NMR spectrum. Although the geometries of oligonucleotides and oligophosphates differ, the distance between two sequential phosphorus atoms in A-RNA (0.59 nm) is only slightly larger than the distance between P_i and P_{i+2} in an extended oligophosphate chain (~ 0.51 nm, (Kielman and Leyte, 1974)).

The results of the CD experiments presented in Table 2.1 show that α -helical conformation is favoured by lowering the temperature and addition of inorganic salts, especially addition of relatively long oligophosphates. Also the proton NMR spectra of P25 recorded under various conditions show effects of changes in secondary structure. A clear correlation is found between the amount of α -helical conformation as determined by CD experiments (Table 2.1) and the down-field shifts of the resonances of the γ -protons of Thr9, one β -proton of Gln12, and the backbone amide proton of Arg10 (Figure 2.3 and Table 2.2). A down-field shift of a proton resonance indicates a small distance between the corresponding proton and an oxygen atom, e.g. in a hydrogen bond (Wagner et al., 1983). Although the γ -protons of Thr9 and the β -proton of Gln12 cannot form hydrogen bonds themselves, the side chains of both these residues contain groups which are able to act as hydrogen bond donor or acceptor. Hydrogen bond formation by these groups may play a role in helix formation in this region.

Table 2.3 shows the results of T_1 measurements giving information about the internal mobility of various types of side chains of P25 in the presence of various oligophosphates. The side chains of P25 are expected to become less mobile going from 25 to 10°C, and all T_1 values in Table 2.3 decrease going from 25 to 10°C. Therefore, a decrease of T_1 value can be correlated with a decrease of internal mobility. This effect and the values measured indicate that the groups involved have correlation times around

10⁻¹⁰ s, in agreement with the mobility observed for long amino acid side chains (Creighton, 1983). Table 2.3 shows that the presence of oligophosphates of increasing length results in decreasing T₁ values for the resonances of γ CH₃ of Thr9, arginyl δ CH₂, and lysyl ϵ CH₂. Thus, the mobility of these side chains decreases with increasing oligophosphate length.

The effects of temperature, presence of inorganic salt, and the length of oligophosphates on the conformation of P25 will be discussed in more detail below. A decrease of temperature results in an increase of α -helical conformation in P25 (see Tables 2.1-2.2 and Figure 2.1). The same phenomenon has been reported for the C-peptide (residue 1-13) and S-peptide (residue 1-20) of RNase A, which show significant α -helix formation in aqueous solution near 0°C (Brown and Klee, 1971; Bierzynski et al., 1982; Kim and Baldwin, 1984). This phenomenon can be explained by the fact that at low temperature hydrophobic interactions stabilizing the helical conformation are stronger than at high temperature (Creighton, 1983).

The addition of inorganic salt results in an increase of α -helical conformation in P25 (see Table 2.1 and Figures 2.2 and 2.3). Shielding of the positive charges by anions reduces the destabilizing mutual Coulombic interactions between the positively charged lysyl and arginyl side chains, which are all present along one side of the amphipathic helix (Vriend et al., 1986). Phosphate induces more helical conformation than fluoride or chloride. This phenomenon can be explained by the fact that phosphate has the possibility to participate in hydrogen bond formation. Especially the down-field shifts of several ϵ NH resonances of the arginyl residues after addition of phosphates (see Figure 2.2) can be explained by hydrogen bond formation (Wagner et al., 1983). The largest down-field shift has been observed for the ϵ NH resonance of Arg10, followed by those of Arg14, Arg18, Arg22, Arg25, and Arg13. This sequence shows that phosphate binds most strongly to Arg10 at the N-terminus of the region 10-17, which has the ability to adopt an α -helical conformation in 200 mM sodium phosphate (Chapter 3). Arg10 can bind more strongly to the negatively charged phosphate group than the other arginyl residues, because it has a larger positive charge as result of the helix dipole (Hol, 1985). However, according to this effect the ϵ NH resonance of Arg 13 should be situated between those of Arg10 and Arg14, which is not the case. A possible explanation for this exception is given below. The phosphate group may act as a 'bridge' by forming hydrogen bonds to arginyl side chains of residues *i* and *i*+4 thereby stabilizing an α -helical conformation. The phosphate group probably cannot bind simultaneously to the side chain of

Arg13 and another positively charged side chain because of an unfavourable orientation of the side chain of Arg13.

The presence of (oligo)phosphates of increasing length results in an increasing amount of α -helical conformation in P25 (Tables 2.1 and 2.2, Figures 2.4 and 2.5). Since longer oligophosphates have more negatively charged groups per molecule, they bind more strongly to the positively charged side chains of the peptide. This is in agreement with the T_1 values presented in Table 2.3 showing a reduction of the internal mobilities of the arginyl and lysyl side chains upon increasing chain length of the oligophosphate present. The T_1 value of the γCH_3 -resonance of Thr9 shows the same effect indicating that also this side chain has less mobility in the presence of long oligophosphates as result of a more stable α -helical conformation. Since oligophosphates have an extended chain conformation in solution (Wunderlich, 1973; Kielman, 1974), optimal binding will occur if P25 attains a conformation with most positively charged side chains pointing in one direction. An amphipathic helix has these properties and will be stabilized by binding of P25 to an oligophosphate.

Figures 2.1-2.3 and Table 2.1 show that the down-field shifts of the characteristic resonances of Thr9, Arg10, and Gln12 occur even at relatively low percentages of α -helical conformation. This indicates that α -helix formation starts in this region, which is in agreement with the results of a two-dimensional NMR study on P25 in 200 mM sodium phosphate at pH 4 (Chapter 3). This study has shown that under these conditions region 9-17, especially the region close to Arg10, has a tendency to adopt an α -helical conformation.

The present results enable an extension of the 'snatch-pull' model (Vriend et al., 1982; 1986) to a more detailed model for the assembly of CCMV coat protein and RNA. Down-field shifts of the characteristic resonances of Thr9 and Gln12 already occur in the absence of phosphates. Therefore, hydrogen bond formation by these side chains, probably between each other, is suggested to initiate α -helix formation in this region. After this initiation, the helix will be extended upon binding of negatively charged phosphate groups to the positively charged side chains. The results show that the phosphate groups bind most strongly to the side chains of the arginyl residues near the N-terminus of the helical region, especially to Arg10. The neutralization of the positive charge at this position by phosphate binding extends the helix in the direction of the C-terminus, because the unfavourable interaction between the positive charge of the arginyl side chain and the macrodipole of the helix has

been removed (Hol, 1985; Shoemaker et al., 1985; 1987). The extension of the helical region results in a proper orientation of the next positively charged side chains for binding to the next phosphate groups of the RNA backbone. In this way, the RNA itself induces the conformation of the protein which is necessary for binding.

ACKNOWLEDGEMENTS

We thank C.J.A.M. Wolfs for performing analyses on the samples and for expert assistance in measuring and analysing the CD spectra, Dr J. Krüse for doing some preliminary experiments, and C.C. van der Linden and Dr W. Norde for stimulating discussions. We thank Professor T.J. Schaafsma for carefully reading the manuscript. We are especially indebted to the SON HF-NMR facility Nijmegen (the Netherlands), where all NMR experiments were carried out.

REFERENCES

- Bancroft, J. B. & Hiebert, E. (1967) *Virology* 32, 354-356.
- Bartlett, G. R. (1959) *J. Biol. Chem.* 234, 466-468.
- Bierzynski, A., Kim, P. S. & Baldwin, R. L. (1982) *Proc. Natl. Acad. Sci. U.S.A.* 79, 2470-2474.
- Brown, J. E. & Klee, W. A. (1971) *Biochemistry* 10, 470-476.
- Cantor, C. R. & Schimmel, P. R. (1980) *Biophysical Chemistry*, W.H. Freeman, San Francisco.
- Chang, R. (1981) *Physical Chemistry with Applications to Biological Systems*, 2nd edn, p. 323, Macmillan Publishin Co., Inc., New York.
- Chen, Y. H., Yang, J. T. & Martinez, H. M. (1972) *Biochemistry* 11, 4120-4131.
- Chen, Y. H., Yang, J. T. & Chau, K. H. (1974) *Biochemistry* 13, 3350-3359.
- Creighton, T. E. (1983) *Proteins, Structure and Molecular Properties*, W. H. Freeman and Company, New York.
- Dasgupta, R. & Kaesberg, P. (1982) *Nucleic Acids Res.* 10, 703-713.
- Englander, S. W., Downer, N. W. & Teitelbaum, H. (1972) *Annu. Rev. Biochem.* 41, 903-924.
- Hol, W. G. J. (1985) *Prog. Biophys. Molec. Biol.* 45, 149-195.
- Kielman, H. S. & Leyte, J. C. (1974) in *Proceedings of the 18th Ampere Congress on Magnetic Resonance and Related Phenomena* (Allen, P. S., Andrew, E. R. & Bates, C. A., eds) vol. 2, pp. 515-516, Nottingham Ampere Committee, Physics Department of the University of Nottingham, Nottingham.

- Kim, P. S. & Baldwin, R. L. (1984) *Nature* 307, 329-334.
- Pearson, G. A. (1977) *J. Magn. Reson.* 27, 265-272.
- Peterson, G. L. (1977) *Anal. Biochem.* 83, 346-356.
- Saxena, V. P. & Wetlaufer, D. B. (1971) *Proc. Natl. Acad. Sci. USA* 68, 969-972.
- Shoemaker, K. R., Kim, P. S., Brems, D. N., Marqusee, S., York, E. J., Chaiken, I. M., Stewart, J. M. & Baldwin, R. L. (1985) *Proc. Natl. Acad. Sci. USA* 82, 2349-2353.
- Shoemaker, K. R., Kim, P. S., York, E. J., Stewart, J. M. & Baldwin, R. L. (1987) *Nature* 326, 563-567.
- Ten Kortenaar, P. B. W., Krüse, J., Hemminga, M. A. & Tesser, G. I. (1986) *Int. J. Pept. Protein Res.* 27, 401-413.
- Verduin, B. J. M. (1978) Ph. D. Thesis, Agricultural University Wageningen, The Netherlands.
- Vriend, G., Hemminga, M. A., Verduin, B. J. M., de Wit, J. L. & Schaafsma, T. J. (1981) *FEBS Lett.* 134, 167-171.
- Vriend, G., Verduin, B. J. M., Hemminga, M. A. & Schaafsma, T. J. (1982) *FEBS Lett.* 145, 49-52.
- Vriend, G., Verduin, B. J. M. & Hemminga, M. A. (1986) *J. Mol. Biol.* 191, 453-460.
- Wagner, G., Pardi, A. & Wüthrich, K. (1983) *J. Am. Chem. Soc.* 105, 5948-5949.
- Wunderlich, B. (1973) *Macromolecular Physics I. Crystal Structure, Morphology, Defects*, pp. 74-76, Academic Press, Inc., New York.

CHAPTER 3

SOLUTION CONFORMATION OF A PEPTIDE FRAGMENT REPRESENTING A PROPOSED RNA-BINDING SITE OF A VIRAL COAT PROTEIN STUDIED BY TWO-DIMENSIONAL NMR

Marinette van der Graaf, Carlo P.M. van Mierlo, and Marcus A. Hemminga

ABSTRACT

The first 25 amino acids of the coat protein of cowpea chlorotic mottle virus are essential for binding the encapsidated RNA. Although an α -helical conformation has been predicted for this highly positively charged N-terminal region (Argos, 1981; Vriend et al., 1986), no experimental evidence for this conformation has been presented so far. In this study two-dimensional proton NMR experiments were performed on a chemically synthesized pentacosapeptide containing the first 25 amino acids of this coat protein (Ten Kortenaar et al., 1986). All resonances could be assigned by a combined use of two-dimensional correlated spectroscopy and nuclear Overhauser enhancement spectroscopy carried out at four different temperatures. Various NMR parameters indicate the presence of a conformational ensemble consisting of helical structures rapidly interconverting to more extended states. Differences in chemical shifts and nuclear Overhauser effects indicate that lowering the temperature induces a shift of the dynamic equilibrium towards the helical structures. At 10°C a perceptible fraction of the conformational ensemble consists of structures with an α -helical conformation between residues 9 and 17, likely starting with a turn-like structure around Thr9 and Arg10. Both the conformation and the position of this helical region agree well with the secondary structure predictions mentioned above.

INTRODUCTION

Cowpea chlorotic mottle virus (CCMV) is a spherical plant virus of the group of bromoviruses. It consists of RNA in an icosahedron composed of 180 identical protein subunits, each 189 residues long (Dasgupta and Kaesberg,

1982). CCMV virions undergo structural changes as a function of pH, ionic strength and temperature (Kaper, 1975). The virus particle is stable around pH 5.0, but it can be dissociated into protein dimers and RNA by raising the pH to 7.5 at high ionic strength ($\mu > 0.3$) (Bancroft and Hiebert, 1967). Both RNA and protein can be isolated and reassembled *in vitro* (Bancroft and Hiebert, 1967). In the absence of RNA, the protein subunits reassociate into empty protein capsids by lowering the pH to 5.0 (Bancroft et al., 1968). These empty protein capsids have structures similar to the native virions with a T=3 icosahedral symmetry (Finch and Bancroft, 1968). The phenomena described above suggest that CCMV virus particles are stabilized by protein-RNA interactions and pH dependent protein-protein interactions.

NMR studies on empty capsids have revealed an increased mobility of the highly basic N-terminal parts of the protein subunits. This mobility is absent upon binding of RNA - as in intact virions - as well as after removal of the first 25 N-terminal amino acids by tryptic digestion (Vriend et al., 1981). Proteins lacking the N-terminal pentacosapeptide do not bind RNA. This indicates that the first 25 amino acid residues (Fig. 1.3) play an essential role in the interaction with RNA. It has been suggested that interactions between the positively charged amino acids in this part of the protein (six Arg and three Lys) and the negatively charged phosphate groups in the RNA are responsible for the protein-RNA binding (Argos, 1981; Vriend et al., 1981; 1986). This suggestion is supported by studies on brome mosaic virus (BMV), a virus closely related to CCMV. For both CCMV and BMV, the positively charged amino acids are situated in the region 7-25 within the significantly conserved first 25 amino acid residues. Sgro et al. (1986) introduced RNA-protein cross-links into brome mosaic virus by a photoreactive cross-linker with a relatively short 0.7-nm span. It was found that within the N-terminal region only the residues 11-19 are involved in cross-linking with RNA. Sacher and Ahlquist (1989) investigated the effect of deletions in the N-terminal region of BMV coat protein on RNA packaging and systemic infection. From their experiments it can be concluded that the RNA binding region is situated somewhere in the region 8-25, which contains all but one of the positively charged amino acids.

It has been predicted that an α -helical conformation exists for the region 8-18 of BMV coat protein (Argos, 1981), and that neutralization of the positively charged arginyl and lysyl side chains initiates α -helix formation in the region 10-20 of CCMV coat protein (Vriend et al., 1986). So far, no experimental evidence for these secondary structure predictions has been

presented. Laser Raman studies on CCMV have shown differences in protein structure in the presence and the absence of RNA, but no conclusions have been drawn about the nature of the secondary structure of the N-terminus (Verduin et al., 1984). High-resolution X-ray crystallographic structures have been obtained for a number of spherical RNA viruses: tomato bushy stunt virus (Harrison et al., 1978), southern bean mosaic virus (Abad-Zapatero et al., 1980), satellite tobacco necrosis virus (Liljas et al., 1982), human common cold virus (Rossmann et al., 1985), turnip crinkle virus (Hogle et al., 1986), and black beetle virus (Hosur et al., 1987). In all structures the N-terminal basic arms could not, or only partly, be observed due to a lack of crystallographic symmetry. Therefore, it seems unlikely that the secondary structure of the N-terminal arm of CCMV can be obtained by X-ray diffraction techniques. High-resolution NMR experiments have provided some information about the behaviour of the N-terminal arm of CCMV coat protein (Vriend et al., 1981; 1986). However, the lines in the NMR spectra are strongly broadened due to the size of the intact virus particles or protein-nucleotide complexes, which makes it extremely difficult to investigate the secondary structure of the N-terminus in these systems by NMR.

Chemical synthesis of the N-terminal pentacosapeptide P25 (Ten Kortenaar et al., 1986) has created the possibility to perform detailed NMR and optical spectroscopic studies on the structure of this N-terminal segment in the absence and the presence of nucleotides. It has been shown that the ^1H NMR spectrum of P25 closely resembles the ^1H NMR difference spectrum of intact coat protein and coat protein lacking the N-terminal region (Hemminga et al., 1985). Therefore, we have used P25 as a model for the N-terminal part of CCMV coat protein.

The objective of the study reported here is the determination of the secondary structure of the synthetic N-terminus P25 in aqueous solution by 2D proton NMR. The experiments indicate the presence of a conformational ensemble consisting of helical structures rapidly interconverting to more extended conformational states. It will be shown that the predominantly helical region is situated between residue 9 and 17, which agrees well with the secondary structure predictions by Argos (1981) and Vriend et al. (1986).

MATERIALS AND METHODS

The N-terminal pentacosapeptide of the coat protein of CCMV was available as the chemically synthesized N α 1-acetyl, C α 25-methylamide P25 (Ten Kortenaar et al., 1986). Samples for 2D NMR measurements contained 6 to 8.5 mM P25 and 200 mM sodium phosphate in a mixture of 10%(v/v) $^2\text{H}_2\text{O}$ and 90%(v/v) H_2O , pH 4.0. This low pH value was chosen to be close to the pH minimum for the rate of chemical exchange of labile protons from amide and guanidium groups of the peptide with the bulk water (Wüthrich and Wagner, 1979). Sodium 3-trimethylsilyl-(2,2,3,3- $^2\text{H}_4$) propionate was used as an internal standard.

All 2D NMR spectra were recorded on a Bruker AM600 spectrometer operating at 600 MHz for protons, interfaced with an Aspect 3000 computer. The carrier frequency was chosen in the middle of the spectrum coinciding with the water resonance. The water signal was suppressed by gated irradiation or in the case of some of the NOESY spectra by using a $(90^\circ)_\phi - \tau - (90^\circ)_{-\phi}$ jump-return read pulse (Plateau and Guéron, 1982) with $\tau = 80 \mu\text{s}$. All spectra were acquired in the phase-sensitive mode using Time Proportional Phase Increments (TPPI) (Marion and Wüthrich, 1983). Spectral widths were generally about 20 ppm in the ω_2 -dimension and 10 ppm in the ω_1 -dimension. The spectral width in the ω_2 -dimension was doubled to obtain a more flattened baseline at the position of the resonance peaks. After the first Fourier transformation the range of the spectrum containing the resonance peaks was selected and further processed. Spectra were generally recorded with 2048 or 4096 data points and 512 t_1 -increments. The number of scans per t_1 -increment varied between 24 and 48.

The double quantum filtered COSY spectrum (Rance et al., 1983) shown in this article was recorded with a spectral width of approximately 10 ppm in the ω_2 -dimension and 8192 data points to obtain the best possible digital resolution. The number of t_1 -increments was 700. The relaxation delay period was randomly varied between 2.88 and 3.12 s to avoid the appearance of double quantum cross peaks. The spectrum was recorded at 10°C, since at this temperature the cross peaks in the fingerprint region ($\omega_1 = 3.9 - 4.9$ ppm, $\omega_2 = 7.9 - 8.9$ ppm) show minimal overlap.

2D Homonuclear Hartmann Hahn (HoHaHa) spectra were recorded at 2, 5, 10 and 25°C with an 80-ms MLEV17 mixing scheme (Bax and Davis, 1985). The MLEV17 cycle was preceded and followed by 2.5-ms trim pulses to defocus magnetization not parallel to the spin-lock axis. The relaxation

delay was 2.5 s.

NOESY spectra (Jeener et al., 1979; Macura and Ernst, 1980) were recorded at 2, 5, 10 and 25°C with a mixing time of 200 ms. At 10°C mixing times of 50, 100 and 150 ms were also used. No zero quantum suppression technique was applied. The relaxation delay was 2.5 s.

2D NMR data were processed on a microVAX II or a VAXstation 2000 using software kindly given by Dr R. Boelens. The free induction decays were multiplied by shifted sine-bell window functions in both dimensions. After zero filling and double Fourier transformation baseline corrections with a fourth order polynomial (Pearson, 1977) were performed in both dimensions. Digital resolution in the final transformed spectrum was usually 3.13 or 6.26 Hz/point in the ω_2 -dimension and 6.26 Hz/point in the ω_1 -dimension. The digital resolution of the DQ filtered COSY spectrum was 0.78 Hz/point in the ω_2 -dimension and 1.57 Hz/point in the ω_1 -dimension.

RESULTS

General remarks

The assignments of the ^1H -NMR resonances of P25 (Table 3.1) were obtained using the sequential assignment methodology developed by Wüthrich and co-workers (Billeter et al., 1982; Wagner and Wüthrich, 1982; Wider et al., 1982; Wüthrich et al., 1982; Wüthrich, 1986). During the first stage of this procedure complete spin systems of individual amino acid residues were identified using DQ filtered COSY and HoHaHa spectra. The HoHaHa spectra were very helpful in determining complete spin systems, particularly in correlating amide protons with side-chain protons. The next step was the establishment of connectivities across the peptide bond. Through-space connectivities appearing in NOESY spectra and the known primary sequence (Fig. 1.3) were used to assign a spin system to a particular residue. Finally, additional NOESY information was used to determine any element of secondary structure. Although P25 is a small peptide, the assignment procedure was complicated by the large number of amino acids with long side-chains and the amount of overlapping resonances. It proved to be an essential factor in the entire assignment procedure that spectra were recorded at different temperatures. Degeneracies of proton resonances appearing at one temperature often disappeared at another temperature, because of temperature-induced changes in the conformation.

Table 3.1 ^1H chemical shifts (ppm) of P25 in 200 mM sodium phosphate buffer pH 4.0, 10°C.

Residue	NH	αH	βH	others	
(Ac)				Ac-CH ₃	2.08
Ser1	8.45	4.50	3.91, 3.86		
Thr2	8.41	4.45	4.30	γCH_3	1.21
Val3	8.21	4.14	2.10	γCH_3	0.97, 0.97
Gly4	8.63	4.05			
Thr5	8.22	4.36	4.31	γCH_3	1.23
Gly6	8.59	3.98			
Lys7	8.23	4.32	1.83, 1.75	γCH_2	1.44, 1.39
				δCH_2	1.68, 1.68
				ϵCH_2	3.01, 3.01
				ζNH_3^+	7.61 ^a
Leu8	8.29	4.56	1.67, 1.57	γCH	1.68
				δCH_3	0.89, 0.84
Thr9	8.57	4.39	4.56	γCH_3	1.30
Arg10	8.84	4.05	1.89, 1.89	γCH_2	1.77, 1.63
				δCH_2	3.24, 3.24
				ϵNH	7.38
Ala11	8.52	4.16	1.43		
Gln12	8.10	4.16	2.27, 2.04	γCH_2	2.44, 2.44
				δNH_2	7.60, 6.89
Arg13	8.59	4.12	1.90, 1.90	γCH_2	1.77, 1.63
				δCH_2	3.25, 3.19
				ϵNH	7.23
Arg14	8.33	4.18	1.89, 1.89	γCH_2	1.78, 1.64
				δCH_2	3.22, 3.22
				ϵNH	7.35
Ala15	8.08	4.19	1.47		
Ala16	8.06	4.20	1.45		
Ala17	7.96	4.26	1.47		
Arg18	7.99	4.25	1.91, 1.85	γCH_2	1.76, 1.67
				δCH_2	3.23, 3.23
				ϵNH	7.32
Lys19	8.12	4.25	1.87, 1.82	γCH_2	1.51, 1.43
				δCH_2	1.71, 1.71
				ϵCH_2	3.01, 3.01
				ζNH_3^+	7.61 ^a
Asn20	8.34	4.69	2.87, 2.80	γNH_2	7.70, 7.01
Lys21	8.29	4.30	1.88, 1.80	γCH_2	1.47, 1.44
				δCH_2	1.70, 1.70
				ϵCH_2	3.02, 3.02
				ζNH_3^+	7.61 ^a
Arg22	8.41	4.31	1.88, 1.81	γCH_2	1.68, 1.63
				δCH_2	3.22, 3.22
				ϵNH	7.28
Asn23	8.58	4.80	2.90, 2.82	γNH_2	7.72, 6.99
Thr24	8.25	4.34	4.27	γCH_3	1.21
Arg25	8.39	4.28	1.87, 1.79	γCH_2	1.67, 1.61
				δCH_2	3.22, 3.22
				ϵNH	7.27
(NHCH ₃)	7.97			CH ₃	2.75

^aThe Lys ζNH_3^+ resonance is broadened around 7.61 ppm due to exchange.

Spin system identification

Initially, the spin systems were divided into three categories, a group of systems with unique side-chain symmetry, a group comprising the $\alpha\text{H}-\beta\text{H}_2$ AMX spin systems, and a group containing amino acids with long side chains (Wüthrich, 1986).

The first category consists of 2 Gly, 4 Ala, 1 Val, 1 Leu, and 4 Thr. The two glycyl residues could be identified by their large geminal coupling constants and the lack of side-chain protons. However, the multiplet patterns in the DQ filtered COSY spectrum differed from the characteristic pattern (Neuhaus et al., 1985). These could only be explained by the presence of a minor concentration of two additional glycines with slightly shifted NH- αH_2 cross peaks, likely originating from an impurity or a second conformation of P25. The four alanyl and the four threonyl residues were identified by the intense cross peaks to the methyl groups. The threonines showed also $\alpha\text{H}-\beta\text{H}$ cross peaks relatively close to the diagonal. The valine and the leucine were identified by their side-chain length and characteristic spin system patterns. Apart from the two glycines mentioned above, two additional threonines and a second valine were found.

P25 contains only three amino acids with AMX spin systems; 1 Ser and 2 Asn. The seryl residue was recognized by the position of the βCH_2 resonances at relatively low field around 4 ppm. Analysis of the NH- αH cross peak revealed also an additional seryl residue. The two asparagines were identified by the low field position of the α -protons and the presence of NOEs from βH_2 to the side-chain amide protons in the NOESY spectra.

The third category contains the amino acids with long side-chains; 1 Gln, 6 Arg, and 3 Lys. The glutamine was identified by the chemical shifts of βH_2 and γH_2 , and by the presence of NOEs from the γ -protons to the side-chain amide protons in the NOESY spectra. The use of HoHaHa spectra was essential for the assignment of the six arginyl and three lysyl residues. The positions of the α -protons of the arginyl and lysyl residues could be determined by the observation of the $\alpha\text{H}-\delta\text{H}_2$ and $\alpha\text{H}-\epsilon\text{H}_2$ cross peaks. The $\alpha\text{H}-\beta\text{H}_2$ cross peaks of three of the arginyl residues (Arg 10, Arg 13 and Arg 14) were well resolved in the DQ filtered COSY spectrum, and were used to determine the chemical shifts of the β -protons. The additional high field resonances connected to the αH resonances in the HoHaHa spectra could be assigned to the γ -protons. The $\alpha\text{H}-\beta\text{H}_2$ cross peaks of the other three arginyl residues overlapped with the $\alpha\text{H}-\beta\text{H}_2$ cross peaks of the lysines. Also the other cross peaks between the side-chain resonances of Arg and Lys showed

varying degrees of mutual overlap. However, cross peaks from ϵNH to δH_2 , γH_2 , βH_2 , and even to αH of the arginyl residues (see Fig. 3.1), and cross peaks between backbone amide resonances and side-chain resonances of both Arg and Lys were well resolved in the HoHaHa spectrum recorded at 10°C . The positions of all these side-chain resonances were compared with the approximate positions of the less well resolved DQ filtered COSY cross peaks to make distinctions between βH_2 , γH_2 , and δH_2 . In this way it was possible to assign all side-chain resonances of the arginyl and lysyl residues.

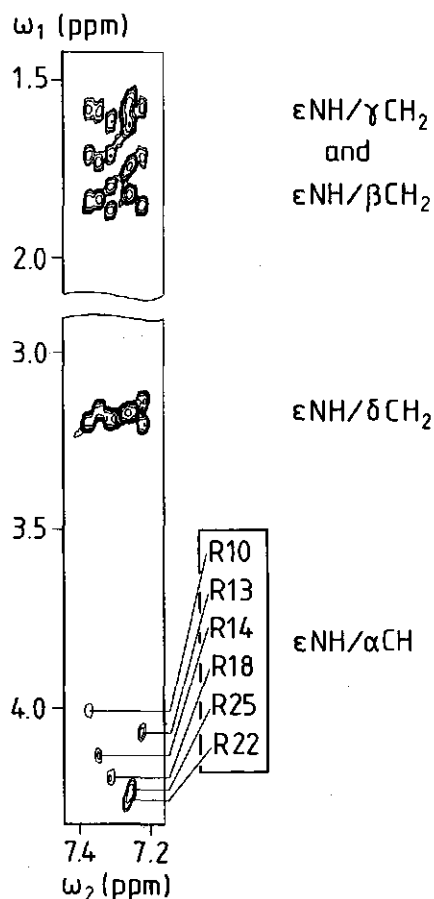


Fig. 3.1 Part of a 600 MHz HoHaHa spectrum of P25 showing the cross peaks from ϵNH (in ω_2 -dimension) to δH_2 , γH_2 , βH_2 , and αH (in ω_1 -dimension) of all arginyl residues. The spectrum was recorded at 10°C with an MLEV17 mixing time of 80 ms. The time domain data consisting of 512 FIDs of 4k data points were multiplied by a sine-bell window function shifted by $\pi/8$ in both dimensions. The digital resolution in the transformed spectrum is 3.13 Hz/point in the ω_2 -dimension and 6.26 Hz/point in the ω_1 -dimension.

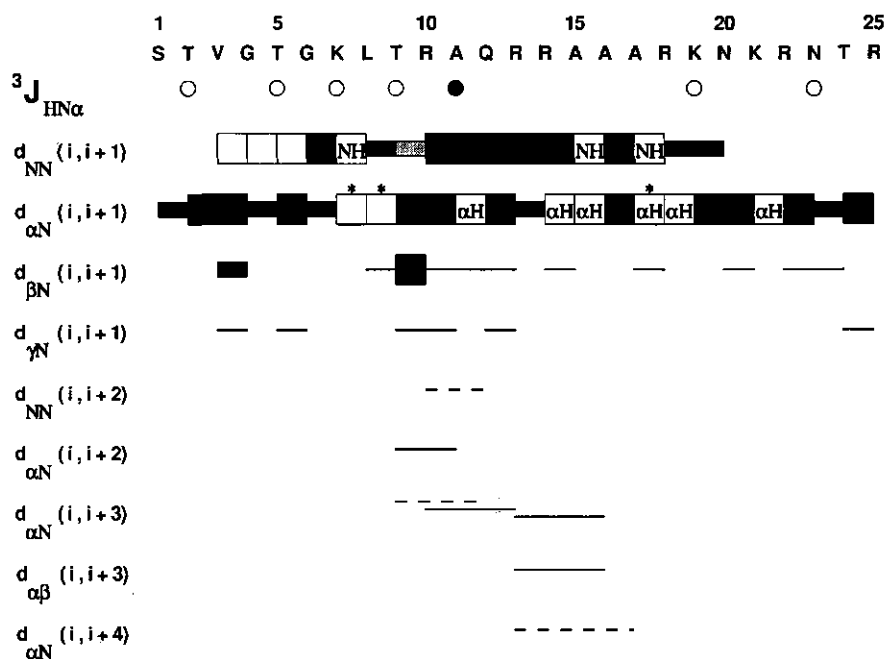


Fig. 3.2 Summary of the $^3J_{HN\alpha}$ coupling constants observed for P25 at 10°C, and the short and medium range NOEs observed at 10 and 2°C. Open and closed circles indicate $^3J_{HN\alpha}$ coupling constants larger than 7 Hz and smaller than 6 Hz, respectively. Three different groups of NOE intensities are distinguished by the thickness of the lines. Open squares indicate that the presence of the connectivity is ambiguous due to overlap problems. In the case of degeneracy of the sequential NH or α H resonances the open square contains 'NH' or ' α H', respectively. An asterisk above an open square indicates that the connectivity is clearly present at lower temperature than 10°C. The dashed lines and the grey filled box indicate NOEs absent at 10°C, but present at 2°C. The presented NOEs were derived from NOESY spectra recorded with mixing times of 200 msec. All presented connectivities were also observed in the NOESY spectra recorded with smaller mixing times.

Sequential assignments

During the sequential assignment step the NOESY spectra were searched for sequential d_{NN} , $d_{\alpha N}$, $d_{\beta N}$ and $d_{\gamma N}$ connectivities to assign every spin system to a specific amino acid residue in the primary sequence. Figure 3.2 shows these sequential connectivities appearing in the NOESY spectrum recorded at 10°C. As indicated in this figure, problems arise if sequential NH or α H resonances are degenerate. NOESY cross peaks between amide protons

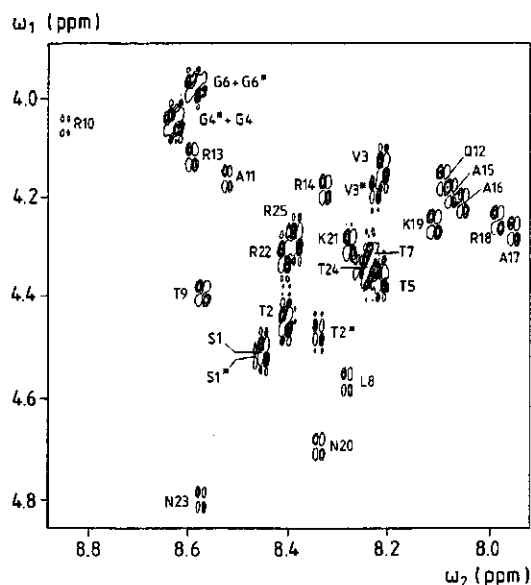
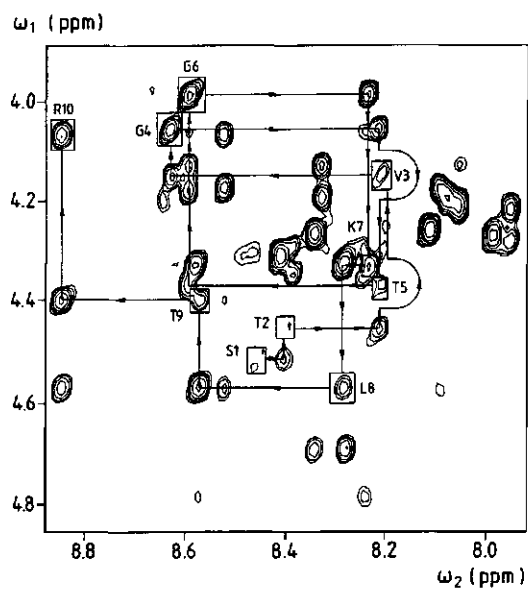
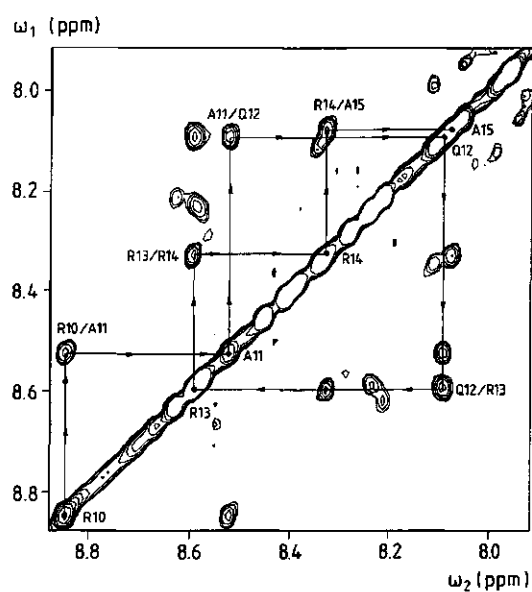


Fig. 3.3 The fingerprint region ($\omega_1 = 3.9 - 4.9$ ppm, $\omega_2 = 7.9 - 8.9$ ppm) of a 600 MHz DQ filtered COSY spectrum of P25 recorded at 10°C. The time domain data were multiplied by a sine-bell window function shifted by $\pi/12$ in t_2 -direction, and by a sine-bell window function shifted by $\pi/6$ in t_1 -direction. The digital resolution in the transformed spectrum is 0.78 Hz/point in the ω_2 -dimension and 1.57 Hz/point in the ω_1 -dimension. Positive peaks are represented as filled circles, and negative peaks as open circles. The NH- α H cross peaks are identified by labels. Labels with asterisks refer to P25* (see text). The NH- α H cross peak of T5* of P25* is not labelled for reason of clarity; this cross peak overlaps with the NH- α H cross peaks of T24 and T7 of P25.

Fig. 3.4 Parts of a 600 MHz NOESY spectrum of P25 recorded at 10°C with a mixing time of 200 msec. The time domain data consisting of 512 FIDs of 2k data points were multiplied by a sine-bell window function shifted by $\pi/6$ in both dimensions. The digital resolution in the transformed spectrum is 6.26 Hz/point for both dimensions. (A) The sequential assignment pathway from S1 to R10 is indicated by arrows leading from the intra-residual (NH- α H)_i cross peak via the sequential $d_{\alpha N}$ connectivity to the intra-residual (NH- α H)_{i+1} cross peak. The intra-residual NH- α H cross peaks indicated by rectangles are labelled. The spectral region overlaps with the fingerprint region ($\omega_1 = 3.9 - 4.9$ ppm, $\omega_2 = 7.9 - 8.9$ ppm) of the DQ filtered COSY spectrum shown in Figure 3.3. (B) The sequential assignment pathway from R10 to A15 is indicated by arrows leading from the NH_i resonance at the diagonal via the sequential d_{NN} connectivity to the NH_{i+1} resonance at the diagonal. The d_{NN} connectivities are labelled ω_2/ω_1 .

A**B**

with almost the same chemical shifts overlap with the diagonal, and cannot be observed. Sequential α Hs with degenerate resonances give rise to inter-residual α H_i-NH_{i+1} connectivities which are not resolved due to overlap with the intra-residual (NH- α H)_{i+1} connectivities. Another problem is the overlap of NH or α H resonances of non-sequential residues (e.g. NH_{Val3} and NH_{Thr5}). Some of the overlap problems were solved at lower temperatures, but others remained. In these cases the presence of the cross peak was ambiguous, and the connectivity could not be used in the sequential assignment procedure.

Figure 3.3 shows the sequential assignments in the fingerprint region of the DQ filtered COSY spectrum recorded at 10°C. Figure 3.4A shows the same region of a NOESY spectrum recorded at this temperature. The assignment pathway from Ser1 to Arg10 is indicated by arrows leading from the (NH- α H)_i intra-residual cross peak via the $d_{\alpha N}$ sequential connectivity to the (NH- α H)_{i+1} intra-residual cross peak. Two serious overlap problems ($d_{\alpha N}$ from Lys7 to Leu8 overlaps with (NH- α H)_{Lys21}, and $d_{\alpha N}$ from Leu8 to Thr9 overlaps with (NH- β H)_{Thr9}) were solved by using spectra recorded at lower temperatures.

Not only $d_{\alpha N}$ contacts but also d_{NN} connectivities were very useful in the sequential assignment procedure. This is demonstrated in Figure 3.4B, which shows the assignment pathway from Arg10 to Ala15 via d_{NN} connectivities. The assignment of the section Ala15-Arg18 gave some problems because of several degenerate resonances (see Fig. 3.2 and Table 3.1). However, the sequential connectivities between Ala16 and Ala17 were obviously present, and at 2°C the $d_{\alpha N}$ connectivity from Ala17 to Arg18 was well enough resolved to make unambiguous assignments. The section from Arg18 to Arg25 was assigned without serious difficulties.

The additional resonances mentioned before (2 Gly, 2 Thr, 1 Val and 1 Ser) could be assigned to a second set of the first six amino acids in the N-terminal region of P25 (see Fig. 3.3). After this observation the sample was analysed to test whether the additional resonances originated from an impurity or a second conformation of P25. An enantioseparation (Fujiwara et al., 1987; Brückner et al., 1989) revealed that 25 - 30% of the valyl residues had been converted from L-Valine to D-Valine during the synthesis. Therefore, the additional resonances were assigned to the presence of 25 - 30% P25*, which can be defined as P25 containing D-Valine instead of L-Valine at position three. Since the resonances of P25 could be separated from those of P25*, no attention will be paid to the presence of P25* in the further analysis.

Presence of secondary structure

Inter-residual NOESY connectivities are the most important tools in secondary structure determination. Strong d_{NN} connectivities in combination with relatively weak $d_{\alpha N}$ connectivities and medium range NOEs from αH of residue i to NH or βH of residue $i+3$ are typical of helices, whereas strong $d_{\alpha N}$ connectivities indicate extended structures such as β -sheets. Additional NMR parameters including $^3J_{HN\alpha}$ spin-spin coupling constants, chemical shift positions and exchange rates of amide protons give further information about the secondary structure (Wüthrich, 1986).

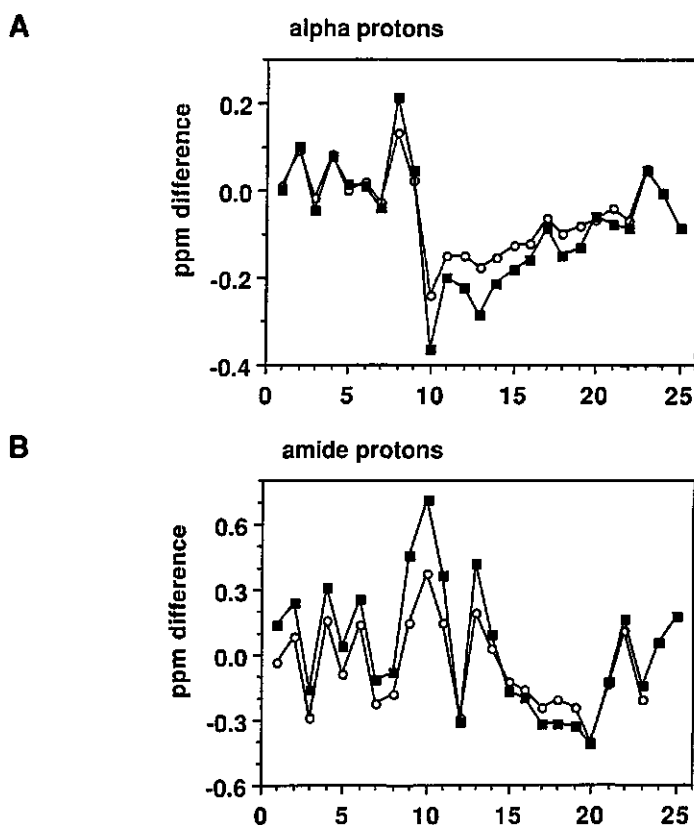


Fig. 3.5 Conformation-dependent chemical shifts of the α -protons (A) and the amide protons (B) at 2°C (—■—) and at 25°C (—○—) presented as function of the residue numbers. These conformation-dependent chemical shifts were obtained by subtraction of the corresponding 'random-coil' chemical shifts (Bundi and Wüthrich, 1979) from the measured chemical shifts. The chemical shift values of the amide and α -protons of T24 and R25 could not be determined at 25°C because of overlap problems.

The short and medium range NOESY connectivities presented in Figure 3.2 are somewhat ambiguous with respect to the secondary structure of P25. The sequential $d_{\alpha N}$ connectivities have rather strong intensities indicating an extended structure. On the contrary, however, the presence of the sequential d_{NN} connectivities is characteristic of folded structures, and the medium range NOESY connectivities in the region between residue 9 and 16 are typical of a helical conformation. The connectivity $d_{\alpha\beta}(8,12)$ and NOEs from side-chain resonances of Leu8 and Thr9 to side-chain resonances of Gln12 are also indicative for the presence of helical secondary structure in the region in the middle of P25. The amide region of the NOESY spectrum recorded at 2°C (not presented) shows additional connectivities in this region: $d_{NN}(9,10)$, $d_{NN}(10,12)$, $d_{\alpha N}(9,12)$ and $d_{\alpha N}(13,17)$ (see Figure 3.2).

The chemical shifts presented in Table 3.1 provide additional evidence for the presence of secondary structure in the region in the middle of P25 (residue 8 - residue 17). Several chemical shifts clearly deviate from their random coil values, and some normally degenerate resonances are separated. For instance, the δ -protons of Leu8 have distinct resonance positions indicating that each proton experiences its own environment. The same applies to the δ -protons of Arg13. The chemical shifts of the backbone protons differ in varying degrees from their random coil values. Figure 3.5 shows the conformation-dependent chemical shifts of the α -protons (Fig. 3.5A) and the amide protons (Fig. 3.5B) at 2 and 25°C. The conformation-dependent chemical shifts were obtained by subtraction of the corresponding 'random-coil' chemical shifts (Bundi and Wüthrich, 1979) from the observed shifts. Positive and negative values indicate shifts to lower and higher field, respectively. The conformation-dependent chemical shifts measured at 5 and 10°C have values between the upper and lower limits of the shifts presented in Figure 3.5.

Connectivities between resonances of non-exchangeable protons and the water resonance

Figure 3.6 shows a part of the NOESY spectrum recorded at 2°C with a mixing time of 200 msec. The water signal was not suppressed by irradiation, but by a jump-return read pulse. In this figure cross peaks can be observed at the ω_2 -resonance positions of the non-exchangeable γ -protons of Thr9 and Gln12 and the ω_1 -resonance position of water. These cross peaks can be the result of direct NOEs or of a 'relay' mechanism. Direct NOEs may originate from sufficiently tightly bound hydration water or from a hydroxyl group with

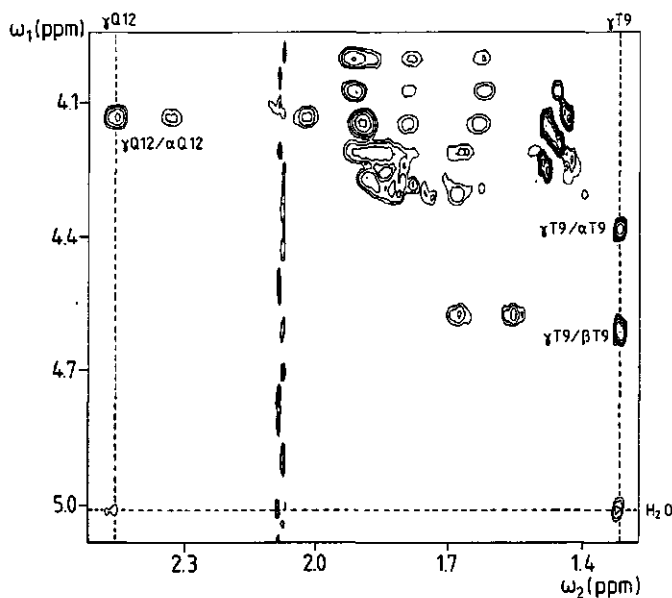


Fig. 3.6 Part of a 600 MHz NOESY spectrum of P25 recorded at 2°C with a mixing time of 200 msec. The water signal was suppressed by using a $(90^\circ)_\phi - \tau - (90^\circ)_{-\phi}$ jump-return read pulse with $\tau = 80 \mu\text{s}$. The time domain data consisting of 512 FIDs of 4k data points were multiplied by a sine-bell window function shifted by $\pi/8$ in t_2 -direction. In t_1 -direction a sine-bell shifted by $\pi/6$ was used. The digital resolution in the transformed spectrum is 3.13 Hz/point in the ω_2 -dimension and 6.26 Hz/point in the ω_1 -dimension. Vertical dotted lines indicate the ω_2 -resonances of the γ -protons of Thr9 and Gln12. The horizontal dotted line indicates the ω_1 -resonance position of water. At the crossings of the dotted lines connectivities are clearly visible. The other connectivities at the ω_2 -resonances of the mentioned γ -protons are labelled ω_2/ω_1 .

the same resonance position as water. A reasonable 'relay' mechanism involves dipolar cross relaxation between the non-exchangeable γ -protons and an exchangeable proton (NH or OH) preceded by chemical exchange of the latter with water (Van de Ven et al., 1988). For the cross peak at the ω_2 -resonance position of the γ -protons of Thr9 a 'relay' mechanism via an exchangeable amide proton can be excluded, because the connectivity at this position is also present in a NOESY spectrum recorded under comparable conditions with irradiation of the amide proton region during the mixing time. In such a MINSY-type experiment the proposed 'relay' pathway via an

exchangeable amide proton is closed off by the saturation of the amide resonances (Massefski and Redfield, 1988). In addition, NOE difference experiments indicated direct NOE growth at the resonance position of the γ -protons of Thr9 after irradiation of the water resonance. These experiments suggest that the connectivity between the ω_1 -resonance position of water and the ω_2 -resonance position of the γ -protons of Thr9 originates from a direct NOE. This could indicate the presence of a sufficiently tightly bound hydration water. However, this explanation is not unique, because distinction between an inter-molecular NOE with hydration water and an intra-molecular NOE with a hydroxyl group (e.g. of Thr9) cannot be made (Otting and Wüthrich, 1989). The above mentioned MINSY-type spectrum and the NOE difference spectra showed no intensity above the noise level at the ω_2 -resonance position of the γ -protons of Gln12.

DISCUSSION

Nature of the conformation of P25 in aqueous solution

The results show a simultaneous presence of $d_{\alpha N}$ and d_{NN} NOEs with almost the same intensities. It is often found that sequential NOEs characteristic of both α and β conformations are present for a small flexible peptide. An explanation for this phenomenon is conformational averaging on the NMR time scale (Wright et al., 1988). The measured NMR parameters such as NOE intensities, coupling constants and chemical shifts are a population-weighted average over all conformations sampled.

Since P25 is a small and flexible peptide in aqueous solution, it is suggested that P25 samples different conformations on the NMR time scale. The strong intensities of several αN connectivities indicate the presence of extended structures. However, several medium range NOEs characteristic of helical conformation suggest that a perceptible fraction of the conformational ensemble of P25 consists of structures with a helical conformation in the region in the middle of P25 (see next paragraph).

Figure 3.5 shows that the conformation-dependent chemical shifts measured at 2°C are larger than those measured at 25°C. Furthermore, at 2°C the NOE connectivities $d_{NN}(9,10)$, $d_{NN}(10,12)$, $d_{\alpha N}(9,12)$ and $d_{\alpha N}(13,17)$ appear in addition to the connectivities present at 10°C. These observations indicate a shift of the dynamic conformational equilibrium towards helical conformations by a decrease of temperature. The same phenomenon has

been reported for the C-peptide (residue 1-13) and S-peptide (residue 1-20) of RNase A, which show significant α -helix formation in aqueous solution near 0°C (Brown and Klee, 1971; Bierzynski et al., 1982; Kim and Baldwin, 1984).

Position of the helical region

For the region Thr9-Ala17 several medium range NOESY connectivities characteristic of α -helical conformation such as $d_{\alpha N}(i,i+3)$, $d_{\alpha\beta}(i,i+3)$ and $d_{\alpha N}(i,i+4)$ (Wüthrich, 1986) are observed: $d_{\alpha N}(10,13)$, $d_{\alpha N}(13,16)$ and $d_{\alpha\beta}(13,16)$ at 10°C, and also $d_{\alpha N}(9,12)$ and $d_{\alpha N}(13,17)$ at 2°C. The connectivity $d_{\alpha N}(9,11)$ is not typical of an α -helix, but indicates a 3_{10} -helix or a reverse turn (Wüthrich et al., 1984). We also note that $d_{\beta N}(9,10)$ is much stronger than the other $d_{\beta N}(i,i+1)$ connectivities. These $d_{\beta N}(i,i+1)$ connectivities are commonly observed in helical structures and tight turns (Wüthrich et al., 1984). The presence of $d_{\alpha N}(9,11)$ and the fact that $d_{\beta N}(9,10)$ is much stronger than the $d_{\beta N}(i,i+1)$ connectivities in the rest of the helical region suggest a turn-like conformation around Thr9 and Arg10.

Most $^3J_{HN\alpha}$ spin-spin coupling constants have values between 6 and 7 Hz (see Fig. 3.2). These values could indicate a random coil conformation, but for the region in the middle of P25 a conformational averaging between a helical ($^3J_{HN\alpha} \leq 5$) and an extended β conformation ($^3J_{HN\alpha} \geq 8$) is a more reasonable explanation. If P25 had entirely a random coil conformation, no medium range NOESY connectivities characteristic of a helical conformation would be present at all.

The conformation-dependent chemical shifts presented in Figure 3.5 provide additional information about the backbone conformation of P25. In general, chemical shift information has been considered to be not very reliable because of a high sensitivity to ring-current fields of aromatic amino acids and shielding effects resulting from secondary and tertiary structure. However, P25 contains no aromatic amino acids, and is too small to obtain tertiary structure. Therefore, in our case, the chemical shifts are only influenced by local electronic structure, protonation equilibria, hydrogen bonding and shielding effects that result from the secondary structure (Wüthrich, 1986).

For both amide and α -protons, close proximity to oxygen atoms has been correlated to large low-field shifts (Pardi et al., 1983; Wagner et al., 1983). Low-field shifts (positive conformation-dependent chemical shifts) occur predominantly in antiparallel β -structures, and high-field shifts (negative conformation-dependent chemical shifts) occur in helical conformations. It has

also been shown by statistical analysis of chemical-shift distributions in 32 polypeptides and proteins that the α -protons of aliphatic amino acids in α -helical conformations shift upfield by 0.4 ppm, on the average (Szilágyi and Jardetzky, 1989). Figure 3.5A shows the strongest conformation-dependent chemical shifts of the α -protons between residue 8 and 10, and gradually decreasing high-field shifts (indicated by negative values) going from Arg10 in the direction of the C-terminus of P25. Figure 3.5B shows a more irregular pattern for the conformation-dependent chemical shifts of the amide protons, but again the largest shifts can be observed around Arg10. The large down-field shift of the amide proton of Arg 10 in combination with the up-field shift of the α -proton of this residue could be indicative for the 'turn-like' structure mentioned before or for the presence of a relatively tightly bound hydration water in close proximity of the amide proton as suggested by Fig. 3.6. The up-field shifts of the α -protons in the region between residue 10 and 20 are indicative for an α -helix conformation (Wagner et al., 1983; Szilágyi and Jardetzky, 1989), in agreement with the observed NOEs. The conformation-dependent chemical shifts of the amide protons in this region are also predominantly down-field, but the pattern is more irregular. The relative shifts of the amide protons are larger than those of the α -protons, which can be explained by a larger influence of hydrogen bonding (Wagner et al., 1983). It was tried to determine the hydrogen bond positions by measuring the exchange rates of the amide protons. However, the exchange rates were too fast to be measured due to the large solvent accessibility of P25 and probably also due to the process of conformational averaging.

All the phenomena described above indicate the presence of structures with a predominantly α -helical conformation between residue 9 and 17. Both termini of the peptide are assumed to have random coil conformations.

Stabilization of the helical conformation

Several interactions have been suggested to be a stabilization factor in helical conformations. Substitution experiments on the ribonuclease C-peptide have shown that charged groups play a critical role in the stability of a helix (Shoemaker et al., 1987). Negative and positive charges close to the positive N-terminal and negative C-terminal poles of the α -helix macrodipole, respectively, induce favourable charge-dipole interactions that stabilize the helix. However, this theory is not applicable to P25, because in this peptide positively charged amino residues are present at both termini of the helical region.

Presta and Rose (1988) have presented a helix hypothesis based on hydrogen bond formation at the helix termini: a necessary condition for helix formation is the presence of residues whose side chains can form hydrogen bonds with the initial four helix N-H groups and final four C=O groups. In P25 the side chains of Thr9 and Gln12 can serve as hydrogen-bond acceptors at the N-terminus of the helix, and the side chains of all amino acids between residue 18 and 25 (Arg, Lys, Asn and Thr) can serve as hydrogen-bond donors at the C-terminus of the helical region. The cross peaks at the ω_1 -resonance position of water in Figure 3.6 could indicate the presence of relatively tightly bound hydration water in close proximity of the γ -protons of Thr9 and Gln12. If this hydration water is present, it can serve as an additional hydrogen-bond acceptor at the N-terminus of the helical region. So, although only two hydrogen-bond acceptors are present at the N-terminus of the helical region instead of four, the helix hypothesis seems to be applicable to P25.

The predominantly α -helical region in P25 has an amphipathic character. At the hydrophobic side of this amphipathic helix hydrophobic interactions between side chains play a role in stabilization of the α -helix (Lim, 1974a,b). However, at the hydrophilic side all positive charges are in close spatial proximity of each other, which is expected to be energetically unfavourable. Circular dichroism experiments have shown that addition of salt or (oligo)phosphates induces an increase of α -helical conformation in P25 (see Chapter 2). Furthermore, previous secondary structure predictions suggested a random coil conformation for the N-terminal arm of CCMV coat protein with charged side-chains, but an α -helix between residues 10 and 20 after charge neutralization (Vriend et al., 1986). This indicates that shielding of the positive charges neutralizes their destabilizing effect on α -helix formation. In CCMV virus particles the positive charges are neutralized by the negatively charged phosphate groups of the encapsidated RNA. Therefore, all samples used for the NMR experiments presented here contained 200 mM sodium phosphate.

It can be concluded that P25 alternates among helical and extended backbone conformations on the NMR time scale. Under our experimental conditions a perceptible fraction of the conformational ensemble consists of structures with an α -helical conformation between residue 9 and 17, likely starting with a turn-like structure around Thr9 and Arg10. Both position and conformation agree well with previous secondary structure predictions (Argos, 1981; Vriend et al., 1986). The amino acid sequence between residues 9 and

18 in CCMV is exactly the same as in BMV, for which virus it has been shown that residues 11-19 are involved in RNA-binding (Sacher and Ahlquist, 1989; Sgro et al., 1986). Therefore, we suggest that ability to form an α -helix in this region may be an essential part of the synergistic interaction with RNA.

ACKNOWLEDGEMENTS

We thank Dr S.S. Wijmenga and J.J.M. Joordens of the HF-SON NMR Facility Nijmegen (The Netherlands) for assistance in recording the NMR spectra, and C.J.A.M. Wolfs and Dr P.B.W. ten Kortenaar for performing chemical analyses of P25.

REFERENCES

- Abad-Zapatero, C., Abel-Meguid, S. S., Johnson, J. E., Leslie, A. G. W., Rayment, I., Rossmann, M. G., Suck, D. & Tsukinara, T. (1980) *Nature* 286, 33-39.
- Argos, P. (1981) *Virology* 110, 55-62.
- Bancroft, J. B. & Hiebert, E. (1967) *Virology* 32, 354-356.
- Bancroft, J. B., Wagner, G. W. & Bracker, C. E. (1968) *Virology* 36, 146-149.
- Bax, A. & Davis, D. G. (1985) *J. Magn. Reson.* 65, 355-360.
- Bierzynski, A., Kim, P. S. & Baldwin, R. L. (1982) *Proc. Natl. Acad. Sci. U.S.A.* 79, 2470-2474.
- Billeter, M., Braun, W. & Wüthrich, K. (1982) *J. Mol. Biol.* 155, 321-346.
- Brown, J. E. & Klee, W. A. (1971) *Biochemistry* 10, 470-476.
- Brückner, H., Wittner, R. & Godel, H. (1989) *J. Chromatogr.* 476, 73-82.
- Bundi, A. & Wüthrich, K. (1979) *Biopolymers* 18, 285-297.
- Dasgupta, R. & Kaesberg, P. (1982) *Nucl. Acids Res.* 10, 703-713.
- Finch, J. T. & Bancroft, J. B. (1968) *Nature* 220, 815-816.
- Fujiwara, M., Ishida, Y., Nimura, N., Toyama, A. & Kinoshita, T. (1987) *Anal. Biochem.* 166, 72-78.
- Harrison, S. C., Olson, A. J., Schutt, C. E., Winkler, F. K. & Bricogne, G. (1978) *Nature* 276, 368-373.
- Hemminga, M. A., Datema, K. P., ten Kortenaar, P. W. B., Krüse, J., Vriend, G., Verduin, B. J. M. & Koole, P. (1985) in *Magnetic Resonance in Biology and Medicine* (Govil, G., Khetrapal, C. L., Saran, A., Eds.) pp 53-76, Tata McGraw-Hill, New Delhi.
- Hogle, J. M., Maeda, A. & Harrison, S. C. (1986) *J. Mol. Biol.* 159, 93-108.
- Hosur, M. V., Schmidt, T., Tucker, R. C., Johnson, J. E., Gallagher, T. M., Selling, B. H. &

- Ruekert, R. R. (1987) *Proteins Struct. Funct. Genet.* 2, 167-176.
- Jeener, J., Meier, B. H., Bachmann, P. & Ernst, R. R. (1979) *J. Chem. Phys.* 71, 4546-4553.
- Kaper, J. M. (1975) *The Chemical Basis of Virus Structure, Dissociation and Reassembly*, North-Holland, Amsterdam.
- Kim, P. S. & Baldwin, R. L. (1984) *Nature* 307, 329-334.
- Liljas, L., Unge, T., Jones, T. A., Fridborg, K., Lövgren, S., Skoglund, U. & Strandberg, B. (1982) *J. Mol. Biol.* 159, 93-108.
- Lim, V. I. (1974a) *J. Mol. Biol.* 88, 857-872.
- Lim, V. I. (1974b) *J. Mol. Biol.* 88, 873-894.
- Macura, S. & Ernst, R. R. (1980) *Molec. Phys.* 41, 95-117.
- Marion, D. & Wüthrich, K. (1983) *Biochem. Biophys. Res. Commun.* 113, 967-974.
- Massefski, W., Jr. & Redfield, A. G. (1988) *J. Magn. Reson.* 78, 150-155.
- Neuhaus, D., Wagner, G., Vasák, M., Kägi, J. H. R. & Wüthrich, K. (1985) *Eur. J. Biochem.* 151, 257-273.
- Otting, G. & Wüthrich, K. (1989) *J. Am. Chem. Soc.* 111, 1987-1875.
- Pardi, A., Wagner, G. & Wüthrich, K. (1983) *Eur. J. Biochem.* 137, 445-454.
- Pearson, G. A. (1977) *J. Magn. Reson.* 27, 265-272.
- Plateau, P. & Guéron, M. (1982) *J. Am. Chem. Soc.* 104, 7310-7311.
- Presta, L. G. & Rose, G. D. (1988) *Science* 240, 1632-1641.
- Rance, M., Sørensen, O. W., Bodenhausen, G., Wagner, G., Ernst, R. R. & Wüthrich, K. (1983) *Biochem. Biophys. Res. Commun.* 117, 479-485.
- Rossmann, M. G., Arnold, E., Erickson, J. W., Frankenberger, E. A., Griffith, J. P., Hecht, H. J., Johnson, J. C., Kamer, G., Luo, M., Mosser, A. G., Rueckert, R. R., Sherry, B. & Vriend, G. (1985) *Nature* 317, 145-153.
- Sacher, R. & Ahlquist, P. (1989) *J. Virol.* 63, 4545-4552.
- Sgro, J., Jacrot, B. & Chroboczek, J. (1986) *Eur. J. Biochem.* 154, 69-76.
- Shoemaker, K. R., Kim, P. S., York, E. J., Stewart, J. M. & Baldwin, R. L. (1987) *Nature* 326, 563-567.
- Szilágyi, L. & Jardetzky, O. (1989) *J. Magn. Reson.* 83, 441-449.
- Ten Kortenaar, P. B. W., Krüse, J., Hemminga, M. A. & Tesser, G. I. (1986) *Int. J. Pept. Protein Res.* 27, 401-413.
- Van de Ven, F. J. M., Janssen, H. G. J. M., Gräslund, A. & Hilbers, C. W. (1988) *J. Magn. Reson.* 79, 221-235.
- Verduin, B. J. M., Prescott, B. & Thomas, G. J., Jr. (1984) *Biochemistry* 23, 4301-4308.
- Vriend, G., Hemminga, M. A., Verduin, B. J. M., de Wit, J. L. & Schaafsma, T. J. (1981) *FEBS Lett.* 134, 167-171.
- Vriend, G., Verduin, B. J. M. & Hemminga, M. A. (1986) *J. Mol. Biol.* 191, 453-460.
- Wagner, G., Pardi, A. & Wüthrich, K. (1983) *J. Am. Chem. Soc.* 105, 5948-5949.

- Wagner, G. & Wüthrich, K. (1982) *J. Mol. Biol.* 155, 347-366.
- Wider, G., Lee, K. H. & Wüthrich, K. (1982) *J. Mol. Biol.* 155, 367-388.
- Wright, P. E., Dyson, H. J. & Lerner, R. A. (1988) *Biochemistry* 27, 7167-7175.
- Wüthrich, K. (1986) *NMR of Proteins and Nucleic Acids*, Wiley, New York.
- Wüthrich, K., Billeter, M. & Braun, W. (1984) *J. Mol. Biol.* 180, 715-740.
- Wüthrich, K. & Wagner, G. (1979) *J. Mol. Biol.* 130, 1-18.
- Wüthrich, K., Wider, G., Wagner, G. & Braun, W. (1982) *J. Mol. Biol.* 155, 311-319.

CHAPTER 4

CONFORMATION OF A PENTACOSAPEPTIDE REPRESENTING THE RNA-BINDING N-TERMINUS OF CCMV COAT PROTEIN IN THE PRESENCE OF OLIGOPHOSPHATES

A TWO-DIMENSIONAL PROTON NMR AND DISTANCE GEOMETRY STUDY

Marinette van der Graaf, Ruud M. Scheek, Catharina C. van der Linden, and Marcus A. Hemminga

ABSTRACT

Conformational studies have been performed on a synthetic pentacosapeptide representing the RNA-binding N-terminal region of the coat protein of cowpea chlorotic mottle virus. Two-dimensional proton NMR experiments were performed on the highly positively charged peptide containing six arginines and three lysines in the presence of an excess of monophosphates, tetra(poly)phosphates or octadeca(poly)phosphates mimicking the phosphates of the RNA. The results show that the peptide alternates between various extended and helical structures in the presence of monophosphate, and that this equilibrium shifts towards the helical structures (with the helical region situated between residues 10 and 20) in the presence of oligophosphates. Distance geometry calculations using distance constraints derived from a NOESY spectrum of the peptide in the presence of tetra(poly)phosphate resulted in eight structures belonging to two structure families. The first family consists of five structures with an α -helix-like conformation in the middle of the peptide, and the second family consists of three structures with a more open conformation. The presence of two structure families indicates that even in the presence of tetra(poly)phosphate the peptide is flexible. The propensity to form an α -helical conformation in the N-terminal part of this viral coat protein upon binding of phosphate groups to the positively charged side chains is suggested to play an essential role in RNA binding.

INTRODUCTION

Cowpea chlorotic mottle virus (CCMV) is an icosahedral plant virus consisting of RNA and 180 identical coat proteins, each 189 residues long (Dasgupta and Kaesberg, 1982). The virus particle can easily be dissociated and reassembled *in vitro* by changing pH and ionic strength (Bancroft and Hiebert, 1967). However, after removal of the first 25 amino acids by tryptic digestion the protein is not able to bind the RNA anymore (Vriend et al., 1981). This indicates that the N-terminal arm containing nine positively charged amino acids (six Arg and three Lys) plays an essential role in RNA binding. Based upon NMR experiments and secondary structure predictions, Vriend et al. (1982, 1986) proposed a model for the assembly of CCMV coat protein and RNA. In this 'snatch-pull' model the N-terminal region of the coat protein has a random coil conformation before interaction with the RNA, but attains an α -helical conformation (between residues 10 and 20) upon binding of the positively charged side chains with the negatively charged phosphates of the RNA (Figure 1.4). Chemical synthesis of the pentacosapeptide P25 containing the first 25 N-terminal amino acids of CCMV coat protein (Ten Kortenaar et al., 1986) allowed detailed conformational studies to test the 'snatch-pull' model. Circular dichroism experiments (Chapter 2) showed that P25 has 15-18% α -helical and about 80% random-coil conformation in the absence of salt at 25°C, and 20-21% α -helical conformation under the same conditions at 10°C. Addition of inorganic salts results in an increase of α -helix content, up to 42% in the presence of octadeca(poly)phosphate. A two-dimensional proton NMR study on P25 in 200 mM sodium monophosphate, pH 4, showed that under these conditions P25 alternates between various extended and helical structures with the helical region situated between residues 9 and 17 (Chapter 3). The objective of the present study is to determine the conformation of P25 in the presence of oligophosphates by two-dimensional proton NMR and distance geometry calculations in order to obtain more information about the conformational change of the N-terminal region of CCMV coat protein upon RNA binding.

MATERIALS AND METHODS

NMR experiments

NMR samples contained 6.9 - 7.7 mM of the synthetic N^α1-acetyl, C^α25-methylamide P25 (Ten Kortenaar et al., 1986) and 200 mM sodium monophosphate P, 20 mM hexaammonium tetraphosphate P₄, or 10 mM sodium octadecaphosphate P₁₈ (sodium phosphate glass nr 15 of Sigma) in 10% (v/v) ²H₂O and 90% (v/v) H₂O. The pH was 4 (for P) or 5 (for P₄ and P₁₈). All samples contained an excess of negatively charged (oligo)phosphates with respect to the amount of positively charged peptide present. Sodium 3-trimethylsilyl(2,2,3,3-²H₄)propionate was used as an internal standard.

Two-dimensional proton NMR spectra were recorded at 2, 5 and 10°C on a Bruker AM 600 spectrometer interfaced with an Aspect 3000 computer. Phase-sensitive double quantum filtered COSY (Marion and Wüthrich, 1983; Rance et al., 1983), NOESY (Bodenhausen et al., 1984) and HoHaHa (Bax and Davis, 1985) spectra were obtained by using time proportional phase incrementation in *t*₁. The carrier frequency was chosen in the middle of the spectrum coinciding with the water resonance. The water signal was suppressed by irradiation at all times except during data acquisition in COSY and NOESY experiments or only during the 2.5-ms relaxation delay in HoHaHa experiments. Further details concerning the 2D-NMR experiments on P25 in 200 mM sodium monophosphate have been described elsewhere (Chapter 3). NOESY spectra of P25 in the presence of oligophosphates were recorded with mixing times of 100 and 200 ms for P25 + P₄ and 80 ms for P25 + P₁₈. No zero quantum suppression technique was applied. HoHaHa spectra were recorded with an MLEV-17 composite pulse of 75 ms for P25 + P₄ and 17 ms for P25 + P₁₈, preceded and followed by two 2.5-ms trim pulses. Spectra were generally recorded with 512 *t*₁-increments of 2048 or 4096 data points. The number of scans per *t*₁-increment varied between 16 and 48 after 2 or 4 dummy scans. Data processing was performed as previously described (Chapter 3).

Distance Geometry Calculations

Inter-proton distance constraints were derived from the NOESY spectrum of P25 in 20 mM P₄ recorded at 5°C with a mixing time of 100 ms. NOE intensities were determined by counting contour levels in the NOESY contour plot. Intensities of peaks originating from overlapping methylene or methyl proton resonances were divided by 2 and 3, respectively. Inter-proton

distances r_{ij} were calculated using the equation:

$$r_{ij} = (\text{NOE}_{\text{ref}} / \text{NOE}_{\text{obs}})^{1/6} \times r_{\text{ref}}$$

with r_{ij} = distance between proton i and j
 r_{ref} = reference distance
 NOE_{obs} = observed NOE intensity
 NOE_{ref} = NOE intensity corresponding to the reference distance

The spectrum of P25 showed no NOESY cross peak between methylene proton resonances which was suitable for being used as a reference peak. Therefore, the NOESY cross peaks between the side-chain amide proton resonances of Gln and Asn, all showing equal intensities, were used as reference peaks ($r_{\text{ref}} = 1.73 \text{ \AA}$). To obtain the upper and lower limit of each inter-proton distance for the distance geometry calculations a value of 0.5 \AA was added to and subtracted from each r_{ij} . Additional pseudo-atom corrections (Wüthrich et al., 1983) were applied in the case of degenerate methylene or methyl resonances (1.0 \AA) and isopropyl groups (2.4 \AA). Distances obtained for non-degenerate proton resonances (e.g. methylene protons) were not corrected, and the corresponding protons were labelled H1 (low field resonance) and H2 (high field resonance). In this way, 98 inter-residual distance constraints were obtained from the NOESY spectrum of P25. In addition, many other upper and lower bounds on distances in the peptide followed directly from the known bond lengths, bond angles and atomic radii (holonomic constraints).

Distance geometry calculations were carried out on a Convex C1-XP computer using a program (written by R. M. Scheek) based upon the metric matrix method developed by Havel, Crippen and Kuntz (Crippen, 1981; Crippen and Havel, 1978; Havel et al., 1983). By repeated random choices of inter-atomic distances between upper and lower bounds 48 different structures were generated. Each structure was optimized by minimizing the error function F_{error} by a 50-step conjugent gradient.

$$F_{\text{error}} = K_{\text{dc}} \left\{ \sum_{d>u} (d^2 - u^2)^2 + \sum_{d<l} (d^2 - l^2)^2 \right\} + K_{\text{chiral}} \left\{ \sum_{\text{C}} (v_{\text{c}} - V_{\text{c}})^2 \right\}$$

with K_{dc} = force constant for the distance constraints
 $(1 \text{ kJ} \cdot \text{mol}^{-1} \cdot \text{\AA}^{-4})$

K_{chiral}	=	force constant for the constraints on the chiral centres (1 kJ·mol ⁻¹ ·Å ⁻⁶)
d	=	inter-proton distance in generated structure
u	=	upper limit distance constraint
l	=	lower limit distance constraint
C	=	chiral centre
v_c	=	signed volume of chiral centre in generated structure
V_c	=	ideal signed volume of chiral centre

The chiral centres involving protons labelled H1 and H2 were not included in the error function resulting in a 'floating chirality' (Weber et al., 1988). The next step was a simplified molecular dynamics step to sample more exhaustively the possible conformations that satisfy the NMR distance constraints: 1000 steps (2 ps) of distance bounds driven dynamics (Kaptein et al., 1988) were performed at 1000K, followed by a 1000-step cooling down to 1K. During this 'shaking up' of the structures the protons labelled H1 and H2 were flipped in a way comparable to the procedure Williamson and Madison (1990) used. Each 10th step H1 and H2 were interchanged, and the error functions corresponding to the situation before and after flipping (F_1 and F_2 , respectively) were calculated. For $F_2 < F_1$ the structure generated by flipping was always chosen, but for $F_2 > F_1$ the structure generated was only chosen if

$$e^{-\Delta F/RT} > \epsilon$$

with ΔF	=	$F_2 - F_1$
R	=	gas constant (8.31 J·mol ⁻¹ ·K)
T	=	temperature
ϵ	=	value randomly chosen between 0 and 1

After this procedure the 32 structures showing the lowest values of F_{error} were selected. For inter-proton distances smaller than 4 Å present in those structures the NOESY spectrum was searched for corresponding cross peaks. In the case that certainly no NOESY cross peak was present, the distance was given a lower limit of 4 Å and an upper limit of 999.9 Å. In this way 36 non-NOE distance constraints were obtained. For the 32 structures generated before, these 36 non-NOE distance constraints were also included during a new run of 300 steps of distance bounds driven dynamics at 1000K, followed by a 1000-step cooling down to 1K. Finally, the 8 structures showing the

NMR experiments

Figure 4.1 shows short- and medium-range NOESY connectivities present in the NOESY spectra of P25 in 200 mM sodium monophosphate pH 4 (Figure 4.1A) and of P25 in 20 mM hexaammonium tetrphosphate pH 5 (Figure 4.1B), both recorded at 10°C. Details about the resonance assignment and determination of the conformation of P25 in 200 mM sodium monophosphate were described previously (Chapter 3). The resonances in the spectrum of P25 in 20 mM hexaammonium tetrphosphate pH 5 could easily be assigned with the help of the resonance assignment of P25 in 200 mM sodium monophosphate. The medium-range NOESY connectivities shown in Figure 4.1 ($d_{\alpha N(i,i+3)}$, $d_{\alpha\beta(i,i+3)}$, and $d_{\alpha N(i,i+4)}$) are characteristic of α -helical conformation (Wüthrich, 1986). Figure 4.2 shows a part of the NOESY spectrum of P25 in 20 mM hexaammonium tetrphosphate with the characteristic $d_{\alpha N(i,i+3)}$ and $d_{\alpha N(i,i+4)}$ connectivities indicated.

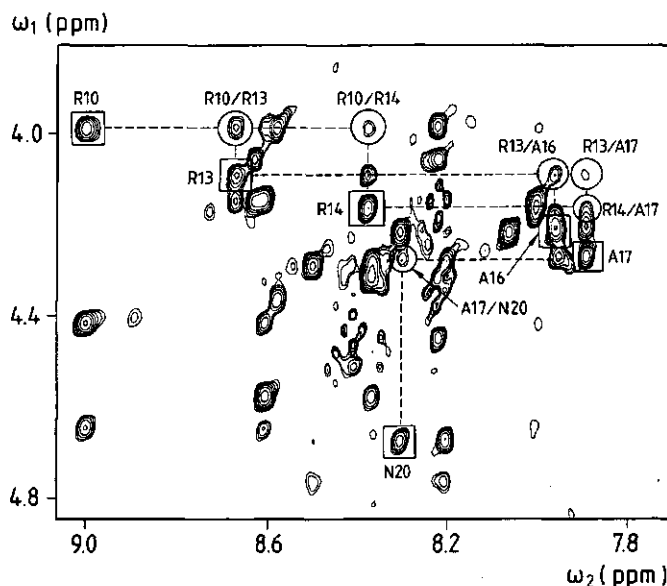


Fig. 4.2 Part of a NOESY spectrum of 6.9 mM P25 in 20 mM hexaammonium tetrphosphate pH 5, recorded with a mixing time of 100 ms at 10°C. The time domain data consisting of 512 free induction decays of 2048 data points were multiplied by a sine-bell window function shifted by $\pi/6$ in both dimensions. The digital resolution in the transformed spectrum is 3.13 Hz/point in the ω_2 -dimension and 6.26 Hz/point in the ω_1 -dimension. Characteristic inter-residual $d_{\alpha N(i,i+3)}$ and $d_{\alpha N(i,i+4)}$ connectivities are indicated by circles and labelled X_i/Y_{i+3} or X_i/Y_{i+4} . The corresponding intra-residual $NH_i-\alpha H_i$ connectivities are indicated by squares and labelled X_i .

Unfortunately it was not possible to analyze the NOESY spectrum of P25 in 10 mM sodium octadecaphosphate in the way as presented in Figure 4.1. In this spectrum only the resonances corresponding to the six first and three last residues of P25 were sharp. All other resonances were broadened due to various interactions between the phosphates and the positively charged residues of P25. Medium-range NOESY connectivities could not be assigned, but it was possible to determine the chemical shifts of the α -protons. Figure 4.3 shows the conformation-dependent chemical shifts of the α -protons of P25 in the presence of monophosphate, tetraphosphate and octadecaphosphate. These conformation-dependent chemical shifts were obtained by subtraction of the corresponding 'random-coil' chemical shifts (Bundi and Wüthrich, 1979) from the observed shifts.

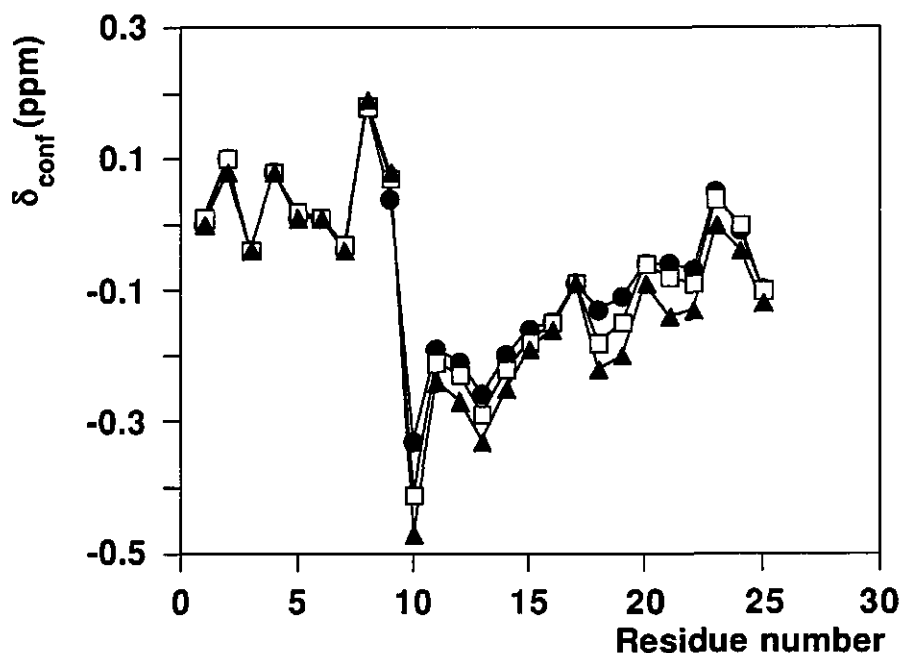


Fig. 4.3 Conformation-dependent chemical shifts (δ_{conf}) of the α -protons of P25 in the presence of monophosphate (●), tetraphosphate (□) and octadecaphosphate (▲) measured at 10°C. The conformation-dependent chemical shifts were obtained by subtraction of the corresponding 'random-coil' chemical shifts (Bundi and Wüthrich, 1979) from the measured chemical shifts.

Table 4.1 ^1H chemical shifts (ppm) of 6.9 mM P25 in 20 mM hexaammonium tetraphosphate, pH 5.0, 5°C.

Residue	NH	αH	βH	others	
(Ac)				Ac-CH ₃	2.08
Ser1	8.50	4.50	3.90, 3.85		
Thr2	8.46	4.44	4.30	γCH_3	1.22
Val3	8.27	4.13	2.10	γCH_3	0.97, 0.97
Gly4	8.68	4.05			
Thr5	8.27	4.36	4.30	γCH_3	1.23
Gly6	8.62	3.97			
Lys7	8.27	4.31	1.82, 1.75	γCH_2	1.44, 1.41
				δCH_2	1.68, 1.68
				ϵCH_2	2.99, 2.99
				ζNH_3^+	7.66 ^a
Leu8	8.42	4.58	1.68, 1.58	γCH	1.70
				δCH_3	0.88, 0.83
Thr9	8.68	4.41	4.67	γCH_3	1.33
Arg10	9.09	3.96	1.99, 1.88	γCH_2	1.78, 1.62
				δCH_2	3.26, 3.26
				ϵNH	7.53
Ala11	8.67	4.13	1.45		
Gln12	8.03	4.13	2.37, 2.02	γCH_2	2.46, 2.46
				δNH_2	7.63, 6.88
Arg13	8.74	4.07	1.96, 1.92	γCH_2	1.81, 1.61
				δCH_2	3.27, 3.19
				ϵNH	7.25
Arg14	8.42	4.15	1.91, 1.91	γCH_2	1.82, 1.71
				δCH_2	3.21, 3.21
				ϵNH	7.45
Ala15	8.03	4.16	1.49		
Ala16	7.99	4.20	1.47		
Ala17	7.92	4.26	1.50		
Arg18	7.98	4.20	1.92, 1.89	γCH_2	1.79, 1.68
				δCH_2	3.23, 3.23
				ϵNH	7.41
Lys19	8.07	4.20	1.90, 1.86	γCH_2	1.52, 1.46
				δCH_2	1.70, 1.70
				ϵCH_2	3.00, 3.00
				ζNH_3^+	7.66 ^a
Asn20	8.32	4.68	2.89, 2.81	γNH_2	7.75, 7.05
Lys21	8.22	4.26	1.91, 1.84	γCH_2	1.51, 1.46
				δCH_2	1.71, 1.71
				ϵCH_2	3.01, 3.01
				ζNH_3^+	7.66 ^a
Arg22	8.39	4.27	1.88, 1.84	γCH_2	1.70, 1.63
				δCH_2	3.22, 3.22
				ϵNH	7.34
Asn23	8.52	4.78	2.92, 2.84	γNH_2	7.78, 7.02
Thr24	8.25	4.33	4.28	γCH_3	1.22
Arg25	8.39	4.27	1.87, 1.79	γCH_2	1.67, 1.61
				δCH_2	3.21, 3.21
				ϵNH	7.30
(NHCH ₃)	7.97			CH ₃	2.75

^aThe Lys ζNH_3^+ resonance is broadened around 7.66 ppm due to exchange.

Distance Constraints

Since the NOESY connectivities shown in Figure 4.1 indicate that P25 has a more stable structure in 20 mM hexaammonium tetrphosphate than in 200 mM sodium monophosphate, distance constraints for distance geometry calculations were derived from a NOESY spectrum of P25 in the presence of tetrphosphate. The NOESY spectrum recorded at 5°C was used, because this spectrum showed less overlap than the NOESY spectrum recorded at 10°C. Table 4.1 presents the complete resonance assignment of the proton NMR resonances of P25 in 20 mM hexaammonium tetrphosphate pH 5, 5°C. Inter-residual NOE distance constraints and non-NOE distance constraints are presented in Appendix A and B (see supplementary material), respectively.

Distance Geometry Structures

During the generation of the eight DG structures some chiral centres had a 'floating chirality'. For each DG structure the chiral volumes of these centres were calculated to find out the positioning of the H1-H2 pairs. It turned out to be possible to assign the β -methylene protons of Arg14 stereospecifically, because the corresponding chiral volume showed a negative value in all eight structures. No further stereospecific assignments could be made. It should be noted that the procedure used only results in stereospecific assignments for protons which are situated in a region well defined by NOE constraints, which is the case for the β -methylene protons of Arg14.

Of each DG structure the conformation was analyzed according to the secondary structure determination procedure (Kabsch and Sander, 1983) present in the QUANTA/CHARMM software package. The results of this analysis (see Figure 4.4) show that the region between residues 10 and 16 has a helical character in all DG structures. After the eight structures had been superimposed on each other thereby optimizing the fit of the backbone atoms of residues 8 to 17, the root mean square deviations of the positions of these backbone atoms were calculated for all structure pairs to compare the backbone conformation in this region (see Table 4.2). Table 4.2 shows that the eight DG structures can be divided into two 'structure families': family 1 consisting of structures 1, 2, 3, 7 and 8 (Figure 4.5A) with an α -helix-like conformation, and family 2 consisting of structures 4, 5 and 6 (Figure 4.5B) with a more open conformation. The structure families were chosen in a such way that within the two families each rmsd value corresponding to a structure pair is smaller than the average rmsd value of 2.328 Å.

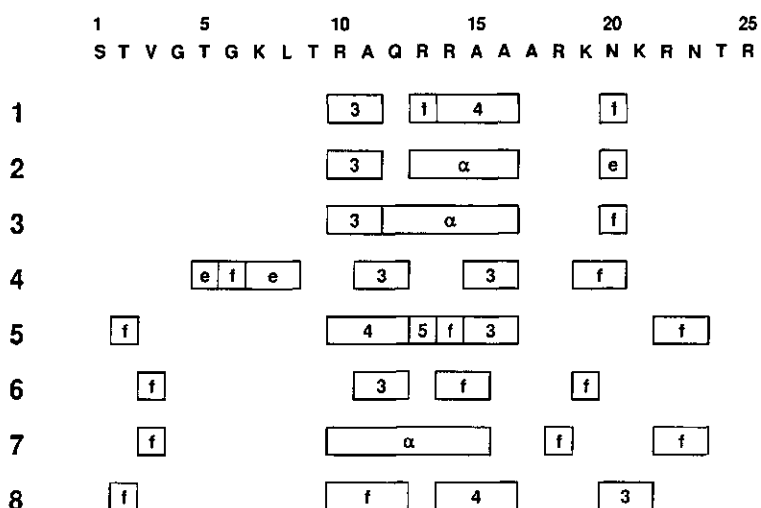


Fig. 4.4 Secondary structure elements present in the DG structures 1 - 8 as determined according to Kabsch and Sander (1983). Definitions used: e = extended: CA torsion between -180° and -130° , or CA torsion between -130° and -100° , $\phi < -100^\circ$ and $\psi > 100^\circ$; f = folded: two or more consecutive residues with CA torsions between 30° and 70° ; 3 = 3-turn: residues $i+1$ and $i+2$ are 3-turn if there exists H-bond $(i, i+3)$; 4 = 4-turn: residues $i+1$, $i+2$, and $i+3$ are 4-turn if there exists H-bond $(i, i+4)$; 5 = 5-turn: residues $i+1$, $i+2$, $i+3$, and $i+4$ are 5-turn if there exists H-bond $(i, i+5)$; α = α -helix: two or more consecutive 4-turns.

Table 4.2 Root mean square deviations (\AA) of the backbone atom positions in the region between residues 8 and 17 for all structure pairs of the eight DG structures.

structure nr.	1	2	3	7	8	4	5	6
1	0.000	1.136	1.221	0.779	1.064	3.174	2.962	3.156
2	1.136	0.000	0.964	0.813	1.857	3.594	3.154	3.405
3	1.221	0.964	0.000	1.181	1.597	3.190	3.439	3.276
7	0.779	0.813	1.181	0.000	1.475	3.313	2.998	3.240
8	1.064	1.857	1.597	1.475	0.000	2.836	3.219	3.166
4	3.174	3.594	3.190	3.313	2.836	0.000	2.324	1.140
5	2.962	3.154	3.439	2.998	3.219	2.324	0.000	1.501
6	3.156	3.405	3.276	3.240	3.166	1.140	1.501	0.000

average rmsd: 2.328 \AA

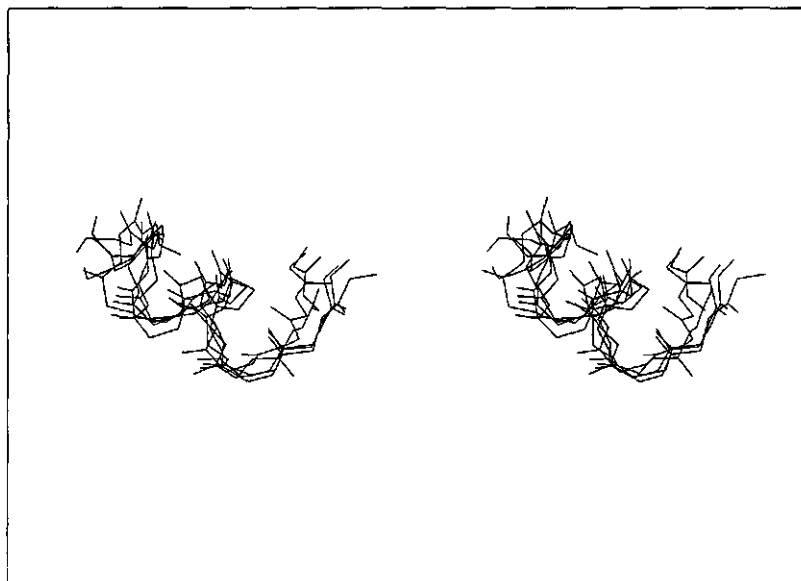
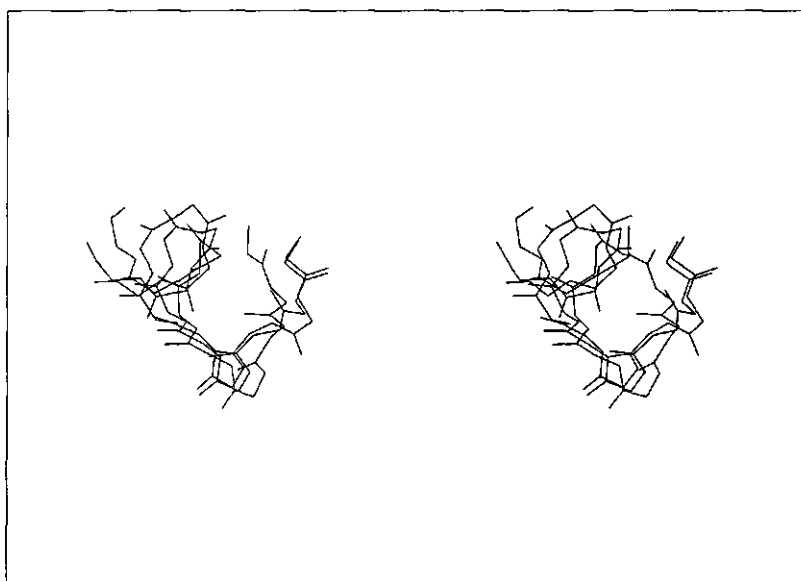
A**B**

Fig. 4.5 (A) Stereoview of a superposition of the backbone structures between residues 17 and 8 (from left to right) of the DG structures 1, 2, 3, 7, and 8. (B) Stereoview of a superposition of the backbone structures between residues 17 and 8 (from left to right) of the DG structures 4, 5, and 6.

Various DG structures were used as starting structures for molecular dynamics simulations in water using the CHARMM program to test the stability of the generated structures. Preliminary results show that structures with an open conformation in the middle of the peptide become α -helical and the other way round. Since no NOE restraints were applied during the simulations, it can be concluded that the region in the middle of the peptide shows a natural tendency to become α -helical.

DISCUSSION

In the study presented here the conformation of P25 in the presence of P, P₄, and P₁₈ was determined by two-dimensional proton NMR. In addition, NOE distance constraints obtained from the NOESY spectrum of P25 in the presence of P₄ were used to generate DG structures. Figure 4.1 shows medium-range NOESY connectivities characteristic of α -helical conformation present in NOESY spectra of P25 in 200 mM P (Figure 4.1A) and of P25 in 20 mM P₄ (Figure 4.1B). This figure shows that in the presence of P₄ the number of these characteristic NOEs and the region where they appear increase. It can be concluded that the α -helical conformation in P25 is stabilized by the presence of P₄ and that the helical region is extended into the direction of the C-terminus. For exactly the same region as where the characteristic NOEs appear (between residues 10 and 20) Vriend predicted α -helix formation upon neutralization of the positive charges in the Arg and Lys side chains (Vriend et al., 1986). The δ_{conf} values presented in Figure 4.3 provide additional information about the backbone conformation of P25 in the presence of P, P₄ or P₁₈. Negative δ_{conf} values of the α -proton resonances are indicative of an α -helical conformation (Szilágyi and Jardetzky, 1989; Wagner et al., 1983). The negative values between residues 10 and 20 suggest that in this region (particularly close to residue 10) an α -helical conformation is favoured, in agreement with the observed medium-range NOEs shown in Figure 4.1. Furthermore, it can be seen that the presence of oligophosphates of increasing length makes the δ_{conf} values of the α -proton resonances of P25 more negative indicating a more stable helical conformation.

A previous 2D-NMR study on P25 in 200 mM sodium phosphate has shown that under the conditions used P25 alternates among extended and more helical structures on the NMR time scale (Chapter 3). Since all NMR

parameters including the NOE intensities are a population-weighted average over all conformations sampled, it is generally not possible to generate distance geometry structures for such systems not violating the distance constraints based upon the NOESY spectrum. Indeed, an attempt to generate DG structures by using distance constraints derived from a NOESY spectrum of P25 in 200 mM sodium monophosphate gave no satisfying results. A possible solution for this problem could be the use of an ensemble averaging (comparable to time-averaging (Torda et al., 1989; 1990)) during the minimization of the error function in the distance geometry calculation generating an ensemble of structures simultaneously. However, since the NMR data indicated that the helical conformation of P25 in the presence of P_4 was stabilized, the distance constraints derived from a NOESY spectrum of P25 and P_4 were used and the error function of each structure was optimized in the normal way. The results show that the eight best DG structures can be divided into two 'structure families' (Figure 4.5) indicating that even in the presence of tetraphosphate P25 has no stable α -helical structure, but alternates between helical and more open conformations.

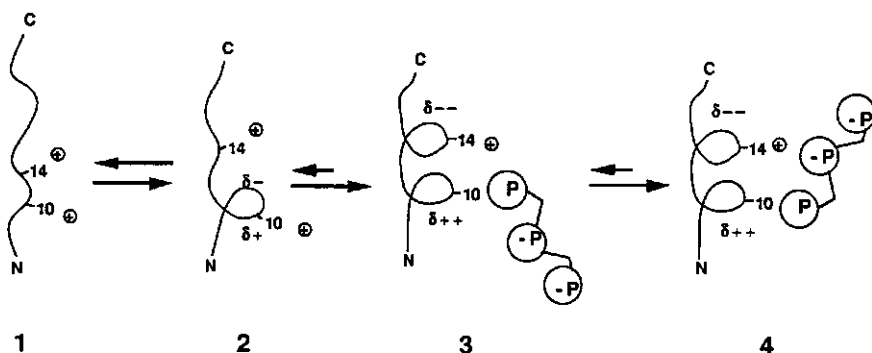


Fig. 4.6 Tentative model showing α -helix formation in the N-terminal part of CCMV coat protein induced by phosphate binding (see text).

Recent studies on P25 (Chapters 2 and 3) in combination with the present results enable an extension of the 'snatch-pull' model (Vriend et al., 1982; 1986) to a more detailed model for the assembly of CCMV coat protein and RNA (see Figure 4.6). It has been suggested before (Chapter 2) that

hydrogen bond formation between the side chains of Thr9 and Gln12 may initiate α -helix formation in P25. After the formation of the first helical turn (stage 2 in Figure 4.6), the positive charge of Arg10 in combination with the induced positive charge of the helix dipole attracts a negatively charged phosphate group. Binding of the phosphate group to the side chain of Arg10 removes an unfavourable interaction between the positive charge in the side chain of Arg10 and the macrodipole of the helix, which may lead to an extension of the helix in the direction of the C-terminus (stage 3 in Figure 4.6) (Hol, 1985; Shoemaker et al., 1985; 1987). The extension of the helical region results in the proper orientation of the next positively charged side chains for binding to the next phosphate groups of the RNA backbone (stage 4 in Figure 4.6). In this way, the RNA induces the conformation of the protein necessary for binding.

ACKNOWLEDGEMENTS

We thank Dr D. Hartmann and S. Keim for performing molecular dynamics simulations. All NMR experiments were carried out at the SON HF-NMR facility in Nijmegen (The Netherlands).

REFERENCES

- Bancroft, J. B. & Hiebert, E. (1967) *Virology* 32, 354-356.
- Bax, A. & Davis, D. G. (1985) *J. Magn. Reson.* 65, 355-360.
- Bodenhausen, G., Kogler, H. & Ernst, R. R. (1984) *J. Magn. Reson.* 58, 370-388.
- Bundi, A. & Wüthrich, K. (1979) *Biopolymers* 18, 285-297.
- Crippen, G. M. (1981) *Distance Geometry and Conformational Calculations*, Research Studies Press, New York.
- Crippen, G. M. & Havel, T. F. (1978) *Acta Cryst.* 34A, 282-284.
- Dasgupta, R. & Kaesberg, P. (1982) *Nucl. Acids Res.* 10, 703-713.
- Havel, T. F., Kuntz, I. D. & Crippen, G. M. (1983) *Bull. Math. Biol.* 45, 665-720.
- Hol, W. G. J. (1985) *Prog. Biophys. Molec. Biol.* 45, 149-195.
- Kabsch, W. & Sander, C. (1983) *Biopolymers* 22, 2577-2637.
- Kaptein, R., Boelens, R., Scheek, R. M. & Gunsteren, W. F. V. (1988) *Biochemistry* 27, 5389-5395.
- Marion, D. & Wüthrich, K. (1983) *Biochem. Biophys. Res. Commun.* 113, 967-974.

- Rance, M., Sørensen, O. W., Bodenhausen, G., Wagner, G., Ernst, R. R. & Wüthrich, K. (1983) *Biochem. Biophys. Res. Commun.* 117, 479-485.
- Shoemaker, K. R., Kim, P. S., Brems, D. N., Marqusee, S., York, E. J., Chaiken, I. M., Stewart, J. M. & Baldwin, R. L. (1985) *Proc. Natl. Acad. Sci. USA* 82, 2349-2353.
- Shoemaker, K. R., Kim, P. S., York, E. J., Stewart, J. M. & Baldwin, R. L. (1987) *Nature* 326, 563-567.
- Szilágyi, L. & Jardetzky, O. (1989) *J. Magn. Reson.* 83, 441-449.
- Ten Kortenaar, P. B. W., Krüse, J., Hemminga, M. A. & Tesser, G. I. (1986) *Int. J. Pept. Protein Res.* 27, 401-413.
- Torda, A. E., Scheek, R. M. & Van Gunsteren, W. F. (1989) *Chem. Phys. Letters* 157, 289-294.
- Torda, A. E., Scheek, R. M. & Van Gunsteren, W. F. (1990) *J. Mol. Biol.* 214, 223-235.
- Vriend, G., Hemminga, M. A., Verduin, B. J. M., de Wit, J. L. & Schaafsma, T. J. (1981) *FEBS Lett.* 134, 167-171.
- Vriend, G., Verduin, B. J. M. & Hemminga, M. A. (1986) *J. Mol. Biol.* 191, 453-460.
- Vriend, G., Verduin, B. J. M., Hemminga, M. A. & Schaafsma, T. J. (1982) *FEBS Lett.* 145, 49-52.
- Wagner, G., Pardi, A. & Wüthrich, K. (1983) *J. Am. Chem. Soc.* 105, 5948-5949.
- Weber, P. L., Morrison, R. & Hare, D. (1988) *J. Mol. Biol.* 204, 483-487.
- Williamson, M. P. & Madison, V. S. (1990) *Biochemistry* 29, 2895-2905.
- Wüthrich, K. (1986) *NMR of Proteins and Nucleic Acids*, Wiley, New York.
- Wüthrich, K., Billeter, M. & Braun, W. (1983) *J. Mol. Biol.* 169, 949-961.

APPENDIX A

NOE constraint list determined from a NOESY spectrum recorded with a mixing time of 100 ms of P25 in 20 mM hexaammonium tetrphosphate pH 5.0, 5°C. Symbols used: HN = NH; HA = α CH; HB = β CH; HG = γ CH; HD = δ CH or δ NH (Asn); HE = ϵ NH (Arg or Gln); MA = pseudo atom for α CH₂ of Gly; MB = pseudo atom for β CH₃ of Ala; MG = pseudo atom for γ CH₂ of Gln or for γ CH₃ of Thr; MD = pseudo atom for one of the two δ CH₃ groups of Leu; QG = pseudo atom for (γ CH₃)₂ of Val. Non-degenerate methylene protons, side-chain amide protons (Gln and Asn), and δ -methyl protons of Leu are labelled 1 (low field resonance) and 2 (high field resonance).

Residue	NOE constraint with		upper limit (Å)	lower limit (Å)
1 SER	HA	2 THR HN	3.35	2.35
2 THR	HN	3 VAL HN	3.60	2.60
2 THR	HA	3 VAL HN	3.15	2.15
3 VAL	HN	4 GLY HN	3.35	2.35
3 VAL	HA	4 GLY HN	2.75	1.75
3 VAL	QG	4 GLY HN	7.45	1.65
3 VAL	QG	4 GLY MA	9.00	1.20
4 GLY	MA	5 THR H	4.21	1.21
4 GLY	MA	5 THR MG	7.05	2.05
5 THR	HA	6 GLY HN	3.15	2.15
5 THR	MG	6 GLY HN	5.90	2.90
6 GLY	HN	7 LYS HN	3.15	2.15
6 GLY	MA	7 LYS HN	4.20	1.20
7 LYS	HA	8 LEU HN	2.75	1.75
7 LYS	HG1	8 LEU HN	3.90	2.90
7 LYS	HG2	8 LEU HN	3.90	2.90
8 LEU	HA	9 THR HN	2.95	1.95
8 LEU	HA	9 THR MG	5.55	2.55
8 LEU	HA	12 GLN HB1	4.15	3.15
8 LEU	HA	12 GLN HB2	4.15	3.15
8 LEU	HB1	9 THR HN	3.90	2.90
8 LEU	HB2	9 THR NH	3.35	2.35
8 LEU	HB2	12 GLN HB1	3.60	2.60
8 LEU	HB2	12 GLN HB2	3.60	2.60
8 LEU	HB2	12 GLN MG	5.62	2.62
8 LEU	MD1	12 GLN HB2	5.55	2.55
8 LEU	MD1	13 ARG HN	5.90	2.90
8 LEU	MD1	13 ARG HA	4.93	1.93

To be continued

Appendix A continued

Residue		NOE constraint with		upper limit (Å)	lower limit (Å)
8 LEU	MD1	16 ALA	MB	6.98	1.98
8 LEU	MD2	9 THR	HN	5.23	2.23
8 LEU	MD2	12 GLN	HB1	5.55	2.55
8 LEU	MD2	12 GLN	HB2	4.93	1.93
8 LEU	MD2	12 GLN	MG	7.44	2.44
8 LEU	MD2	12 GLN	HE1	5.90	2.90
8 LEU	MD2	12 GLN	HE2	5.55	2.55
8 LEU	MD2	13 ARG	HA	5.55	2.55
8 LEU	MD2	16 ALA	MB	7.79	2.79
9 THR	HN	12 GLN	HB1	3.15	2.15
9 THR	HN	12 GLN	HB2	3.60	2.60
9 THR	HN	12 GLN	HG2	4.98	1.98
9 THR	HA	10 ARG	HN	2.95	1.95
9 THR	HB	10 ARG	HN	3.35	2.35
9 THR	HA	11 ALA	MB	5.90	2.90
9 THR	MG	10 ARG	HN	5.55	2.55
9 THR	MG	12 GLN	MG	7.05	2.05
9 THR	MG	12 GLN	HE1	5.90	2.90
9 THR	MG	12 GLN	HE2	5.90	2.90
10 ARG	HN	11 ALA	HN	3.15	2.15
10 ARG	HA	11 ALA	HN	3.35	2.35
10 ARG	HA	13 ARG	HN	3.60	2.60
10 ARG	HA	14 ARG	HN	3.90	2.90
10 ARG	HA	13 ARG	HD2	4.15	3.15
10 ARG	HA	13 ARG	HE	4.15	3.15
10 ARG	HB1	11 ALA	HN	3.60	2.60
10 ARG	HB2	11 ALA	HN	3.35	2.35
11 ALA	HN	12 GLN	HN	3.15	2.15
11 ALA	MB	12 GLN	HN	4.65	1.65
11 ALA	MB	12 GLN	MG	7.05	2.05
12 GLN	HN	13 ARG	HN	2.95	1.95
12 GLN	HN	13 ARG	HD2	4.15	3.15
12 GLN	HA	13 ARG	HN	3.35	2.35
12 GLN	HB1	13 ARG	HN	3.60	2.60
12 GLN	HB2	13 ARG	HN	3.90	2.90
12 GLN	MG	13 ARG	HN	5.29	2.29
13 ARG	HN	14 ARG	HN	2.95	1.95

To be continued

Appendix A continued

Residue		NOE constraint with		upper limit (Å)	lower limit (Å)
13 ARG	HA	14 ARG	HN	3.35	2.35
13 ARG	HA	16 ALA	HN	3.60	2.60
13 ARG	HA	16 ALA	MB	4.65	1.65
13 ARG	HA	17 ALA	HN	4.15	3.15
14 ARG	HN	15 ALA	HN	2.95	1.95
14 ARG	HA	17 ALA	HN	3.60	2.60
14 ARG	HB1	15 ALA	HN	2.95	1.95
14 ARG	HB2	15 ALA	HN	4.15	3.15
15 ALA	HA	16 ALA	HN	3.35	2.35
16 ALA	HA	17 ALA	HN	3.15	2.15
16 ALA	MB	17 ALA	HN	4.65	1.65
16 ALA	MB	20 ASN	HD2	5.90	2.90
17 ALA	HA	18 ARG	HN	2.95	1.95
17 ALA	HA	20 ASN	HN	3.90	2.90
17 ALA	HA	20 ASN	HB1	3.60	2.60
17 ALA	HA	20 ASN	HB2	3.90	2.90
17 ALA	HA	20 ASN	HD1	4.15	3.15
17 ALA	MB	18 ARG	HN	4.40	1.40
18 ARG	HN	19 LYS	HN	3.35	2.35
19 LYS	HN	20 ASN	HN	3.15	2.15
19 LYS	HA	20 ASN	HN	2.95	1.95
20 ASN	HN	21 LYS	HN	3.15	2.15
20 ASN	HA	21 LYS	HN	3.15	2.15
20 ASN	HB1	21 LYS	HN	3.60	2.60
20 ASN	HB2	21 LYS	HN	3.60	2.60
21 LYS	HN	22 ARG	HN	3.60	2.60
22 ARG	HA	23 ASN	HN	2.95	1.95
23 ASN	HN	24 THR	HN	3.35	2.35
23 ASN	HN	25 ARG	HN	3.35	2.35
23 ASN	HA	24 THR	HN	3.35	2.35
23 ASN	HB1	24 THR	HN	4.15	3.15
23 ASN	HB2	24 THR	HN	3.90	2.90
24 THR	HA	25 ARG	HN	3.15	2.15

APPENDIX B

Non-NOE constraint list determined from a NOESY spectrum recorded with a mixing time of 100 ms of P25 in 20 mM hexaammonium tetrphosphate pH 5.0, 5°C. The symbols are identical to those used in appendix A.

Residue	non-NOE with	Residue	non-NOE with
8 LEU HA	10 ARG HN	10 ARG HA	12 GLN MG
8 LEU HB1	12 GLN HB2	10 ARG HA	12 GLN HE1
8 LEU HB2	11 ALA HN	10 ARG HG1	13 ARG HE
8 LEU HB2	12 GLN HA	10 ARG HE	13 ARG HE
8 LEU HB2	12 GLN HE1	11 ALA HN	13 ARG HG1
8 LEU HB2	12 GLN HE2	12 GLN HN	13 ARG HD1
8 LEU HG	12 GLN HA	12 GLN HB2	14 ARG HN
8 LEU HG	12 GLN HB2	12 GLN MG	13 ARG HD2
8 LEU HG	12 GLN HE1	12 GLN HE1	13 ARG HB2
8 LEU MD1	11 ALA HA	12 GLN HE1	13 ARG HD2
8 LEU MD2	10 ARG HN	13 ARG HA	16 ALA HA
9 THR HA	12 GLN HA	16 ALA HA	20 ASN HD2
9 THR HA	12 GLN HB1	17 ALA HN	20 ASN HB1
9 THR HA	12 GLN MG	17 ALA HA	19 LYS HN
9 THR HB	12 GLN MG	17 ALA HA	20 ASN HA
10 ARG HN	13 ARG HN	17 ALA MB	20 ASN HB1
10 ARG HN	13 ARG HD2	18 ARG HN	20 ASN HB1
10 ARG HA	12 GLN HB1	18 ARG HG1	19 LYS HN

CHAPTER 5

CONFORMATION AND MOBILITY OF THE RNA-BINDING N-TERMINAL PART OF THE INTACT COAT PROTEIN OF COWPEA CHLOROTIC MOTTLE VIRUS

A TWO-DIMENSIONAL PROTON NUCLEAR MAGNETIC RESONANCE STUDY

Marinette van der Graaf, Gerard J.A. Kroon, and Marcus A. Hemminga

ABSTRACT

Two-dimensional proton NMR experiments were performed on the coat protein of cowpea chlorotic mottle virus (molecular mass: 20.2 kDa) present as dimer (pH 7.5) or as capsid consisting of 180 protein monomers (pH 5.0). The spectra of both dimers and capsids showed resonances originating from the flexible N-terminal region of the protein. The complete resonance assignment of a synthetic pentacosapeptide representing this N-terminus made it possible to interpret the spectra in detail. The capsid spectrum showed backbone amide proton resonances arising from the first 8 residues having a flexible random coil conformation, and side-chain resonances arising from the first 25 N-terminal amino acids. The dimer spectrum showed also side-chain resonances of residues 26 to 33, which are flexible in the dimer but immobilized in the capsid. The NMR experiments indicated that the conformation of the first 25 amino acids of the protein in dimers and capsids is comparable to the conformation of the synthetic peptide, which alternates among extended and helical conformations on the NMR time scale. It is suggested that the α -helical region, situated in the region between residues 10 and 20, binds to the RNA during assembly of the virus particle.

INTRODUCTION

Cowpea chlorotic mottle virus (CCMV) is a spherical plant virus consisting of RNA surrounded by 180 identical protein subunits with a molecular mass of 20.2 kDa (Dasgupta and Kaesberg, 1982). The virus particle is stable around pH 5.0, but it can be dissociated into protein dimers

1985). However, these absolute value spectra have rather low resolution due to very broad lines. In the study reported here, the resolution of the 2D-NMR spectra of protein capsids is considerably improved as a result of new developments in NMR methodology.

The objective of the present study is to obtain detailed information about the structure and flexibility of the N-terminal region of the coat protein in capsids and dimers. It will be shown that the first 25 amino acids of the protein in both aggregation states have a conformation comparable to that of P25, and that the side chains of the residues 26 to 33 are more mobile in dimers than in capsids.

MATERIALS AND METHODS

(a) Sample preparation

CCMV was isolated and purified as described by Verduin (1978). The coat protein was separated from the RNA according to the CaCl_2 method (Verduin, 1974), and associated into empty capsids in 50 mM sodium acetate buffer (pH 5.0) containing 1 M sodium chloride, 1 mM sodium azide and 1 mM dithiothreitol. All NMR samples were prepared in measuring buffer, which is defined as buffer containing 300 mM sodium chloride, 10 mM magnesium chloride and 10 mM sodium phosphate, pH 5.0 or 7.5. After dialysis against measuring buffer pH 5.0, the empty capsids were concentrated by centrifugation (3 h at 180 000 g). The pellet containing the capsids was resuspended in 1 ml of measuring buffer made up in a mixture of 15%(v/v) $^2\text{H}_2\text{O}$ and 85%(v/v) H_2O or in almost pure $^2\text{H}_2\text{O}$, pH 5.0. For all solutions pH meter readings were taken without correction for the presence of $^2\text{H}_2\text{O}$. Centrifugation was repeated for the samples in $^2\text{H}_2\text{O}$ to substitute most H_2O by $^2\text{H}_2\text{O}$. In this way capsid samples with concentrations from 40 to 74 mg/ml were obtained. Dimer samples were prepared by dialysing capsid samples against measuring buffer pH 7.5. At high protein concentrations the solutions remained opalescent indicating that the capsids were not completely dissociated. Therefore, the dimer samples were diluted until the opalescence disappeared. The final concentrations were 31 mg/ml in 15%(v/v) $^2\text{H}_2\text{O}$ and 85%(v/v) H_2O , and 14 mg/ml in $^2\text{H}_2\text{O}$. To compare the spectra of intact protein with those of the synthetic N-terminus, a sample of 4 mM P25 was prepared in measuring buffer pH 5.0 made up in 15%(v/v) $^2\text{H}_2\text{O}$ and 85%(v/v) H_2O . Of all preparations 500 to 600 μl was used for the NMR experiments.

NMR experiments

The NMR spectra were recorded on a Bruker AM600 spectrometer operating at 600 MHz for protons. The carrier frequency was chosen in the middle of the spectrum coinciding with the water resonance. The water signal was suppressed by gated irradiation during the relaxation delay (2 s for intact protein and 2.5 s for P25) or in case of a NOESY experiment at all times, except during the data acquisition period. For the H₂O samples a saturation power at 8-20 dB attenuation of 0.2 Watt was used. For the samples in ²H₂O a saturation power at 35 dB attenuation of 0.2 Watt was sufficient.

All 2D-NMR spectra were acquired in the phase-sensitive mode using Time Proportional Phase Increments (Marion and Wüthrich, 1983). Spectral widths were generally about 10 ppm in the ω_1 -dimension and doubled to 20 ppm in the ω_2 -dimension to obtain a more flattened baseline at the position of the resonance peaks. After the first Fourier transformation the range of the spectrum containing the resonance peaks was selected and further processed. 2D-NMR spectra were recorded with 2k or 4k data points and 370 to 512 t_1 -increments. The number of scans per t_1 -increment varied between 40 and 96, dependent on the protein concentration in the sample. 1D-NMR spectra of intact protein were recorded with 128 scans of 8k data points. Two dummy scans were performed for both the 1D and 2D experiments.

NOESY spectra (Jeener et al., 1979; Macura and Ernst, 1980) using a mixing time of 100 ms were recorded of all samples. For the sample containing capsids in H₂O also a mixing time of 50 ms was used. No zero quantum filter technique was applied. A Clean TOCSY spectrum (Griesinger et al., 1988) was recorded of the sample containing capsids in H₂O. Delays of 2.6 times the duration of the 90° pulse were applied before and after the 180° pulses during the MLEV16 sequence to compensate for rotating frame cross-relaxation. The extended MLEV17 cycle was preceded and followed by 2.5-ms trim pulses to defocus magnetization not parallel to the spin-lock axis. The total mixing time was 24.7 ms. For P25 a Homonuclear Hartmann Hahn spectrum (Bax and Davis, 1985) was recorded with a 75-ms MLEV17 cycle preceded and followed by 2.5-ms trim pulses.

2D-NMR data were processed on a VAXstation 2000 using software kindly given by Dr R. Boelens. Free induction decays were generally multiplied by a sine-bell window function shifted by $\pi/6$ in both dimensions. In the case of the NOESY spectrum of dimers in ²H₂O, a squared sine-bell shifted by $\pi/10$ was used in t_2 -direction, because multiplication by this

window-function resulted in a better resolution in this spectrum. After zero filling and double Fourier transformation baseline corrections with a fourth order polynomial (Pearson, 1977) were performed in both dimensions. Digital resolution in the final transformed spectra was 3.13 Hz/point in the ω_2 -dimension and 6.26 Hz/point in the ω_1 -dimension. In case of the 1D-NMR experiments, a line broadening of 1 Hz was applied before zero filling. The final digital resolution was 1.57 Hz/point.

All NMR spectra were recorded at 10°C. Before and after every 2D-NMR experiment a 1D-NMR spectrum was recorded to check the stability of the protein solution. No indications for denaturation were observed. All chemical shifts refer to sodium 3-trimethylsilyl-(2,2,3,3- $^2\text{H}_4$) propionate, and were determined by taking the resonance of the N-terminal acetyl group (see Figure 5.1) as an internal standard at 2.08 ppm.

RESULTS

One-dimensional NMR experiments

The 600 MHz proton NMR spectra of dimers (Fig. 5.2A) and capsids (Fig. 5.2B) show several sharp resonances arising from the flexible N-terminal region of the coat protein (Fig. 5.1). The assignments indicated in Figure 5.2 are based upon chemical shift values (Bundi and Wüthrich, 1979) and upon comparison with the spectrum of P25 (Chapter 3). In the dimer spectrum the backbone amide proton resonances (a) are all broadened, and the resonances of the side-chain ϵN and guanidium protons (c,d) of the arginyl residues are absent. The corresponding protons have a higher rate of chemical exchange with the bulk water in the dimer sample (pH 7.5) than in the capsid sample (pH 5.0) (Wüthrich and Wagner, 1979). However, the resonances originating from the exchangeable side-chain amide protons of Gln and Asn (b) are clearly visible in both spectra. The resonances arising from the β -protons of Asn (e) and from the β and γ -protons of Gln (f) are sharper in the dimer spectrum than in the capsid spectrum. In addition, the dimer spectrum shows more intensity at the resonance positions of the β -proton of Val (g), the γ -protons of Val (h) and the δ -protons of Leu (i). The presence of more sharp resonances in the aliphatic region (0 - 5 ppm) of the dimer spectrum indicates that the N-terminal region is more flexible in the dimer than in the capsid.

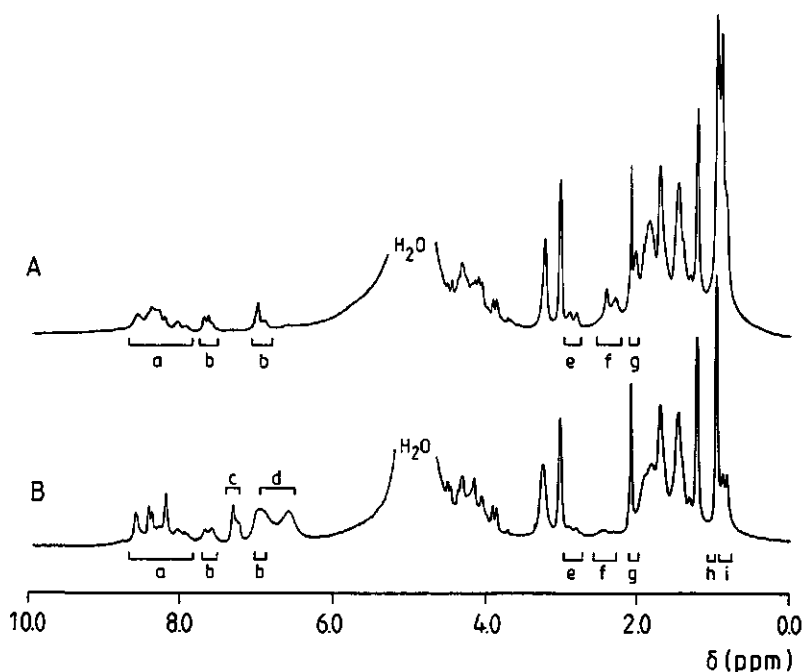


Fig. 5.2 600 MHz ^1H -NMR spectra of (A) 31 mg/ml dimers, and (B) 45 mg/ml capsids in measuring buffer in H_2O . The indices (a to i) refer to the resonance positions of the following protons: (a) backbone NH, (b) side-chain NH of Asn and Gln, (c) ϵNH of Arg, (d) guanidium protons of Arg, (e) βH of Asn, (f) βH and γH of Gln, (g) βH of Val, (h) γCH_3 of Val, and (i) δCH_3 of Leu.

Two-dimensional NMR experiments in H_2O

In this paragraph only the resonances assigned to water exchangeable protons will be discussed. Figure 5.3 shows the amide part of the NOESY spectrum of 45 mg/ml capsids in H_2O recorded with a mixing time of 50 ms. The indices (a-d) refer to the same spectral regions as in the 1D-NMR spectrum in Figure 5.2B. Between the resonance positions indicated by (b) two different cross peaks are observed: a very weak peak between the resonance positions 7.60 and 6.90 ppm, and a more intense one between the resonance positions 7.70 and 7.02 ppm. In accordance with the resonance assignment of P25 (Chapter 3), the weak cross peak was assigned to the δN -protons of Gln12 and the intense cross peak to the γN -protons of the asparagyl residues at positions 20 and 23. The resonances indicated by (c) and (d) were assigned to at least three different arginyl ϵNH protons and

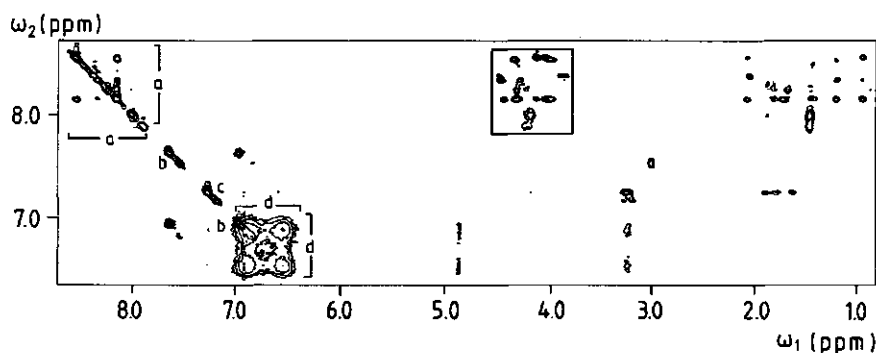


Fig. 5.3 Part of a 600 MHz NOESY spectrum of 45 mg/ml capsids in measuring buffer in H₂O recorded with a mixing time of 50 ms. A saturation power at 20 dB attenuation of 0.2 Watt was used to suppress the water signal. The time domain data consisted of 400 FIDs of 2k data points. N.B. this spectrum is rotated by 90° with respect to the other spectra presented. The characters (a) - (d) indicate the same spectral regions as in Figure 5.2B, and the spectral region indicated by a box is presented in more detail in Figure 5.4A.

mutual exchanging guanidium protons, respectively. The ϵ NH and guanidium proton resonances show weak cross peaks to each other and to the δ H₂-resonances around $\omega_1 = 3.2$ ppm. One ϵ NH-resonance gives also NOE cross peaks to the resonance positions of the γ - and β -protons of the arginyl residues ($\omega_1 = 1.6 - 1.9$ ppm). The cross peak between $\omega_2 = 7.6$ ppm and $\omega_1 = 3.0$ ppm (not indicated) is an intra-residual connectivity between a ζ NH₃⁺-resonance (ω_2) and an ϵ H-resonance (ω_1) of a lysine residue.

The part of Figure 5.3 containing the cross peaks between backbone NH and α H-resonances ($\omega_2 = 7.8 - 8.6$; $\omega_1 = 3.8 - 4.6$) is shown in detail in Figure 5.4A. The same region of a Clean-TOCSY spectrum of capsids is shown in Figure 5.4B. Both spectra show cross peaks between resonances which could be assigned to the extreme N-terminal region of the protein (see Table 5.1 and Fig. 5.1). Sequential assignments up to Thr5 were made by a combined interpretation of the NOESY spectrum (Figures 5.3 and 5.4A) and the Clean-TOCSY spectrum (Figure 5.4B). The resonances of Gly6, Lys7, and Leu8 could be assigned after comparison of the spectrum of capsids with that of P25. Apart from resonances originating from the first 8 residues Figure 5.5 shows some weak broadened cross peaks, which could not be assigned unambiguously.

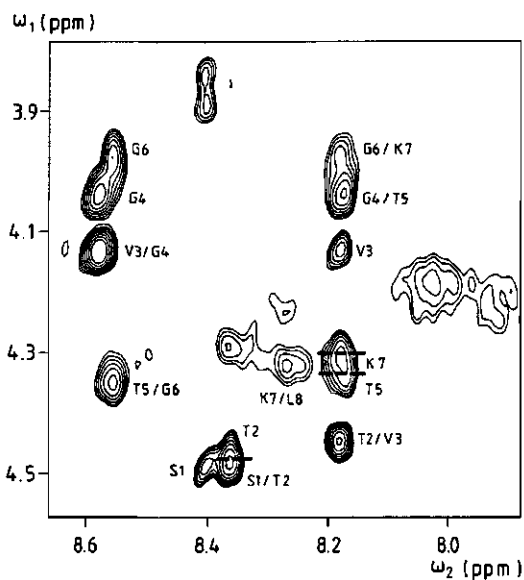


Fig. 5.4A Part of the 600 MHz NOESY spectrum of capsids presented in Figure 5.3. The intra-residual $\alpha\text{H}_i\text{-NH}_i$ cross peaks are labelled by a single code (X_i), and the sequential $\alpha\text{H}_i\text{-NH}_{i+1}$ cross peaks by a double code (X_i/Y_{i+1}).

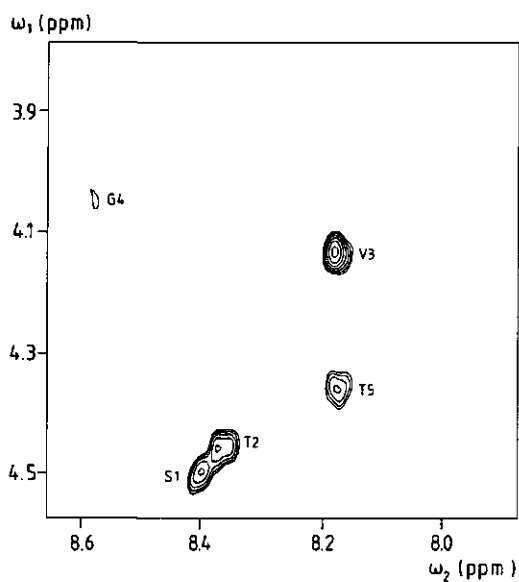


Fig. 5.4B The same spectral part of a 600 MHz Clean TOCSY spectrum of 43 mg/ml capsids in measuring buffer in H_2O . The total mixing time was 24.7 ms. A saturation power at 8 dB attenuation of 0.2 Watt was used to suppress the water signal. 375 FIDs of 2048 data points were recorded.

Table 5.1 NOE connectivities from the backbone amide protons of the first eight amino acids of CCMV coat protein assembled in capsids.

NH of residue:		intra-residual contacts ^a		inter-residual contacts ^{a,b}		
Ser1	(8.45)	α H	(4.51)	Ac	CH ₃	(2.08)
		β H ₂	(3.92, 3.87)			
Thr2	(8.40)	α H	(4.46)	Ser1	α H	(4.51)
		β H	(4.31)	Val3	γ CH ₃	(0.97)
		γ CH ₃	(1.22)			
Val3	(8.21)	α H	(4.15)	Thr2	α H	(4.46)
		β H	(2.10)	Thr2	β H	(4.31)
		γ CH ₃	(0.97)			
Gly4	(8.61)	α H	(4.06)	Val3	α H	(4.15)
				Val3	β H	(2.10)
Thr5	(8.21)	α H	(4.36)	Gly4	α H	(4.06)
		γ CH ₃	(1.23)			
Gly6	(8.59)	α H	(4.00)	Thr5	α H	(4.36)
				Thr5	γ CH ₃	(1.23)
Lys7	(8.21)	α H	(4.34)	Gly6	α H	(4.00)
Leu8	(8.39)	δ CH ₃	(0.89)	Lys7	α H	(4.34)

The NOE connectivities are obtained from the NOESY spectrum of 45 mg/ml capsids recorded with a mixing time of 50 ms at 10°C. Chemical shift values (ppm) are presented between brackets. ^a If a cross peak could be assigned to both an intra-residual and an inter-residual NOE, it was assigned to an intra-residual NOE which is more likely to appear (Wüthrich, 1986). ^b In addition to the inter-residual connectivities presented in this table, the two following NH-NH contacts are present: (1) from Thr2 to Val3, Thr5 or Lys7, and (2) from Gly4 or Gly6 to Val3, Thr5 or Lys7. Since those contacts could not be assigned uniquely, they are not presented in this table.

After the sequential assignment of the first 8 N-terminal amino acids the NOESY spectrum was searched for medium range connectivities, which could supply secondary structure information. However, all assigned inter-residual cross peaks between NH-resonances and side-chain proton resonances appeared to be sequential (see Table 5.1). The rather intense sequential cross peaks between α H_{*i*} and NH_{*i+1*} are characteristic of extended structures and the two NH-NH cross peaks (see Fig. 5.3 and footnote *b* to Table 5.1) are characteristic of folded structures (Wüthrich, 1986). The simultaneous

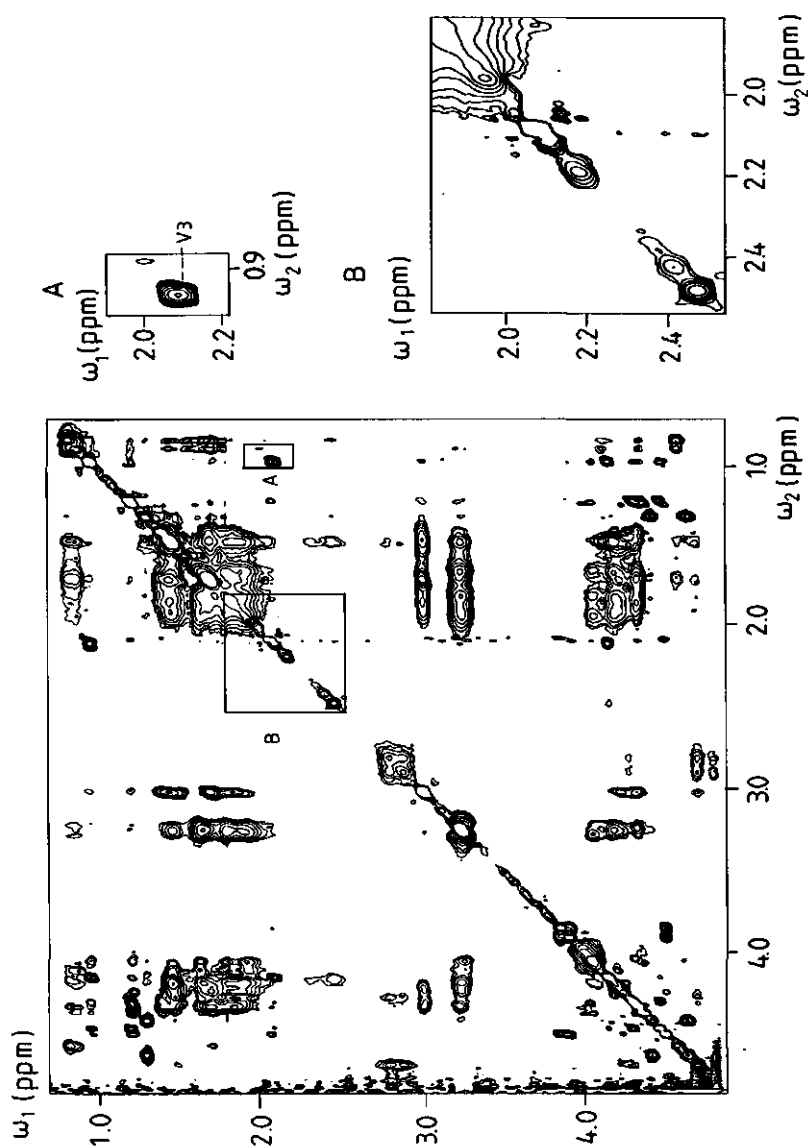


Fig. 5.5 600 MHz NOESY spectrum of 55 mg/ml capsids in measuring buffer in $2\text{-H}_2\text{O}$ recorded with a mixing time of 100 ms. A saturation power at 35 dB attenuation of 0.2 Watt was used to suppress the water signal. The time domain data consisted of 372 FIDs of 2k data points. Two spectral regions indicated by (A) and (B) are enlarged to allow comparison of these regions with the comparable regions of the NOESY spectrum of dimers in Figure 5.6.

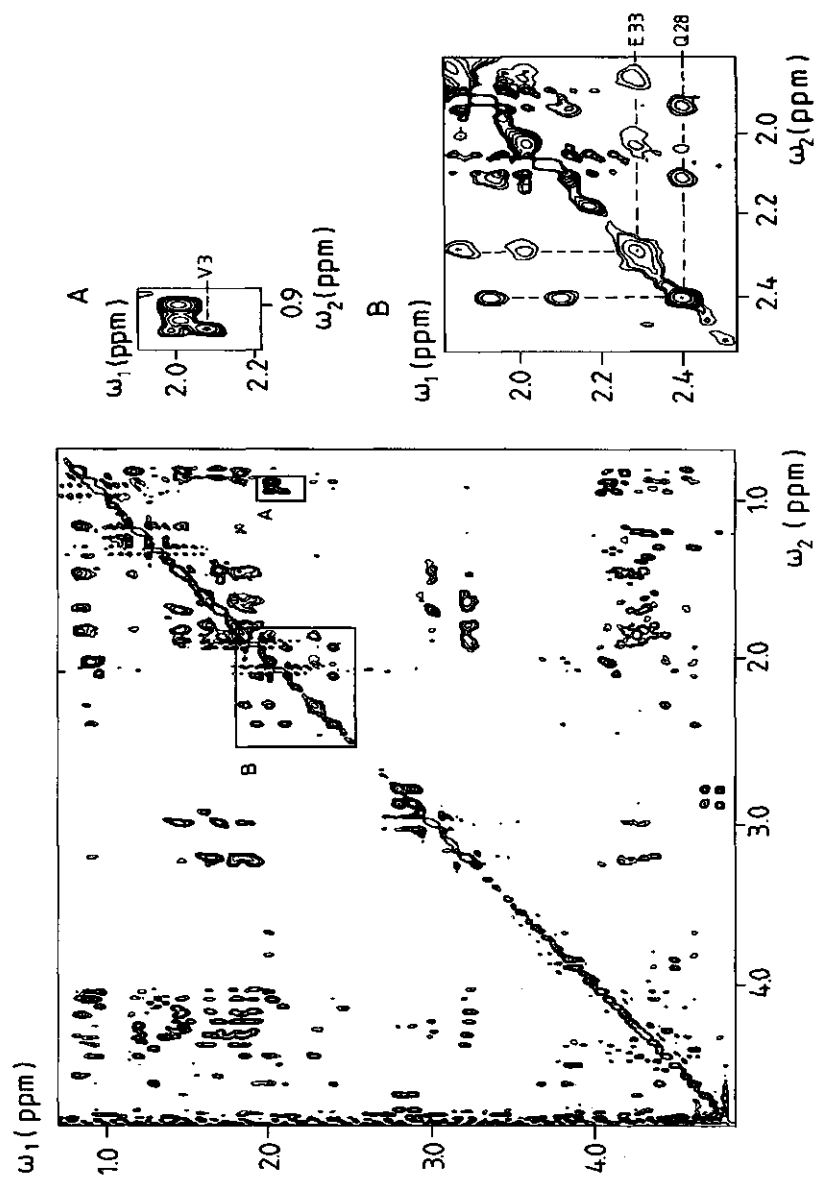


Fig. 5.6 600 MHz NOESY spectrum of 14 mg/ml capsids in measuring buffer in $2\text{-H}_2\text{O}$ recorded with a mixing time of 100 ms. A saturation power at 35 dB attenuation of 0.2 Watt was used to suppress the water signal. 380 FIDs of 2k data points were recorded. Spectral region (A) shows cross peaks between βH and γCH_3 of the valyl residues, and region (B) shows intra-residual cross peaks between βH_2 and γH_2 of Gln28 and Glu33.

presence of these two types of cross peaks with comparable intensity indicates that the extreme N-terminal part of the coat protein associated in capsids rapidly alternates among extended and more folded conformations (Wright et al., 1988).

The NOESY spectrum of dimers in H_2O (not presented) showed only very weak broadened cross peaks between backbone NH-resonances and side-chain proton resonances due to the high exchange rate of the backbone amide protons with the bulk water at pH 7.5. However, four relatively sharp cross peaks between the resonance positions of the side-chain amide protons of Asn and Gln were present. In addition to the cross peaks which were also observed for capsids, a rather sharp cross peak between the NH-resonances at 6.96 and 7.63 ppm was present. Both these NH-resonances showed sharp cross peaks to a ω_1 -resonance at 2.41 ppm (the γH resonances position of Gln), indicating that in dimers an additional Gln is flexible enough to give rise to observable resonances. Furthermore, weaker cross peaks from these NH-resonances to two different ω_1 -resonances around 0.9 ppm (the resonance position of methyl protons of Leu, Val or Ile) are present. This indicates that the additional Gln must be in close proximity of Leu, Val or Ile.

Two-dimensional NMR experiments in 2H_2O

The NOESY spectrum of capsids in 2H_2O (Fig. 5.5) strongly resembles that of the synthetic P25. This corroborates the theory that only the first 25 N-terminal amino acids of the coat protein in capsids have enough flexibility to give rise to observable resonances (Vriend et al., 1981). A detailed comparison of the two spectra reveals three major differences: Firstly, the resonances in the capsid spectrum are more broadened, especially in the region from Leu8/Thr9 to Arg25. Secondly, the αH -resonance of Arg25 has shifted from 4.29 ppm in P25 to 4.41 ppm in capsids. Thirdly, no cross peaks between the aliphatic side-chain protons of Gln12 are visible in the capsid spectrum (see Figure 5.5B), whereas the spectra of P25 clearly show cross peaks between the γH_2 -resonances (2.45, 2.45 ppm) and the βH_2 -resonances (2.03, 2.29 ppm) of Gln12.

The NOESY spectrum of dimers in 2H_2O (Fig. 5.6) shows sharper and more cross peaks than the capsid spectrum (Fig. 5.5). Figure 5.6A shows five cross peaks (with two overlapping cross peaks giving rise to the most intense peak at $\omega_2 = 0.9$ ppm) between the resonance positions of the β - and γ -protons of valyl residues, whereas Figure 5.5A shows only one cross peak assigned to Val3. The additional valyl resonances are assigned to valines at

the positions 26, 27, 30 and 32 (see Fig. 5.1). Figure 5.6B shows cross peaks in the spectral region between 1.8 and 2.5 ppm, whereas the same region of the spectrum of capsids (Figure 5.5B) shows no cross peaks at all. The chemical shift positions and the spin patterns of the resonances present in Figure 5.6B are characteristic of β - and γ -protons of Gln or Glu (Bundi and Wüthrich, 1979). Both γH_2 -resonances (at 2.41 and 2.30 ppm, respectively) show cross peaks to γCH_3 -resonances of valines in the region 26 - 32 (see above), indicating that the resonances must be assigned to Gln28 and Glu33. NOEs between side-chain NH-resonances and the resonance at 2.41 ppm make clear that the resonances at 2.41, 2.11 and 1.94 ppm arise from Gln28, and that the resonances at 2.30, 2.04 and 1.87 ppm arise from Glu33. In addition, resonances of Pro29 (βH and/or γH_2 2.02 ppm; δH_2 3.82 and 3.67 ppm) and Ile31 (αH 4.21 ppm; βH 1.84 ppm; γCH_2 1.48 and 1.18 ppm; γCH_3 0.90 ppm; δCH_3 0.86 ppm) can be observed in the dimer spectrum. Thus, side-chain proton resonances arising from amino acids up to and including residue 33 are present in the NOESY spectrum of dimers.

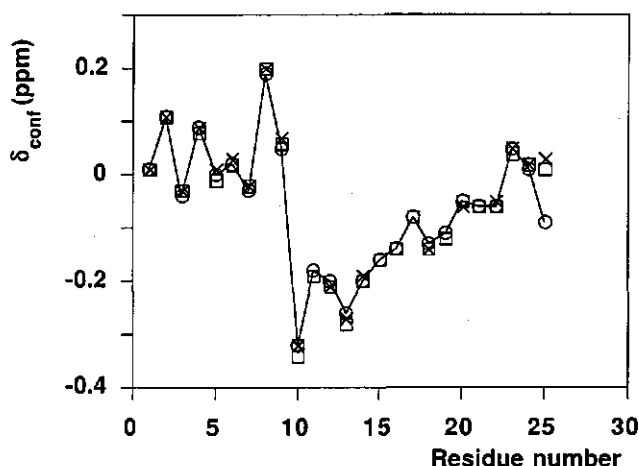


Fig. 5.7 Conformation-dependent chemical shifts (δ_{conf}) of the α -protons as function of the residue numbers for P25 (\circ), dimers (\square), and capsids (\times). The conformation-dependent chemical shifts were calculated by subtraction of the corresponding 'random-coil' chemical shifts (Bundi and Wüthrich, 1979) from the measured chemical shifts. The αH chemical shift values of P25 were obtained from a Homonuclear Hartmann Hahn spectrum of P25 in measuring buffer pH 5.0, 10°C. The αH chemical shift values of capsids and dimers were obtained from the NOESY spectra presented in Figure 5.5 and 5.6, respectively. For capsids, the αH resonance positions of Ala11, Ala15, Ala16, Ala17, Lys19 and Lys21 could not be determined due to overlap problems.

Since no medium range NOEs could be assigned unambiguously, chemical shift information was used to gain insight into the secondary structure of the N-terminal region in CCMV coat protein. Figure 5.7 shows the conformation-dependent chemical shifts of the α -protons of the first 25 residues in P25, dimers, and capsids. The δ_{conf} values were calculated by subtraction of the corresponding 'random-coil' chemical shifts (Bundi and Wüthrich, 1979) from the measured chemical shifts. Figure 5.7 shows that several δ_{conf} values of the α -protons deviate from zero, indicating that some secondary structure is present. The δ_{conf} values of the α -protons of the first 24 residues of P25, dimers and capsids almost coincide, but the δ_{conf} values of the α -proton of Arg25 in P25 differs from those in dimers and capsids. This indicates that the first 24 residues have comparable conformations in P25, dimers, and capsids. The difference observed for residue 25 can be explained by the fact that Arg25 is the terminal residue in P25, while it is attached to the protein core in dimers and capsids.

DISCUSSION

The NMR study on CCMV coat protein presented here is an extension of previous work by our group (Vriend et al., 1981, 1985, 1986). The phase sensitive 2D-NMR spectra (Figures 5.3-5.6) have much better resolution than the absolute value NOESY spectrum of capsids presented previously (Vriend et al., 1985), because the lines are not broadened by dispersive components (Marion and Wüthrich, 1983). In addition, the excellent sensitivity of the spectrometer made it possible to use protein concentrations as low as 14 mg/ml with lower viscosities as compared to the previous experiments.

Vriend et al. (1981) have demonstrated that the sharp resonances in the proton NMR spectrum of capsids are absent after removal of the first 25 N-terminal amino acids by tryptic digestion or after binding to RNA. This shows that the sharp resonances in the NMR spectrum arise from the flexible N-terminal region, which is immobilized after RNA-binding. The complete resonance assignment of P25 (Chapter 3) was necessary to be able to interpret the spectra of intact coat protein. This 2D-NMR study on P25 in 200 mM sodium phosphate (pH 4) has shown that P25 alternates among helical and extended backbone conformations on the NMR time scale. Under the conditions used a significant fraction of the accessible conformations of P25 consists of structures with an α -helical conformation between the residues 9

and 17, likely starting with a turn-like structure around Thr9 and Arg10. The presence of helical conformation in P25 was indicated by high-field shifts of α H-resonances (see Fig. 5.7), and the presence of sequential NH-NH and characteristic medium range NOEs (Chapter 3).

The δ_{conf} values of the α -protons of the first 24 residues of P25, dimers and capsids (Fig. 5.7) indicate that the conformation of the first 24 amino acids must be comparable in all cases. Negative δ_{conf} values of α -protons are indicative for an α -helical conformation (Szilágyi and Jardetzky, 1989; Wagner et al., 1983). This suggests that in the conformational equilibrium an α -helical conformation between the residues 10 and 20 (particularly close to residue 10) is favoured. The cross peaks between the side-chain proton resonances of Gln12 are broadened beyond detection in the spectra of dimers and capsids. This broadening can be explained by a reduced mobility by α -helix formation. Also the δ -protons of Arg13 are affected by α -helix formation in all three spectra; these δ -protons give rise to two distinct resonances indicating that each proton experiences its own environment.

It has been shown for brome mosaic virus, a bromovirus closely related to CCMV, that the residues 11-19 are involved in RNA-binding (Sgro et al., 1986). Since the amino acid sequence in the region 9-18 of the coat protein is identical for both viruses, it is suggested that this region binds in an α -helical conformation to the RNA. This conformation is in agreement with previous secondary structure predictions (Argos, 1981; Vriend et al., 1986).

In capsids only the backbone amide protons of the first 8 residues give rise to observable resonances (see the Figures 5.2-5.4). According to the δ_{conf} values of these residues (Fig. 5.7) and the conformation of P25 (see Chapter 3), it is suggested that this extreme N-terminal region of CCMV coat protein has a flexible random coil conformation. This is in agreement with the NOEs $\alpha\text{H}_i\text{-NH}_{(i+1)}$ and NH-NH observed for capsids (Fig. 5.3 and Table 5.1), which indicate that this region alternates among extended and more folded structures. Backbone amide proton resonances of other residues in the N-terminal region are broadened because of a reduced mobility. Unfortunately, it was not possible to obtain information about the flexibility and conformation of the backbone amide protons in dimers. At the pH value necessary to dissociate the capsids into dimers (pH 7.5) the exchange rate of the backbone amide protons with the bulk water is so high that the corresponding resonances are extremely broadened (see Fig. 5.2A).

In the dimer spectrum (Figure 5.6) resonances originating from side-chain protons of residues 26-33 are present, whereas those resonances are

absent in the capsid spectrum (Figure 5.5). This indicates that these residues are flexible in dimers, but immobilized in capsids. Since previous secondary structure predictions suggested a β -structure for the region 25-32 (Vriend, 1983), these residues may be immobilized by β -sheet formation. The difference in flexibility in dimers and capsids of these mostly aliphatic residues is in agreement with the results of a laser Raman study on CCMV coat protein showing a change in environment of aliphatic amino acid side chains with capsid disassembly (Verduin et al., 1984). The amino acid sequence in the region 28-34 is identical in the coat protein of all three bromoviruses CCMV, brome mosaic virus, and broad bean mottle virus (Verduin, personal communication), suggesting an essential role of this region in the formation of capsid structure. The carboxyl group of Glu33 may play a role in the pH-dependent association of the coat protein. Neutralization of this acidic residue by low pH or by the presence of positively charged bases of the RNA (Verduin et al., 1984) possibly allows the formation of β -structure, which changes the conformational alignment of two protein subunits to the alignment necessary for capsid formation.

Both dimer and capsid have very slow overall motions. The rotational correlation time of the dimer can be estimated to be about 2.2×10^{-8} s, as calculated from the Stokes-Einstein equation, and the value for the capsid is 2×10^{-6} s. However, the linewidths in the spectra show that the N-terminal arm is more flexible with a correlation time between 10^{-9} and 10^{-8} s. This is in agreement with a ^{13}C -NMR relaxation study on capsids indicating correlation times of about 3×10^{-9} s for almost all amino acids in the N-terminal region of the protein (Vriend, 1983). The slow overall motions of dimers and capsids make it impossible to obtain structural information about the core protein by high resolution NMR. However, the study presented shows that detailed information about the conformation and flexibility of the mobile N-terminal region of CCMV coat protein can be obtained by high resolution 2D NMR.

ACKNOWLEDGEMENTS

We thank the department of Virology for the kind gift of CCMV infection material and for the use of their green house. We thank Dr B.J.M. Verduin for stimulating discussions, and C.J.A.M. Wolfs for assistance in isolation and purification of the CCMV coat protein. We especially thank the SON NMR facility Nijmegen (The Netherlands), where all NMR experiments were performed.

REFERENCES

- Argos, P. (1981) *Virology* 110, 55-62.
- Bancroft, J. B. & Hiebert, E. (1967) *Virology* 32, 354-356.
- Bancroft, J. B., Wagner, G. W. & Bracker, C. E. (1968) *Virology* 36, 146-149.
- Bax, A. & Davis, D. G. (1985) *J. Magn. Reson.* 65, 355-360.
- Bundi, A. & Wüthrich, K. (1979) *Biopolymers* 18, 285-297.
- Dasgupta, R. & Kaesberg, P. (1982) *Nucl. Acids Res.* 10, 703-713.
- Griesinger, C., Otting, G., Wüthrich, K. & Ernst, R. R. (1988) *J. Am. Chem. Soc.* 110, 7870-7872.
- Jeener, J., Meier, B. H., Bachmann, P. & Ernst, R. R. (1979) *J. Chem. Phys.* 71, 4546-4553.
- Macura, S. & Ernst, R. R. (1980) *Molec. Phys.* 41, 95-117.
- Marion, D. & Wüthrich, K. (1983) *Biochem. Biophys. Res. Commun.* 113, 967-974.
- Pearson, G. A. (1977) *J. Magn. Reson.* 27, 265-272.
- Sgro, J., Jacrot, B. & Chroboczek, J. (1986) *Eur. J. Biochem.* 154, 69-76.
- Szilágyi, L. & Jardetzky, O. (1989) *J. Magn. Reson.* 83, 441-449.
- Ten Kortenaar, P. B. W., Krüse, J., Hemminga, M. A. & Tesser, G. I. (1986) *Int. J. Pept. Protein Res.* 27, 401-413.
- Verduin, B. J. M. (1974) *FEBS Lett.* 45, 50-54.
- Verduin, B. J. M. (1978) *J. Gen. Virol.* 39, 131-147.
- Verduin, B. J. M., Prescott, B. & Thomas, G. J., Jr. (1984) *Biochemistry* 23, 4301-4308.
- Vriend, G. (1983) Ph.D. Thesis, Agricultural University Wageningen, The Netherlands, Chapters 7 and 9.
- Vriend, G., Hemminga, M. A., Haasnoot, C. A. G. & Hilbers, C. W. (1985) *J. Magn. Reson.* 64, 501-505.
- Vriend, G., Hemminga, M. A., Verduin, B. J. M., de Wit, J. L. & Schaafsma, T. J. (1981) *FEBS Lett.* 134, 167-171.
- Vriend, G., Verduin, B. J. M. & Hemminga, M. A. (1986) *J. Mol. Biol.* 191, 453-460.
- Wagner, G., Pardi, A. & Wüthrich, K. (1983) *J. Am. Chem. Soc.* 105, 5948-5949.
- Wright, P. E., Dyson, H. J. & Lerner, R. A. (1988) *Biochemistry* 27, 7167-7175.
- Wüthrich, K. (1986) *NMR of Proteins and Nucleic Acids*, Wiley, New York, Chapters 7-9.
- Wüthrich, K. & Wagner, G. (1979) *J. Mol. Biol.* 130, 1-18.

CHAPTER 6

CONFORMATIONAL CHANGES IN OLIGONUCLEOTIDES UPON BINDING TO A PEPTIDE REPRESENTING THE N-TERMINAL REGION OF CCMV COAT PROTEIN

AN OPTICAL SPECTROSCOPY STUDY

Marinette van der Graaf, Cor J. A. M. Wolfs, and Marcus A. Hemminga

ABSTRACT

Conformational changes of the oligonucleotides $r(A)_{12}$, $d(GC)_5$, and $d(AT)_5$ upon binding to a pentacosapeptide representing the RNA-binding N-terminus of the coat protein of cowpea chlorotic mottle virus were studied by using absorption and circular dichroism spectroscopy. The peptide has only a minor effect on the single-stranded structure of $r(A)_{12}$ at pH 7.2, but disrupts the double-stranded structure of $r(A)_{12}$ at pH 5.0. However, at pH 4.0, the peptide is not able to disrupt this double-stranded structure. The double-stranded structures of $d(GC)_5$ and $d(AT)_5$ with Watson-Crick base-pairing are stabilized upon binding to the peptide. All conformational changes observed indicate that the positively charged side chains of the peptide have strong electrostatic interactions with the negatively charged phosphate groups of the oligonucleotides.

INTRODUCTION

Cowpea chlorotic mottle virus (CCMV) is a spherical bromovirus, consisting of RNA and 180 identical coat proteins, each 189 residues long (Dasgupta and Kaesberg, 1982). It has been shown (Vriend et al., 1981) that the first 25 N-terminal amino acids are essential for RNA binding. The positively charged side chains of six arginines and three lysines present in this part of the protein (see Chapter 1) are suggested to bind to the negatively charged phosphates of the RNA backbone. Secondary structure predictions (Vriend et al., 1986), and CD and NMR experiments on the synthetic peptide P25 representing the N-terminus of CCMV coat protein (see Chapters 2 to 5)

have shown that the region between residues 10 and 20 of the coat protein has the tendency to adopt an α -helical conformation upon neutralization of the positively charged side chains. This is in agreement with the 'snatch-pull' model proposed for the assembly of CCMV coat protein and RNA (Vriend et al., 1982, 1986), in which model the N-terminal region of CCMV coat protein attains an α -helical conformation upon RNA binding. Although it has been suggested that nucleotides must have a double-stranded structure for binding to the N-terminal region of CCMV coat protein (Hemminga et al., 1985; Vriend et al., 1986), no detailed information about the conformation of the RNA in the complex has been obtained so far. The objective of the present study is to determine the effect of protein binding on the RNA by studying the effect of P25 on the stability and conformation of various oligonucleotides.

MATERIALS AND METHODS

Samples

r(A)₁₂ was obtained from P.L. Biochemicals, and d(AT)₅ and d(GC)₅ have been synthesized by H. van den Elst (University of Leiden, the Netherlands). The N-terminal pentacosapeptide of the coat protein of CCMV was available as the chemically synthesized N α 1-acetyl, C α 25-methylamide P25 (Ten Kortenaar et al., 1986). All other chemicals used were from Sigma and of analytical grade. Nucleotide concentrations were determined spectrophotometrically at pH 7.2 using the following molar extinction coefficients (per nucleotide residue): r(A)₁₂, 12 500 M⁻¹cm⁻¹ at 260 nm according to a phosphorus determination (Bartlett, 1959); d(AT)₅, 6 650 M⁻¹cm⁻¹ at 262 nm as given for poly(AT) by Inman and Baldwin (1962); and d(GC)₅, 8 400 M⁻¹cm⁻¹ at 254 nm as given for poly(GC) by Wells et al. (1970). Peptide concentrations were determined by a bicinchoninic acid assay (Smith et al., 1985). For titration experiments, small volumes of a stock solution containing 0.5 mg/ml P25 were added to a sample volume of 1 ml containing oligonucleotide to vary the ratio N/P. This ratio N/P is defined as number of nucleotides residues per peptide.

UV absorption and melting experiments

UV absorption spectra and melting curves were recorded on a Kontron Uvikon 810 spectrophotometer interfaced with a Commodore PC30 AT computer. For all experiments a 1.0 ml cuvette with a 1-cm light path was

used. UV absorption spectra were recorded at room temperature in double beam mode. Melting curves were recorded in single beam mode. The temperature of the thermostated cuvette housing was controlled by a LKB Multitemp water bath, and the temperature was monitored by a thermocouple placed in the reference cuvette. Temperature and OD were measured every 30 seconds. The increase in OD upon melting was recorded at $\lambda_{\max} = 260$ nm for d(AT)₅, and at 275 nm for d(GC)₅. For d(GC)₅ the OD shows a larger hyperchromic effect upon melting at 275 nm than at $\lambda_{\max} = 257$ nm.

Circular dichroism experiments

CD spectra were measured at room temperature on a Jobin-Yvon Auto-Dichrograph Mark V spectrometer interfaced with an AT Genisys microcomputer. A home written computer program in ASYST 3.1 (Asyst Software Technologies) was used for data collection. Each spectrum is the result of the average of two scans recorded of one sample minus the average of two scans of a reference sample containing an identical buffer solution without nucleotide and peptide. For all experiments a 1-ml sample cuvette with a light path of 1 cm was used.

RESULTS

The effect of P25 on the conformation and stability of r(A)₁₂

Like poly(rA), r(A)₁₂ exists as a single stranded helix at neutral pH, and as a stacked double-stranded helix with parallel strands at pH ≤ 5.8 (Causley and Johnson, 1982; Saenger, 1984). Figure 6.1A shows the UV absorption spectrum of r(A)₁₂ in the single stranded form at pH 7.2 with λ_{\max} at 257 nm. At this neutral pH, addition of P25 has no significant effect on the absorption spectrum of the oligo-ribonucleotide. Figure 6.1B shows the UV absorption spectrum of r(A)₁₂ in the double stranded form at pH 5.0. The absorption maximum has shifted to 252 nm and the intensity of the absorption peak has decreased as result of stacking interactions between the bases in the double-stranded helix. At pH 5.0, addition of P25 (up to N/P = 4-5) results in an increased absorbance and a shift of λ_{\max} to longer wavelengths (up to 257 nm).

The CD spectra of r(A)₁₂ at pH 7.2 (Figure 6.2A) and at pH 5.0 (Figure 6.2B) are comparable to the spectra of poly(rA) at neutral and acidic pH (Causley and Johnson, 1982). At pH 7.2, the CD spectrum of r(A)₁₂ in the

single-stranded form shows a slight decrease in intensity upon addition of P25, but the shape of the spectrum remains the same (see Figure 6.2A). At pH 5.0, however, both intensity and shape of the CD spectrum of $r(A)_{12}$ change upon addition of P25 (see Figure 6.2B). At the ratio $N/P = 4-5$, the CD spectrum of the oligo-ribonucleotide at pH 5.0 is comparable to the spectrum recorded at pH 7.2, and further addition of P25 has no significant effect. Although addition of P25 results in large spectral changes of the UV absorption and CD spectrum of $r(A)_{12}$ at pH 5.0, the spectra of the oligo-ribonucleotide are not affected by addition of P25 at pH 4.0 (not presented).

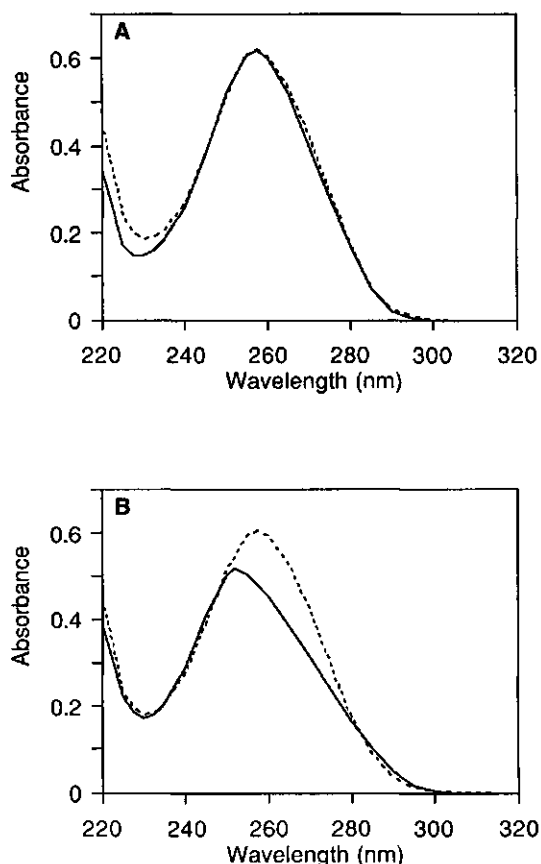


Fig. 6.1 UV absorption spectra of $r(A)_{12}$ (50 nmole nucleotide residues/ml) in the absence and the presence of P25 in (A) 10 mM sodium phosphate buffer pH 7.2 or (B) 10 mM sodium acetate buffer pH 5.0. — $r(A)_{12}$ without P25; - - - $r(A)_{12}$ with P25 at $N/P = 5$.

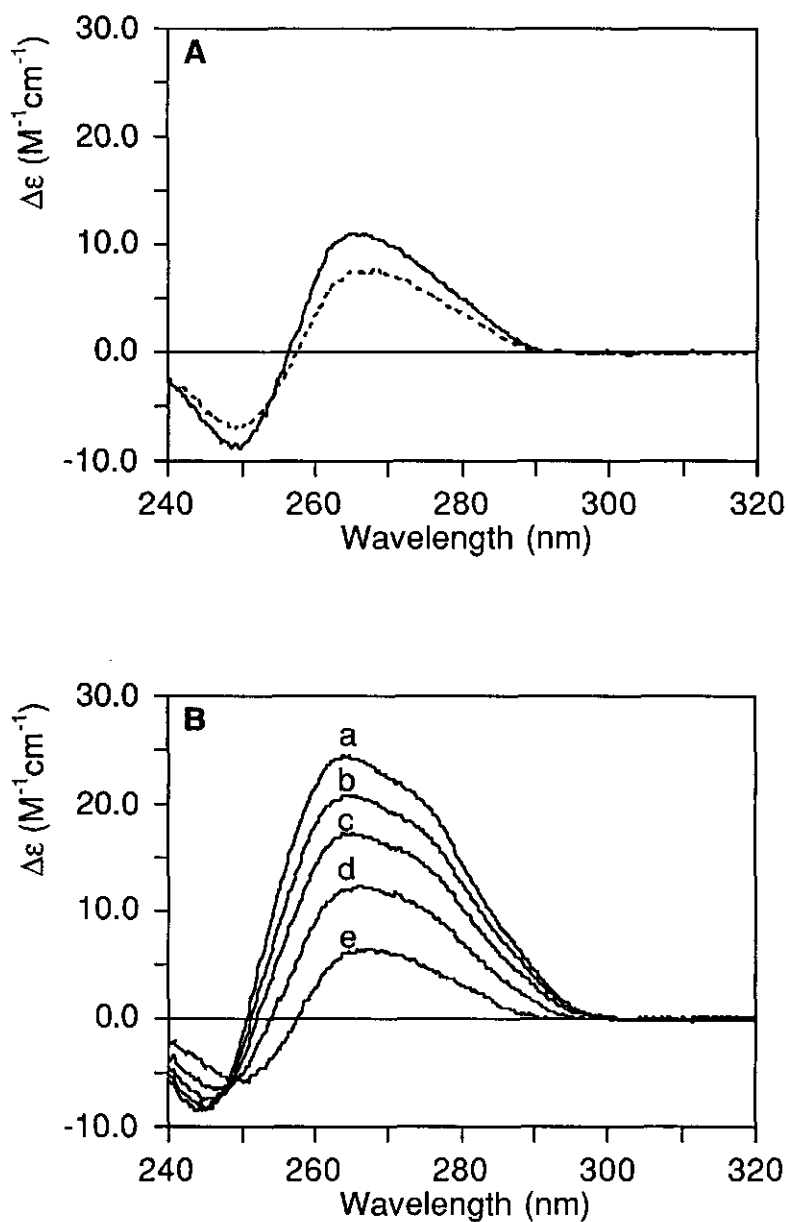


Fig. 6.2 CD spectra of $r(A)_{12}$ (25 nmole nucleotide residues/ml) in the absence and the presence of P25 in 10 mM sodium phosphate buffer (A) pH 7.2 and (B) pH 5.0. (A) — $r(A)_{12}$ without P25; - - - $r(A)_{12}$ with P25 at $N/P = 5$. (B) (a) $r(A)_{12}$ without P25; (b)-(e) $r(A)_{12}$ with P25 at (b) $N/P = 28$, (c) $N/P = 14$, (d) $N/P = 9$, and (e) $N/P = 5$.

The effect of P25 on the conformation and stability of d(GC)₅ and d(AT)₅

The oligonucleotides d(GC)₅ and d(AT)₅ are expected to form double-stranded structures with Watson-Crick base-pairing. However, the melting curves of d(GC)₅ and d(AT)₅ in the Figures 6.3 and 6.4, respectively, show no large cooperativity upon melting in the absence of P25. This indicates that these oligonucleotides do not form very stable double stranded helical structures because of insufficient chain length (Saenger, 1984). In the presence of P25, the double stranded structures of both oligonucleotides are more stabilized resulting in a more cooperative hyperchromicity (see Figures 6.3 and 6.4). Figure 6.4 shows that the presence of 250 mM sodium chloride has a stabilizing effect on the double stranded structure of d(AT)₅ in the absence of P25, but a destabilizing effect on d(AT)₅ in the presence of P25.

Fig. 6.3 Melting curves of d(GC)₅ (33 nmole nucleotide residues/ml) in 10 mM sodium phosphate buffer pH 7.2.

- ● - d(GC)₅ without P25;
- ○ - d(GC)₅ with P25 at N/P = 10.

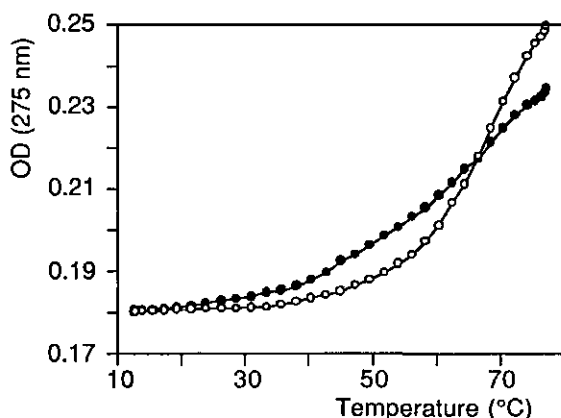
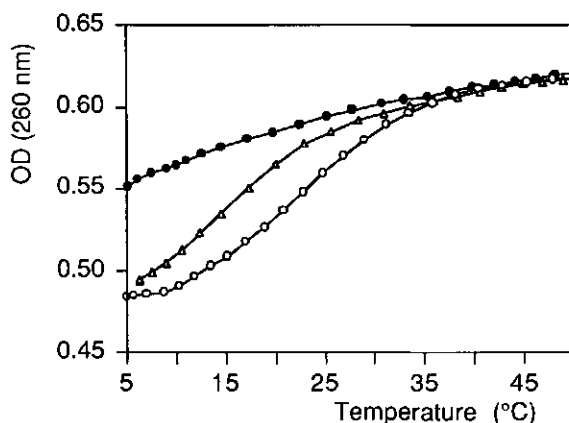


Fig. 6.4 Melting curves of d(AT)₅ (95 nmole nucleotide residues/ml) in 10 mM sodium phosphate buffer pH 7.2.

- ● - d(AT)₅ without P25;
- ○ - d(AT)₅ with P25 at N/P = 10;
- Δ - d(AT)₅ with or without P25 in 250 mM NaCl.



DISCUSSION

The results show that addition of P25 to $r(A)_{12}$ at neutral pH has no significant effect on the conformation of the oligo-ribonucleotide. The small decrease in intensity of the CD spectrum upon addition of P25 (Figure 6.2A) can be explained by a small change in the tilt of the bases, or rotation per base. At pH 5.0, however, addition of P25 to $r(A)_{12}$ results in significant spectral changes (see Figures 6.1B and 6.2B). Below pH 5.8, the oligo-ribonucleotide $r(A)_{12}$ exists as a protonated duplex (Causley and Johnson, 1982). In this duplex the adenine amino group forms two hydrogen bonds (see Figure 6.5): one between N_{10} -H and N_7 of an adjacent adenine, and another between N_{10} -H and a free phosphate oxygen (Rich et al., 1961). The last mentioned hydrogen bond is stabilized by protonation of the adenine at the N_1 position ($pK_a \sim 3.5 - 4.2$) (Saenger, 1984). Figures 6.1B and 6.2B show that addition of P25 changes the UV absorption and CD spectrum of $r(A)_{12}$ in the double-stranded form into spectra characteristic for single-stranded $r(A)_{12}$ (as in Figures 6.1A and 6.2A). This indicates that P25 is able to disrupt the double stranded structure of $r(A)_{12}$ at pH 5.0. Binding of the positively charged side chains of P25 to the negatively charged phosphates of the backbone of $r(A)_{12}$ probably destabilizes the hydrogen bond between the phosphate oxygen and the amino group of the adenine, resulting in a disruption of the double-stranded structure. All changes appear up to $N/P = 4-5$ indicating that 4 to 5 nucleotides are involved in peptide binding. At pH 4.0, P25 is not able to destroy the double-stranded structure, because at this lower pH value the hydrogen bond between the phosphate oxygen and the amino group of the adenine is more stabilized by protonation of the adenine at the N_1 position (about 50% is protonated at pH 4.0).

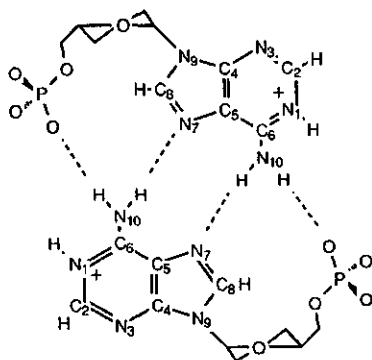


Fig. 6.5 Schematic representation of the base-pairing in double-stranded $r(A)_{12}$ after Rich et al. (1961).

Figures 6.3 and 6.4 show that the cooperativity in the melting behaviour of $d(GC)_5$ and $d(AT)_5$ increases upon addition of P25 or salt. It has been shown that DNA has a slightly expanded conformation at low ionic strength as result of electrostatic repulsions between the phosphate groups of the DNA backbone (Scruggs and Ross, 1964; Eigner and Doty, 1965; Rosenberg and Studier, 1969; Triebel and Reinert, 1971). Addition of salt shields the negative charges of the phosphate groups, and stabilizes a more compact stacked double-stranded structure with a cooperative melting behaviour (Dove and Davidson, 1962). Figure 6.4 shows an increase in cooperativity for the melting behaviour of $d(AT)_5$ in the presence of 250 mM sodium chloride, and even a larger cooperativity in the presence of P25. Binding of the positively charged side chains of P25 to the negatively charged phosphates of the nucleotide backbone stabilizes the double stranded structures of $d(GC)_5$ and $d(AT)_5$. This effect can be compared with the stabilization of the B-DNA double helix upon complexation of the DNA with nucleoprotamine or with homopolymer polypeptides like polylysine or polyarginine (Suwalsky and Traub, 1972). The fact that the stabilizing effect of P25 disappears after addition of 250 mM sodium chloride (see Figure 6.4) shows that the electrostatic interactions between the positively charged side chains of P25 and the negatively charged phosphate backbone of the oligonucleotide are essential for complex formation.

The effects upon binding of P25 to $r(A)_{12}$, $d(AT)_5$, and $d(GC)_5$ on the conformation and stability of the oligonucleotides all indicate that the positively charged side chains of the peptide have strong electrostatic interactions with the negatively charged phosphate groups of the oligonucleotides. These strong interactions disturb the non-Watson-Crick base pairing in $r(A)_{12}$ at pH 5.0, but stabilize the double-stranded structures of $d(AT)_5$ and $d(GC)_5$.

The results of a melting study on CCMV RNA have shown that polyamines induce a compact RNA conformation with stable double-stranded helices (Adolph, 1975). However, the results of a laser Raman study on intact CCMV and protein-free RNA indicate a slightly less ordered secondary structure of the protein-bound RNA in the virus particle (Verduin et al., 1984). The results of the present study and the melting study on CCMV RNA mentioned above (Adolph, 1975) suggest that this structure-distorting effect is not caused by the positively charged N-termini, but by other regions of the protein.

ACKNOWLEDGEMENTS

We thank Professor J. H. van Boom and H. van den Elst for the synthesis of d(GC)₅ and d(AT)₅, and Professor Dr. R. van Grondelle and Dr. H. van Amerongen for stimulating discussions.

REFERENCES

- Adolph, K. W. (1975) *J. Gen. Virol.* 28, 137-145.
- Bartlett, G. R. (1959) *J. Biol. Chem.* 234, 466-468.
- Causley, G. C. & Johnson, W. C., Jr. (1982) *Biopolymers* 21, 1763-1780.
- Dasgupta, R. & Kaesberg, P. (1982) *Nucl. Acids Res.* 10, 703-713.
- Dove, W. F. & Davidson, N. (1962) *J. Mol. Biol.* 5, 467-478.
- Eigner, J. & Doty, P. (1965) *J. Mol. Biol.* 12, 549-580.
- Hemminga, M. A., Datema, K. P., ten Kortenaar, P. W. B., Krüse, J., Vriend, G., Verduin, B. J. M. & Koole, P. (1985) in *Magnetic Resonance in Biology and Medicine* (Govil, G. Khetrapal, C. L. & Saran, A., Eds.) pp 53-76, Tata McGraw-Hill, New Delhi.
- Inman, R. B. & Baldwin, R. L. (1962) *J. Mol. Biol.* 5, 172-184.
- Rich, A., Davies, D. R., Crick, F. H. C. & Watson, J. D. (1961) *J. Mol. Biol.* 3, 71-86.
- Rosenberg, A. H. & Studier, F. W. (1969) *Biopolymers* 7, 765-774.
- Saenger, W. (1984) *Principles of Nucleic Acid Structure*, Springer-Verlag New York, Inc., New York.
- Scruggs, R. I. & Ross, P. D. (1964) *Biopolymers* 2, 593-609.
- Smith, P. K., Krohn, R. I., Hermanson, G. T., Mallia, A. K., Gartner, F. H., Provenzano, M. D., Fujimoto, E. K., Goeke, N. M., Olson, B. J. & Klenk, D. C. (1985) *Anal. Biochem.* 150, 76-85.
- Suwaïsky, M. & Traub, W. (1972) *Biopolymers* 11, 2223-2231.
- Ten Kortenaar, P. W. B., Krüse, J., Hemminga, M. A. & Tesser, G. I. (1986) *Int. J. Pept. Protein Res.* 27, 401-413.
- Triebel, H. & Reinert, K. E. (1971) *Biopolymers* 10, 827-837.
- Verduin, B. J. M., Prescott, B. & Thomas, G. J., Jr. (1984) *Biochemistry* 23, 4301-4308.
- Vriend, G., Hemminga, M. A., Verduin, B. J. M., de Wit, J. L. & Schaafsma, T. J. (1981) *FEBS Lett.* 134, 167-171.
- Vriend, G., Verduin, B. J. M. & Hemminga, M. A. (1986) *J. Mol. Biol.* 191, 453-460.
- Vriend, G., Verduin, B. J. M., Hemminga, M. A. & Schaafsma, T. J. (1982) *FEBS Lett.* 145, 49-52.
- Wells, R. D., Larson, J. E., Grant, R. C., Shortle, B. E. & Cantor, C. R. (1970) *J. Mol. Biol.* 54, 465-497.

SUMMARY

The objective of the study described in this thesis was to obtain information about protein-RNA interactions in cowpea chlorotic mottle virus (CCMV). CCMV consists of RNA and a protective protein coat, composed of 180 identical coat proteins. The positively charged N-terminal arm of the coat protein is essential for binding the encapsidated RNA. Previously, the so-called 'snatch-pull' model has been suggested for the assembly of coat protein and RNA. According to this model the N-terminal region has a flexible random-coil conformation in the absence of RNA, but attains an α -helical conformation upon RNA-binding. In the present study a synthetic peptide containing the first 25 amino acids of CCMV coat protein (P25) was used as a model for the N-terminus, and oligophosphates and oligonucleotides were used as models for the viral RNA. The conformation of the peptide was studied by nuclear magnetic resonance (NMR) and circular dichroism (CD). Changes in the conformation of the oligonucleotides were studied by CD and absorbance spectroscopy. The results confirm the snatch-pull model and allow an extension to a more detailed model for the assembly of CCMV coat protein and RNA (see below).

Chapter 2 describes the effects of ionic strength, addition of (oligo) phosphates, and temperature on the conformation of the peptide P25 containing six arginines and three lysines. CD experiments show that the peptide has 15-18% α -helical and about 80% random coil conformation in the absence of inorganic salt at 25°C. Lowering the temperature to 10°C increases the α -helix content to 20-21%. Addition of inorganic salts results in a larger increase of the amount of α -helical conformation, up to 42% in the presence of oligophosphate with an average chain length of eighteen phosphates. One-dimensional proton NMR experiments show that the α -helix formation starts in the region between Thr9 and Gln12, and is extended in the direction of the C-terminus. NMR relaxation measurements show that binding to oligophosphates of increasing length results in reduced internal mobilities of the positively charged side chains of the arginyl and lysyl residues and of the side chain of Thr9 at the beginning of the α -helical region.

Chapter 3 gives a description of two-dimensional proton NMR experiments on P25 in the presence of sodium monophosphate. All resonances could be assigned by a combined use of two-dimensional correlated spectroscopy and nuclear Overhauser enhancement spectroscopy carried out at four different temperatures. Various NMR parameters indicate

the presence of a conformational ensemble consisting of helical structures rapidly interconverting to more extended states. Differences in chemical shifts and nuclear Overhauser effects indicate that lowering the temperature induces a shift of the dynamic equilibrium towards the helical structures. At 10°C a perceptible fraction of the conformational ensemble consists of structures with an α -helical conformation between residues 9 and 17, likely starting with a turn-like structure around Thr9 and Arg10. The region close to Arg10 shows the strongest tendency to attain an α -helical conformation.

Chapter 4 presents a two-dimensional proton NMR study on the effect of (oligo)phosphates on the conformation of P25. NMR experiments were performed on the highly positively charged peptide in the presence of an excess of monophosphate, tetraphosphate or octadecaphosphate. The peptide alternates between various extended and helical structures in the presence of monophosphate, but this equilibrium shifts towards the helical structures in the presence of oligophosphates. In the presence of tetraphosphate the α -helical region is situated between residues 10 and 20. NMR distance constraints obtained for P25 in the presence of tetraphosphate have been used to generate peptide structures by distance geometry calculations. These calculations resulted in eight structures belonging to two structure families. The first family consists of five structures with an α -helix-like conformation in the middle of the peptide, and the second family consists of three structures with a more open conformation. The presence of two structure families indicates that even in the presence of tetraphosphate the peptide is flexible.

Chapter 5 describes a two-dimensional proton NMR study on the intact coat protein of cowpea chlorotic mottle virus (molecular mass: 20.2 kDa) present as dimer (pH = 7.5) or as capsid consisting of 180 protein monomers (pH = 5.0). The spectra of both dimers and capsids show resonances originating from the flexible N-terminal region of the protein. The complete resonance assignment of P25 made it possible to interpret the spectra in detail. The capsid spectrum shows backbone amide proton resonances arising from the first eight residues having a flexible random coil conformation, and side-chain resonances arising from the first 25 N-terminal amino acids. The dimer spectrum shows also side-chain resonances of residues 26 to 33, which are flexible in the dimer but immobilized in the capsid. It is suggested that the carboxyl group of Glu33 plays a role in the pH-dependent association of the coat protein. Neutralization of this acidic residue by low pH or by the presence of positively charged bases of the RNA possibly results in a

conformation necessary for capsid formation. The NMR experiments indicate that the conformation of the first 25 amino acids of the intact viral coat protein in dimers and capsids is comparable to the conformation of the synthetic peptide P25.

Finally, Chapter 6 deals with the effect of P25 on the structure of oligonucleotides. The experiments described in this chapter have been carried out on samples containing micromolar concentrations of both P25 and oligonucleotides. For NMR measurements samples with concentrations of more than 100 times higher are necessary. Unfortunately, it was not possible to avoid precipitation at such high concentrations of P25 and oligonucleotides in aqueous solution. However, conformational changes of the oligonucleotides $r(A)_{12}$, $d(GC)_5$, and $d(AT)_5$ upon binding to P25 could be studied by using absorption and CD spectroscopy. $r(A)_{12}$ has a single-stranded structure at pH = 7.2, and exists as a protonated duplex at pH-values below 5.8. In this duplex a phosphate oxygen of the RNA backbone forms a hydrogen bond to the amino group of the adenine. The oligonucleotides $d(GC)_5$ and $d(AT)_{12}$ form duplexes with Watson-Crick base-pairing. The results show that P25 has only a minor effect on the single-stranded structure of $r(A)_{12}$ at pH 7.2, but disrupts the double-stranded structure of $r(A)_{12}$ at pH = 5.0. At pH = 4.0, the double stranded structure of $r(A)_{12}$ is stabilized by protonation of the adenine at the N_1 position and the peptide is not able to disrupt the double-stranded structure. The double-stranded structures of $d(GC)_5$ and $d(AT)_5$ with Watson-Crick base-pairing are stabilized upon binding to the peptide. All conformational changes observed indicate that the positively charged side chains of the peptide have strong electrostatic interactions with the negatively charged phosphate groups of the oligonucleotides.

The results of the study described in this thesis confirm the snatch-pull model mentioned in the beginning of this summary. Although P25 alternates between various conformations in aqueous solution, the region between residues 10 and 20 shows a tendency to adopt an α -helical conformation. This α -helical structure is stabilized by low temperature, high ionic strength, and the addition of (oligo)phosphates, mimicking the RNA. It has been shown that the α -helix formation starts in the region between Thr9 and Gln12. Based upon this observation, a more detailed model for the assembly of CCMV coat protein and the viral RNA is proposed. It is suggested that hydrogen bond formation by the side chains of Thr9 and Gln12 initiates α -helix formation. After this initiation, the helix is extended in the direction of the C-terminus

upon binding of negatively charged phosphate groups to the positively charged side chains present in the N-terminal region of the coat protein. The results indicate a strong effect of the presence of phosphates on Arg10. Phosphate binding to this residue may extend the helix in the direction of the C-terminus because of the removal of an unfavourable interaction between the positive charge at this position and the macrodipole of the helix. The extension of the helical region results in a proper orientation of the positively charged side chains for binding to the phosphate groups of the RNA backbone. In an α -helical conformation the distance between the arginines at positions 10, 14, 18 and 22 ($\sim 6 \text{ \AA}$) is comparable to the distance between two neighbouring phosphate groups in an A-type RNA helix ($\sim 5.9 \text{ \AA}$).

SAMENVATTING

Het doel van het in dit proefschrift beschreven onderzoek was het verkrijgen van informatie over interacties tussen eiwit en RNA in cowpea chlorotic mottle virus (CCMV). Het plantevirus CCMV is opgebouwd uit RNA en een beschermende eiwitmantel, bestaande uit 180 dezelfde eiwit-moleculen. Elk manteleiwit heeft een sterk positief geladen N-terminale arm, die essentieel is voor de binding met het RNA. Al eerder was er een model opgesteld voor de binding van het manteleiwit aan het RNA. Volgens dit zogenaamde 'grijp-trek' model heeft het N-terminale deel van het eiwit een flexibele ongedefinieerde structuur in afwezigheid van RNA, maar neemt het een α -helixstructuur aan bij RNA-binding. Een peptide bestaande uit de eerste 25 aminozuren van het manteleiwit werd gebruikt als model voor deze N-terminale arm. Oligofosfaten en oligonucleotiden werden gebruikt als modellen voor het virale RNA. De conformatie van het peptide werd bestudeerd met behulp van kernspinresonantie (NMR) en circulair dichroïsme (CD). Veranderingen in de conformatie van de oligonucleotiden werden bestudeerd met CD en absorptiespectroscopie. De resultaten van het onderzoek ondersteunen het 'grijp-trek' model en maken het mogelijk dit model verder te verfijnen (zie hieronder).

Hoofdstuk 2 beschrijft de effecten van zoutsterkte, toevoeging van (oligo)fosfaten en temperatuur op de structuur van het peptide P25, dat zes arginines en drie lysines bevat. CD-experimenten laten zien dat bij 25°C de structuur van het peptide in water bestaat uit 15-18% α -helix en ongeveer 80% ongedefinieerde structuur. Verlaging van de temperatuur tot 10°C resulteert in een kleine toename van het gehalte α -helix tot 20-21%. Toevoeging van anorganische zouten geeft een grotere toename van α -helix structuur: tot aan 42% in de aanwezigheid van oligofosfaten met een gemiddelde ketenlengte van achttien fosfaten. Eéndimensionale proton-NMR-experimenten laten zien dat de α -helixstructuur begint in het gebied tussen Thr9 en Gln12. De α -helixconformatie kan zich uitbreiden in de richting van de C-terminus. NMR-relaxatiemetingen laten zien dat de interne beweeglijkheid van de positief geladen zijketens van de arginines en lysines afneemt bij binding aan steeds langere oligofosfaten. Ditzelfde geldt voor de zijketen van Thr9, een aminozuur aan het begin van het gebied met α -helixstructuur.

Hoofdstuk 3 geeft een beschrijving van tweedimensionale proton-NMR-experimenten aan P25 in de aanwezigheid van natriummonofosfaat. Alle

resonanties konden worden toegekend met behulp van tweedimensionale gecorreleerde spectroscopie en nuclear Overhauser enhancement (NOE) spectroscopie, uitgevoerd bij vier verschillende temperaturen. Verschillende NMR-parameters duiden op de aanwezigheid van een ensemble van structuren met zowel helixachtige als meer uitgestrekte conformaties. Verschillen in chemische verschuivingen en NOEs laten zien dat temperatuursverlaging resulteert in een verschuiving van het dynamisch evenwicht naar de helixachtige structuren. Bij 10°C bestaat een waarneembare fractie van het ensemble uit structuren met een α -helix tussen aminozuur 9 en 17, waarschijnlijk beginnend met een vreemde draai in de buurt van Thr9 en Arg10. Het gebied dicht bij Arg10 vertoont de sterkste neiging tot α -helixvorming.

In Hoofdstuk 4 wordt beschreven hoe het effect van (oligo)fosfaten op de structuur van P25 in meer detail is bestudeerd met behulp van tweedimensionale proton-NMR. NMR-experimenten werden uitgevoerd op het sterk positief geladen peptide in de aanwezigheid van een overmaat mono-, tetra-, of octadecafosfaat. In een monofosfaatbuffer neemt het peptide afwisselend uitgestrekte en helixachtige conformaties aan en in de aanwezigheid van de langere fosfaten verschuift het evenwicht naar de helixachtige structuren. Met tetrafosfaat bevindt de α -helixconformatie zich tussen aminozuur 10 en 20. Voor P25 in de aanwezigheid van tetrafosfaat werden afstanden tussen de verschillende protonen berekend uit de gemeten NOE-intensiteiten. Met behulp van distance geometry werden uit deze afstanden acht structuren berekend, die onderverdeeld konden worden in twee groepen van vergelijkbare structuren. De eerste groep bestaat uit vijf structuren met een α -helixachtige conformatie in het midden van het peptide, en de tweede groep bestaat uit drie structuren met een meer open conformatie. Het feit dat er twee verschillende structuurgroepen gegenereerd werden, duidt erop dat P25 ook in de aanwezigheid van tetrafosfaat beweeglijk is.

Hoofdstuk 5 presenteert een onderzoek aan het intacte manteleiwit van cowpea chlorotic mottle virus ($M_w = 20,2$ kDa) met behulp van tweedimensionale proton-NMR. Het manteleiwit komt voor als dimeer (bij pH = 7,5) of als een lege bol bestaande uit 180 eiwitmoleculen, het zogenaamde capside (bij pH = 5,0). De NMR-spectra van het eiwit in beide aggregatietoestanden bevatten alleen resonanties die afkomstig zijn van het flexibele N-terminale uiteinde. De spectra konden in detail worden geanalyseerd met behulp van de informatie die met P25 verkregen was. Het NMR-spectrum van

het eiwitcapside bevat resonanties van amideprotonen van de eerste acht aminozuren en van zijketenprotonen van de eerste 25 aminozuren. Het spectrum van het eiwitdimeer laat ook resonanties zien van zijketenprotonen van de aminozuren 26 tot 33. Dit gebied van het eiwit is beweeglijk in een dimeer, maar onbeweeglijk in een capside. Mogelijk speelt de carboxylgroep van Glu33 een rol in de zuurgraad-afhankelijke associatie van het manteleiwit. Neutralisatie van deze zure groep bij lage pH of in aanwezigheid van positief geladen RNA-basen kan resulteren in de conformatie die nodig is voor capsidevorming. De NMR-experimenten geven aan dat de conformatie van de eerste 25 aminozuren van het intacte manteleiwit in beide aggregatievormen vergelijkbaar is met de structuur van het synthetisch peptide P25.

Tenslotte gaat hoofdstuk 6 over het effect van P25 op de structuur van oligonucleotiden. De in dit hoofdstuk beschreven experimenten zijn uitgevoerd aan monsters met micromolaire concentraties van zowel P25 als oligonucleotiden. Voor NMR-metingen zijn monsters met zo'n honderd maal hogere concentratie nodig. Helaas was het niet mogelijk om bij die hoge concentraties in een waterige oplossing neerslagvorming van P25 en oligonucleotiden te vermijden. Met behulp van CD en absorptiespectroscopie was het echter mogelijk om bij zeer lage concentraties het effect van P25 op de structuur van de oligonucleotiden $r(A)_{12}$, $d(GC)_5$ en $d(AT)_5$ te meten. $r(A)_{12}$ is enkelstrengs bij pH = 7,2, maar dubbelstrengs bij pH-waarden beneden 5,8. In deze dubbelstrengsstructuur wordt er een waterstofbrug gevormd tussen een vrij zuurstofatoom van de fosfaatgroep in de RNA-backbone en de aminogroep van het adenine. De oligonucleotiden $d(GC)_5$ en $d(AT)_5$ vormen dubbelstrengsstructuren met Watson-Crick baseparing. De resultaten laten zien dat P25 een zeer klein effect heeft op de enkelstrengsstructuur van $r(A)_{12}$ bij pH = 7,2. De dubbelstrengsstructuur van $r(A)_{12}$ bij pH = 5,0 wordt echter verbroken bij binding van P25. Bij pH = 4,0 wordt de dubbelstrengsstructuur van $r(A)_{12}$ gestabiliseerd door de protonering van de base op de N1-positie. Bij deze pH-waarde is P25 niet meer in staat om de dubbelstrengsstructuur te verbreken. Bij binding van P25 aan $d(GC)_5$ en $d(AT)_5$ worden deze dubbelstrengsstructuren met Watson-Crick baseparing gestabiliseerd. Alle waargenomen conformatieveranderingen duiden erop dat de positief geladen zijketens van het peptide sterke electrostatistische interacties hebben met de negatief geladen fosfaatgroepen van de oligonucleotiden.

De resultaten van het hier beschreven onderzoek ondersteunen het 'grijp-trek' model, dat aan het begin van deze samenvatting genoemd werd.

Hoewel P25 in waterige oplossing verschillende structuren aanneemt, vertoont het gebied tussen aminozuur 10 en 20 de neiging een α -helix te vormen. Deze α -helixconformatie wordt gestabiliseerd bij lage temperatuur, hoge zoutsterkte en de aanwezigheid van (oligo)fosfaten. De resultaten maken het mogelijk om een gedetailleerder model voor de assemblage van CCMV-manteleiwit en het virale RNA voor te stellen. De suggestie wordt gedaan dat de α -helixvorming begint met waterstofbrugvorming door de zijketens van Thr9 en Gln12. Vervolgens wordt de helix uitgebreid in de richting van de C-terminus door binding van negatief geladen fosfaatgroepen aan de positief geladen zijketens in het N-terminale deel van het eiwit. De resultaten laten zien dat Arg10 sterk beïnvloed wordt door de aanwezigheid van fosfaten. Het is mogelijk dat fosfaatbinding aan de zijketen van dit aminozuur resulteert in een verlenging van de α -helix in de richting van de C-terminus aangezien daarbij een ongewenste interactie wordt verwijderd tussen de positieve lading op deze positie en de macrodipool van de helix. De verlenging van de helix heeft als gevolg dat positief geladen zijketens in het eiwit de juiste oriëntatie krijgen voor binding met de fosfaatgroepen in de RNA-backbone. In een α -helixachtige conformatie is de afstand tussen de arginines op de posities 10, 14, 18 en 22 ($\sim 6 \text{ \AA}$) vergelijkbaar met de afstand tussen twee opeenvolgende fosfaatgroepen in een A-type RNA-helix ($\sim 5,9 \text{ \AA}$).

CURRICULUM VITAE

Marinette van der Graaf werd op vrijdag de 13^e september 1963 geboren te Lekkerkerk. In 1981 legde zij het eindexamen Gymnasium- β af aan de scholengemeenschap "De Krimpenervaard" te Krimpen aan den IJssel, waarna zij begon met de studie Plantenveredeling aan de toenmalige Landbouwhogeschool in Wageningen. Na het behalen van het propaedeutisch examen in mei 1982 stapte zij over op de studie Moleculaire Wetenschappen, waarvan zij de fysisch-chemische oriëntatie volgde. Het doctoraalpakkiet bestond uit een verzwaard hoofdvak Moleculaire Fysica, een hoofdvak Kolloïdchemie en de bijvakken Natuurkunde, Wiskunde en Pedagogiek en Algemene Didactiek. Tevens werd een eerste graads onderwijsbevoegdheid in de scheikunde behaald. Het doctoraalexamen werd in januari 1988 met lof afgelegd.

Van mei 1987 tot september 1987 en van januari 1988 tot januari 1991 werkte zij als assistent-onderzoeker bij de vakgroep Moleculaire Fysica van de Landbouwuniversiteit te Wageningen aan het onderzoek dat tot dit proefschrift heeft geleid. Gedurende het studiejaar 1989 - 1990 was zij tevens lid van de Universiteitsraad waar zij deel uitmaakte van de Overleggroep Onderwijs en Onderzoek. Sinds april 1991 is zij in tijdelijke dienst van de Nederlandse Organisatie voor Wetenschappelijk Onderzoek (NWO) en werkt zij in het kader van een samenwerkingsproject tussen de vakgroep Biochemie van de Rijksuniversiteit Leiden en de vakgroep Biofysische Chemie van de Katholieke Universiteit Nijmegen aan de structuuropheldering van pseudoknopen in RNA.